

*Thesis titled:*



# “Development of a BIPCON Apparatus to Probe Subtle Phenomena Associated with Carbocations”

submitted for the Degree of Doctor of Philosophy (Ph.D.)

by

Ian R. Milne

B.Sc. (Hons.) Adel.

from the

Department of Chemistry,  
The University of Adelaide.



December 2001.

## Table of Contents:

<b>Table of Contents:</b>	<b>3</b>
<b>Table of Figures:</b>	<b>7</b>
<b>Abstract:</b>	<b>12</b>
<b>Statement of Originality:</b>	<b>13</b>
<b>Acknowledgements:</b>	<b>14</b>
<b>Chapter 1: Introduction and Development of Hypothesis.</b>	<b>16</b>
<b>1.1 Introduction.</b>	<b>17</b>
1.1.1 The $S_N1$ / $S_N2$ Reaction Classification.	18
<b>1.2 The Solvolytic Reaction.</b>	<b>19</b>
1.2.1 Significant Developments Elucidated Through the Analysis of Solvolytic Reactions.	22
1.2.2 The Grunwald-Winstein Correlation	22
1.2.3 Refinement of the Description of Solvolytic Processes.	24
1.2.4 Identification of the $S_N2$ Nature of the Solvolysis of <i>t</i> -Butyl Halides and the Development of Additional Scales of Solvent Ionising Strength.	27
1.2.5 The Effect on the Rate of Solvolysis of the 1-Adamantyl System with Substitution at the 3-Position.	29
<b>1.3 Comparison to Other Polycyclic Alkanes.</b>	<b>30</b>
1.4.1 Choice of Kinetic Substrates.	33
<b>1.5 Establishment of the BIPCON Suite.</b>	<b>34</b>
1.5.1 Kinetic Data Determined by Monitoring Solvolyses by Titration.	35
1.5.2 Kinetic Data Determined by Monitoring Solvolyses by Chromatography.	36
1.5.3 Kinetic Data Determined by Monitoring Solvolyses by Spectroscopy	36
1.5.4 Kinetic Data Determined by Monitoring Solvolyses by Conductometric Methods.	37
1.5.5 Automation of the Collection of Kinetic Data Through Conductometric Techniques.	37
<b>1.6 Anticipated Results from the Kinetic Study.</b>	<b>39</b>
<b>1.7 Further Investigation of Other Substrates of Interest.</b>	<b>40</b>
<b>Chapter 2: Development of the BIPCON Suite at the Department of Chemistry, the University of Adelaide.</b>	<b>41</b>
<b>2.1 Development of the BIPCON Suite</b>	<b>42</b>
2.1.1 The BIPCON System	42
2.1.2 BIPCON Software	45
2.1.3 The Conductance Cells	45
2.1.4 Temperature Control	53

2.1.5 Other Components	53
<b>2.2 Set-up of the BIPCON Hardware.</b>	<b>54</b>
2.2.1 Radio Frequency Shielding.	54
2.2.2 Temperature Maintenance.	55
2.2.3 Electrical Isolation.	56
2.2.4 Ideal Physical Location.	56
<b>2.3 Preparation of the BIPCON Suite for Conductometric Experiments.</b>	<b>59</b>
2.3.2 Binary Solvent Mixtures.	61
2.3.3 Cell Preparation.	61
2.3.4 Development of the BRAT and Other Software Improvements.	63
<b>Chapter 3: Development of a Complete BIPCON Suite Users Manual</b>	<b>65</b>
<b>3.1 Set Up of the Components of the BIPCON Suite.</b>	<b>66</b>
<b>3.2 Turing On the BIPCON Suite.</b>	<b>66</b>
<b>3.3 First Time Use.</b>	<b>67</b>
<b>3.4 Cell Calibration.</b>	<b>73</b>
<b>3.5 Setting Up a New BIPCON Run.</b>	<b>73</b>
3.5.1 Preparation of the Cells for Conductometric Experiments.	73
3.5.2 Entering Run Data.	74
<b>3.6 The Relevance of the S-alpha and Lambda-0 Values.</b>	<b>77</b>
<b>3.7 Completion of the Run Setup.</b>	<b>80</b>
<b>3.8 Initiating the BIPCON Run.</b>	<b>81</b>
<b>3.9 Modifying a Run.</b>	<b>82</b>
<b>3.10 Run Completion and Data Saving.</b>	<b>82</b>
<b>3.11 Other Commands For Channel and Data Manipulation.</b>	<b>83</b>
<b>3.12 Data Analysis.</b>	<b>84</b>
3.12.2 Kinetic Data Calculation.	86
<b>3.13 Preparation of the BIPCON Suite for a New Run.</b>	<b>91</b>
<b>Chapter 4: Synthetic Approaches to Precursors of Kinetic Interest.</b>	<b>92</b>
<b>4.1 The Preparation of the Substrates Used for Calibration.</b>	<b>93</b>
<b>4.2 Synthetic Approaches Towards the 3-R-Substituted, 1-Adamantyl Tosylates.</b>	<b>93</b>
<b>4.3 Direct Tosylation of the Adamantly Alcohols Utilising <i>p</i>-Toulenesulfonyl Chloride.</b>	<b>97</b>
<b>4.4 Use of Silver Tosylate and the Corresponding Adamantly Bromides.</b>	<b>98</b>

<b>4.5 Friedel Crafts Arylation of the Bridgehead Bromide to Introduce a Phenyl Substituent.</b>	<b>100</b>
4.5.1 Preparation of the Desired Tosylate (15).	101
<b>4.6 Synthetic Approach to Other Required Substrates.</b>	<b>102</b>
<b>4.7 Synthetic Approaches from Adamantane-1-Carboxylic Acid.</b>	<b>103</b>
<b>4.9 Alternate Approach to the Desired Ester (32).</b>	<b>105</b>
<b>4.10 Introduction of a Cyano Group.</b>	<b>106</b>
<b>4.11 Synthetic Approaches to Other Substrates Through Reduction of the Ester (32).</b>	<b>108</b>
<b>4.12 Introduction of Primary Acetate Functionality.</b>	<b>109</b>
<b>4.14 Tosyl-Halde Reaction Conditions.</b>	<b>110</b>
<b><i>Chapter 5: Kinetic Study of the Adamantyl System, and the Mechanistic Implications of the Results.</i></b>	<b>111</b>
5.1 Conductometric Analysis.	112
5.2 Solvolytic study of 1-adamantyl tosylate (10) ( $\sigma_I = 0$ ).	115
5.3 Solvolytic Study of 3-Phenyl, 1-Adamantyl Tosylate (15) ( $\sigma_I = 0.12$ ).	117
5.4 Solvolytic Study of (3-[(tosyl)oxy]-1-adamantyl) methyl acetate (22) ( $\sigma_I = 0.15$ ).	118
5.5 Solvolytic Study of (3-[(tosyl)oxy]-1-adamantyl) methyl tosylate (21) ( $\sigma_I = 0.23$ ).	119
5.6 Solvolytic Study of Methyl 3-[(tosyl)oxy]-1-Adamantane Carboxylate (23) ( $\sigma_I = 0.32$ ).	119
5.7 Solvolytic Study of 3-Cyano 1-Adamantyl Tosylate (11) ( $\sigma_I = 0.57$ ).	120
5.8 Observation of the Developing Trend in "m" Value Decrease.	121
5.9 Hammett Relationship Between the Rate of Solvolysis and the Electron Withdrawing Nature of the Substituent ( $\sigma_I$ ).	123
5.10 Investigation of the Convergence Between the Hammett Plots.	125
5.11 Investigation of the Relationship Between "m" and $\sigma_I$ .	127
<b><i>Chapter 6: Synthetic Approach to Further Systems of Kinetic Interest Through the Trapping of the 3-Halobicyclo[1.1.1]pent-1-yl Cation.</i></b>	<b>131</b>
6.1 Preparation of Additional Solvolytic Substrates.	132
6.2 Choice of Kinetic Model	138
6.3 Mechanistic Implications of the Proposed Synthesis.	139



<b>6.4: Synthetic Approach Towards the Desired Di-Substituted, Bicyclo[1.1.1]pentanes.</b>	<b>140</b>
<b>6.5 Preparation of 1,3-Diiodobicyclo[1.1.1]pentane (54).</b>	<b>141</b>
<b>6.6 Synthesis of 1,3-Dibromobicyclo[1.1.1]pentane (59).</b>	<b>141</b>
<b>6.7 Synthesis of Mixed Dihalide Bicyclo[1.1.1]pentanes.</b>	<b>143</b>
<b>6.8 Preparation of 1-Bromo, 3-Iodobicyclo[1.1.1]pentane (62).</b>	<b>144</b>
<b>6.9 Formation of 1-Bromo, 3-Chlorobicyclo[1.1.1]pentane (64).</b>	<b>145</b>
<b>6.10 Synthetic Approach to 1-Chloro, 3-Iodobicyclo[1.1.1]pentane (67).</b>	<b>147</b>
<b>6.11 Alternate Synthetic Approach to the Formation of 1-Bromo, 3-Iodobicyclo[1.1.1]pentane (62).</b>	<b>147</b>
<b>6.12 Formation of 1-Azido, 3-Iodobicyclo[1.1.1]pentane (56)</b>	<b>148</b>
<b>6.13 Attempted Syntheses Utilising Iodine Monochloride as the Halogen Source.</b>	<b>149</b>
<b>6.14 Hypothesis for the observed stability of the bridgehead cations.</b>	<b>150</b>
<b>6.15 Future directions.</b>	<b>151</b>
<b><i>Chapter 7: Experimental</i></b>	<b>152</b>
<b><i>Appendices</i></b>	<b>164</b>
<b>DOS Glossary:</b>	<b>164</b>
<b>BIPCON Flowchart 1</b>	<b>165</b>
<b>BIPCON Flowchart 2</b>	<b>166</b>
<b>BIPCON Flowchart 3</b>	<b>167</b>
<b>BIPCON Analysis Flowchart</b>	<b>168</b>
<b>About this thesis:</b>	<b>169</b>
<b><i>References</i></b>	<b>170</b>

## Table of Figures:

FIGURE 1.1: THE TRADITIONAL MECHANISTIC DESCRIPTION OF THE SOLVOLYTIC PROCESS. <sup>1</sup> .....	17
FIGURE 1.2: THE TRADITIONAL VIEW OF THE S <sub>N</sub> 1 AND S <sub>N</sub> 2 PROCESSES.....	18
FIGURE 1.3: "SPECIES PROPOSED AS INTERMEDIATES IN SOLVOLYSIS REACTIONS." <sup>2</sup> .....	20
EQUATION 1.1: THE RELATIONSHIP USED IN THE DEVELOPMENT OF THE SCALE OF SOLVENT IONISING STRENGTHS, BASED ON THE SOLVOLYSIS OF <i>T</i> -BUTYL CHLORIDE (1).....	22
EQUATION 1.2: THE GRUNWALD-WINSTEIN EQUATION: RELATIONSHIP BETWEEN THE RATE OF SOLVOLYSIS OF ANY SUBSTRATE AND THE SOLVENT IONISING STRENGTH (Y) BASED ON THE SOLVOLYSIS OF <i>T</i> -BUTYL CHLORIDE (1).....	23
EQUATION 1.3: THE EXPANDED GRUNWALD-WINSTEIN EQUATION.....	23
FIGURE 1.4: "A PLOT OF SOLVENT NUCLEOPHILICITY (N) AGAINST SOLVENT IONISING POWER (Y, BASED ON 2-ADAMANTYL TOSYLATE (2)) FOR AQUEOUS ETHANOL AND AQUEOUS 2,2,2-TRIFLUOROETHANOL. ....	25
FIGURE 1.5: RABER-HARRIS PLOTS OF 2-ADAMANTYL TOSYLATE (2), 1-ADAMANTYL CHLORIDE, <i>EXO</i> -2-NORBORNYL TOSYLATE, 2-PROPYL BROSYLATE AND METHYL TOSYLATE (3) VERSUS 1-ADAMANTYL BROMIDE (4) .....	26
FIGURE 1.6: "CORRELATION OF LOGARITHMS OF SOLVOLYSIS RATES FOR 1-ADAMANTYL CHLORIDE (6) VS. <i>TERT</i> -BUTYL CHLORIDE (1) AT 25°C.".....	28
FIGURE 1.7: "PLOT OF LOG <i>K</i> FOR 3-SUBSTITUTED 1-ADAMANTYL TOLUENESULFONATES VS. INDUCTIVE SUBSTITUENT CONSTANTS $\sigma_1^Q$ " IN 80E AT 25°C. ....	29
FIGURE 1.8: "PLOTS OF LOG <i>K</i> FOR 3-SUBSTITUTED 1-ADAMANTYL <i>P</i> -TOLUENESOLFONATES IN 97% TFE (FILLED CIRCLES) AND 80% ETOH (OPEN CIRCLES) VS. $\sigma_1^Q$ ." .....	30
FIGURE 1.9: "PLOT OF THE FREE ENERGIES OF SOLVOLYSIS VERSUS THE MM2 CALCULATED STRAIN ENERGY DIFFERENCE ( $\Delta E_S(R^+ - RH)$ ).". ....	31
FIGURE 1.10: PLOT OF LOG <i>K</i> OF SOLVOLYSIS OF (I) 1-BROMOBICYCLO[1.1.1]PENTANE (7), (II) 3- <i>TERT</i> -BUTYL BICYCLO[1.1.1]PENTYL BROMIDE (8) AND (III) 3-PHENYL BICYCLO[1.1.1]PENTYL BROMIDE AGAINST LOG <i>K</i> FOR SOLVOLYSIS OF 1-ADAMANTYL BROMIDE (4) IN VARIOUS BINARY SOLVENTS.....	32
FIGURE 1.11: THE PROPOSED 3-SUBSTITUTED 1-ADAMANTYL TOSYLATES TO BE PREPARED, AND THEIR ASSOCIATED $\sigma_I$ VALUES.....	34
FIGURE 1.12: THEORETICAL RABER-HARRIS PLOT FOR A SUBSTRATE IN FIVE SOLVENT SYSTEMS.....	35
FIGURE 1.13: 1,3-DISUBSTITUTED BICYCLO[1.1.1]PENTANES OF INTEREST (X AND/OR Y = I, Br, Cl, N <sub>3</sub> , OH) .....	40
FIGURE 2.1. A SIMPLIFIED DIAGRAM OF THE BIPCON SYSTEM SHOWING THE RELATIONSHIP OF THE VARIOUS COMPONENTS. ....	42
FIGURE 2.2: EQUATION DETAILING THE MEASUREMENT OF A RESISTANCE POINT, AND THE SCHEMATIC DIAGRAM OF THIS RESISTANCE MEASUREMENT.....	44
FIGURE 2.3: CELL TYPES.....	46

FIGURE 2.4: THE PHILIPS PW 95 SERIES CELL. ....	47
FIGURE 2.5: THE SHINER CELL. ....	48
FIGURE 2.6: THE ELECTRODE HOUSING CONSTRUCTED FROM A MODIFIED YOUNG TAP, USED IN THE CELLS CONSTRUCTED AT THE UNIVERSITY OF ADELAIDE. ....	50
FIGURE 2.7: CELL DESIGN CONSTRUCTED AT THE UNIVERSITY OF ADELAIDE. ....	51
FIGURE 2.8: THE SIMPLIFIED CELL DESIGN, CONSTRUCTED AT THE UNIVERSITY OF ADELAIDE. ....	51
FIGURE 2.9: THE INSERT FOR THE ADELAIDE CELLS, UTILISING THE SPL SEALS. ....	52
FIGURE 2.10: PHOTOGRAPHIC AND SCHEMATIC REPRESENTATIONS OF THE BIPCON SUITE AT THE UNIVERSITY OF ADELAIDE. ....	58
FIGURE 2.11: PINACOLYL ( 2,2-DIMETHYL-2-BUTYL) BROSYLATE (12) ....	62
FIGURE 2.12: THE SOLVOLYSIS OF PINACOLYL BROSYLATE. ....	63
FIGURE 3.1. THE BIPCON STARTUP MENU. ....	68
FIGURE 3.2: THE MAIN MENU OF THE BIPREAD PROGRAM. ....	69
FIGURE 3.3: THE CHANNEL AND ACQUISITION MODE SELECTION MENU. ....	70
FIGURE 3.4: THE CALIBRATION PROGRAM WITHIN THE BIPREAD SOFTWARE. ....	71
FIGURE 3.5: PREVIOUSLY USED RUN NUMBER OPTIONS. ....	75
FIGURE 3.6: RUN SET-UP MENU. ....	76
EQUATION 3.1: THE RELATIONSHIP BETWEEN THE SPECIFIC CONDUCTIVITY AND THE CONCENTRATION OF THE SOLUTION. ....	77
EQUATION 3.2: THE FUOSS ONSAGER EQUATION. ....	78
EQUATION 3.3: A SIMPLIFIED VERSION OF THE FUOSS ONSAGER EQUATION. ....	78
FIGURE 3.7: CHANNEL 1 IS LOADED WITH THE RUN DATA FOR RUN NUMBER 1234.01 ....	81
FIGURE 3.8: RUN MODIFICATION OPTIONS. ....	82
FIGURE 3.9: THE DEFAULTS.TRN SETTINGS AS SHOWN IN THE DOS EDITOR. ....	84
FIGURE 3.10: THE TRANSHDR PROGRAM. ....	86
FIGURE 3.11: THE OPENING INFORMATION REQUIRED BY THE KINPROG PROGRAM. ....	87
FIGURE 3.12: EXTERNAL VARIABLES CAN BE MODIFIED FROM WITHIN THE KINPROG PROGRAM. ....	88
FIGURE 3.13: THE DATA SHOWN AT THE COMPLETION OF A KINPROG ANALYSIS. ....	90
FIGURE 4.1: THE SYNTHESIS OF PINACOLYL BROSYLATE (12). ....	93
FIGURE 4.2: PROPOSED 3-R-SUBSTITUTED ADAMANT-1-YL TOSYLATES FOR THE ENVISIONED KINETIC STUDY. ....	94
FIGURE 4.3: THE MAIN INTERCONVERSIONS UTILISED IN THE FORMATION OF THE REQUISITE TOSYLATES. ....	94
SCHEME 4.1: SIMPLIFIED SCHEME OF THE PROPOSED SYNTHESIS OF THE TOSYLATES 10, 15, 16, 17 AND 18 FROM ADAMANTANE (19). ....	95
SCHEME 4.2: SIMPLIFIED SCHEME OF THE PROPOSED SYNTHESIS OF THE TOSYLATES 11, 20, 21, 22 AND 23 FROM ADAMANTANE CARBOXYLIC ACID (24). ....	96
FIGURE 4.4: ATTEMPTED CONVERSION OF THE ALCOHOL 25 TO THE TOSYLATE 10 UTILISING TOSYL CHLORIDE, YIELDING THE CHLORIDE (6). ....	98

FIGURE 4.5: INTERCONVERSION OF THE BROMIDE (4) TO 1-PHENYL ADAMANTANE (26), AND SUB SEQUENTIAL TRANSFORMATION TO 3-PHENYL, 1-ADAMANTYL TOSYLATE (15)...	101
FIGURE 4.6: THE SYNTHETIC APPROACH TO THE SYNTHESIS OF THE TOSYLATES 16, 17 AND 18.....	103
FIGURE 4.7: SYNTHETIC APPROACH TO THE REQUIRED TOSYLATES 11 AND 23.....	104
FIGURE 4.8: OXIDATION OF 1-ADAMANTANE CARBOXYLIC ACID (24) FOLLOWED BY BROMINATION TO GIVE THE PRECURSOR 31 (VIA METHOD B).....	105
FIGURE 4.9: APPROACH TO 3-CYANO-1-ADAMANTANOL (35).....	107
FIGURE 4.10: REDUCTION OF THE ESTER 32 TO GIVE THE PRIMARY ALCOHOL 38, AND FURTHER TRANSFORMATION TO THE DESIRED SUBSTRATES 21 AND 22.....	109
FIGURE 5.1: 3-SUBSTITUTED 1-ADAMANTYL TOSYLATES, 7-ANTI-SUBSTITUTED 2-EXO AND 7-ANTI-SUBSTITUTED 2-ENDO NORBORNYL TOSYLATES.....	113
FIGURE 5.2: PLOTS OF LOG <i>K</i> FOR (I) 3-SUBSTITUTED 1-ADAMANTYL TOSYLATES, 7-ANTI- SUBSTITUTED 2-EXO AND 7-ANTI-SUBSTITUTED 2-ENDO NORBORNYL TOSYLATES V'S $\sigma_I$ .....	113
CHART 5.1: THE RABER HARRIS PLOT OF THE SOLVOLYSIS OF 1-ADAMANTYL TOSYLATE (10) VERSUS THE SOLVOLYTIC RATE FOR 1-ADAMANTYL BROMIDE (4).....	116
CHART 5.2: THE RABER HARRIS PLOT OF THE KINETIC RATE DATA GENERATED THROUGH THE SOLVOLYSIS OF 3-PHENYL-1-ADAMANTYL TOSYLATE (15) VERSUS THE SOLVOLYTIC RATE FOR 1-ADAMANTYL BROMIDE (4).....	117
CHART 5.3: THE RABER HARRIS PLOT OF THE KINETIC RATE DATA GENERATED THROUGH THE SOLVOLYSIS OF (3-[(TOSYL)OXY]-1-ADAMANTYL) METHYL ACETATE (22) VERSUS THE SOLVOLYTIC RATE FOR 1-ADAMANTYL BROMIDE (4).....	118
CHART 5.4: THE RABER HARRIS PLOT OF THE KINETIC RATE DATA GENERATED THROUGH THE SOLVOLYSIS OF (3-[(TOSYL)OXY]-1-ADAMANTYL) METHYL TOSYLATE (21) VERSUS THE SOLVOLYTIC RATE FOR 1-ADAMANTYL BROMIDE (4).....	119
CHART 5.5: THE RABER HARRIS PLOT OF THE KINETIC RATE DATA GENERATED THROUGH THE SOLVOLYSIS OF METHYL 3-[(TOSYL)OXY]-1-ADAMANTANE CARBOXYLATE (23) VERSUS THE SOLVOLYTIC RATE FOR 1-ADAMANTYL BROMIDE (4).....	120
CHART 5.6: THE RABER HARRIS PLOT OF THE KINETIC RATE DATA GENERATED THROUGH THE SOLVOLYSIS OF 3-CYANO 1-ADAMANTYL TOSYLATE (11) VERSUS THE SOLVOLYTIC RATE FOR 1-ADAMANTYL BROMIDE (4).....	121
TABLE 5.1: THE EXPERIMENTAL KINETIC RATE DATA COLLECTED FOR THE TOSYLATES 10, 11, 15, 21, 22 AND 23. IN ADDITION, THE GENERATED "M" VALUES AND THE $\sigma_I$ VALUES FOR THESE SUBSTRATES. THE $\sigma_I$ VALUES WERE OBTAINED FROM PROGRESS IN PHYSICAL ORGANIC CHEMISTRY. <sup>49</sup> .....	122
CHART 5.7: THE RABER HARRIS PLOTS OF THE TOSYLATES 10, 11, 15, 21, 22 AND 23 VERSUS <i>K</i> <sub>0</sub> , 1-ADAMANTYL BROMIDE (4).....	122
CHART 5.8 HAMMET PLOT OF THE RATE OF SOLVOLYSIS IN 80E OF TOSYLATES 10, 11, 15, 21, 22 AND 23 VERSUS THE $\sigma_I$ VALUE OF THEIR SUBSTITUENT.....	123
CHART 5.9 HAMMET PLOT OF THE RATE OF SOLVOLYSIS IN 97T OF TOSYLATES 10, 11, 15, 21, 22 AND 23 VERSUS THE $\sigma_I$ VALUE OF THEIR SUBSTITUENT.....	124

CHART 5.10 HAMMET PLOT OF THE RATE OF SOLVOLYSIS IN 70T OF TOSYLATES <b>11, 21, 22</b> AND <b>23</b> VERSUS THE $\sigma_I$ VALUE OF THEIR SUBSTITUENT. ....	124
CHART 5.11 HAMMET PLOT OF THE RATE OF SOLVOLYSIS IN 70E OF TOSYLATES <b>11, 15, 21,</b> <b>22</b> AND <b>23</b> VERSUS THE $\sigma_I$ VALUE OF THEIR SUBSTITUENT. ....	125
CHART 5.12: HAMMET PLOTS OF THE RATE OF SOLVOLYSIS IN 97T AND 80E OF TOSYLATES <b>10, 11, 15, 21, 22</b> AND <b>23</b> VERSUS THE $\sigma_I$ VALUE OF THEIR SUBSTITUENT. ....	126
TABLE 5.2: CORRELATION BETWEEN THE SEPARATION OF THE HAMMET PLOTS OF THE TOSYLATES <b>10, 11, 15, 21, 22</b> AND <b>23</b> IN 80E AND 97T WITH THE "M" VALUES FROM THEIR INDIVIDUAL RABER HARRIS PLOTS. ....	126
CHART 5.13: THE RELATIONSHIP BETWEEN THE DETERMINED "M" VALUES FOR THE TOSYLATES <b>3, 6, 21, 23, 18</b> AND <b>16</b> AND THE $\sigma_I$ VALUES OF THEIR SUBSTITUENTS. ....	127
CHART 5.14: HAMMET PLOTS OF THE RATES OF SOLVOLYSIS IN 97T, 70T, 70E AND 80E OF THE TOSYLATES <b>10, 11, 15, 21, 22</b> AND <b>23</b> VERSUS THE $\sigma_I$ VALUE OF THEIR SUBSTITUENTS. ....	128
FIGURE 6.1: RELATIVE RATES OF SOLVOLYSIS OF SOME BRIDGEHEAD SUBSTITUTED HALIDES, RELATIVE TO <i>T</i> -BUTYL BROMIDE, MEASURED IN 80E AT 25°C. ....	133
FIGURE 6.2: "PLOTS OF THE FREE ENERGIES OF SOLVOLYSIS ( $\Delta G^\ddagger$ ) VERSUS STRAIN ENERGY DIFFERENCES BETWEEN CATION AND PARENT HYDROCARBON ( $\Delta E_S(R^+ - RH)$ ) FOR THE SYSTEMS OF INTEREST." <sup>21</sup> ....	134
FIGURE 6.3: THE ORBITAL INTERACTIONS BETWEEN C <sup>1</sup> AND C <sup>3</sup> (N=1-3) ( <b>47</b> : N=1 <b>48</b> : N=2 <b>49</b> : N=3) ....	135
FIGURE 6.4: 3-METHOXY CARBOXYLBICYCLO[2.1.1]HEXYL TRIFLATE ( <b>50</b> ) AND 1- BROMOBICYCLO[3.1.1]HEPTANE ( <b>46</b> ) ....	136
FIGURE 6.5: THE TWO POSSIBLE PATHWAYS AND PRODUCTS AVAILABLE FOR THE SOLVOLYSIS OF THE 1,3-DISUBSTITUTED BICYCLO[1.1.1]PENTANES. ....	137
FIGURE 6.6: TRAPPING OF THE INTERMEDIATE CARBOCATION FROM THE IONISATION OF 1,3-DIODOBICYCLO[1.1.1]PENTANE ( <b>54</b> ). ....	138
FIGURE 6.7: ORIGINALLY PROPOSED RADICAL MECHANISM <sup>70</sup> ....	139
FIGURE 6.8: CARBOCATION MECHANISM, SHOWING FORMATION OF (I) TRAPPED BRIDGEHEAD CARBOCATION WITH A GIVEN NUCLEOPHILE ( <b>53</b> ) AND (II) REARRANGED PRODUCT ( <b>52A/B</b> ) ....	140
FIGURE 6.9: PREPARATION OF [1.1.1]PROPELLANE ( <b>58</b> ) FROM 1,1-DIBROMO-2,2- <i>BIS</i> (CHLOROMETHYL)CYCLOPROPANE ( <b>60</b> ) ....	140
FIGURE 6.10: QUANTITATIVE FORMATION OF THE 1,3-DIIDO BICYCLO[1.1.1]PENTANE ( <b>54</b> ) FROM THE REACTION OF [1.1.1]PROPELLANE ( <b>58</b> ) WITH IODINE. ....	141
FIGURE 6.11: PREPARATION OF 1,3-DIBROMOBICYCLO[1.1.1]PENTANE ( <b>59</b> ) THROUGH THE REACTION OF [1.1.1]PROPELLANE ( <b>58</b> ) WITH BROMINE, IN THE PRESENCE OF LITHIUM BROMIDE. ....	142
FIGURE 6.12: SYNTHESIS OF 1-BROMO, 3-IODOBICYCLO[1.1.1]PENTANE ( <b>62</b> ). ....	144
FIGURE 6.13: FORMATION OF 1-BROMO, 3-CHLOROBICYCLO[1.1.1]PENTANE ( <b>64</b> ). ....	146
FIGURE 6.14: PREPARATION OF 1-CHLORO, 3-IODOBICYCLO[1.1.1]PENTANE ( <b>67</b> ). ....	147

FIGURE 6.15: THE ATTEMPTED SYNTHESIS OF 1-BROMO, 3-IODOBICYCLO[1.1.1]PENTANE (62), THROUGH THE REACTION OF [1.1.1]PROPELLANE (58) AND BROMINE, IN THE PRESENCE OF LITHIUM IODIDE. ....	148
FIGURE 6.16: FORMATION OF 1-AZIDO, 3-IODOBICYCLO[1.1.1]PENTANE (56). ....	149
FIGURE 6.17: THE REACTION BETWEEN [1.1.1]PROPELLANE (58) AND IODINE MONOCHLORIDE. ....	149

## Abstract:

The relationship between the rate of solvolysis and the withdrawing nature of any substituent for remotely substituted "model  $S_N1$ " substrates is well understood. The correlation between these molecular characteristics as described through a linear Hammett plot, has been shown to be true in a great many systems. Equally a linear correlation for these systems can be seen between their rate of solvolysis and that of the "model  $S_N1$  system" 1-bromo adamantane, in a range of binary solvent systems providing a spectrum of solvent ionising strengths and nucleophilicities, thus indicating that they undergo solvolysis via the same mechanistic pathway, and thus all show  $S_N1$  character.

However, previously detailed analysis of the effect of remote substituents on this Raber Harris correlation has not been shown.

This thesis details such a study, including the development of the BIPCON Suite at the University of Adelaide, utilised in the conductometric analysis of the solvolyses of a series of 3-substituted adamantyl 1-tosylates in a range of solvents.

The observed decrease in the degree of effect of the solvent ionising strength on the solvolysis of these substrates as the electron withdrawing nature of the remote substituent increased will be shown, and potential explanations for this unexpected decrease in  $S_N1$  character given.

Furthermore, the synthesis of some kinetically interesting 1,3-disubstituted bicyclo[1.1.1]pentanes, through the trapping of the intermediate bridgehead cation will be discussed.

**Statement of Originality:**

This work contains no material which has been accepted for the award of any degree or diploma in any university or other tertiary institution and, to the best of my knowledge and belief, contains no material previously published or written by another person except where due reference has been made in the text

I give consent to this copy of my thesis, when deposited in the University library, being available for loan and photocopying.

Date: 18/12/2001.....

Ian R. Milne



## Acknowledgements:

This thesis, and the research that it represents could not have been completed without the friendship, love and support of many people. Unfortunately, I am unable to thank many of them individually here, as I fear the acknowledgements would outweigh the rest of the thesis. There are however, certain people that I wish to thank specifically, for without them my Ph.D. would never have been completed.

I wish to thank Dr. Dennis Taylor, for taking me on as his first Ph.D. student, and providing guidance, support and supervision throughout this project. This Ph.D. has presented us with many challenges, and I would like to take this opportunity to thank Dennis for the many hours of work he has put into solving these problems with me.

In addition, the assistance and guidance of members of the academic and technical staff of the Department of Chemistry has been invaluable in the completion of this project. I wish to acknowledge the continued support of Dr. George Gream, Dr. Simon Pyke and Dr. Geoff Crisp throughout my Ph.D. Each has been called on numerous times for advice in many facets of chemistry and have always been willing to help in any way possible.

Due to the developmental nature of this project, it would have been impossible without the skills and inventiveness of the technical staff. To Tony Snigg, Barry, Hyde-Parker, Peter Apoefis and Brendon Edwards go my heart felt thanks for creating, reviving, repairing and generally nursing the various equipment that has been required to carry out the research detailed in this thesis. The greeting of "What have you broken this time?" still brings a smile to my face.

Likewise the skills of Phil Clements, Jeff Borkent and Andrew Johnson in the areas of NMR spectroscopy and general computing have been essential in every part of this project. Thanks especially go to Phil, who allowed me to justify my Star Wars customisable card game addiction by sharing the desire to collect and play this very expensive habit. In a similar way, thanks to Simon, Andrew and Jeff for the discussions on Macintosh computers, and helping me defend the purchase of the PowerMac this thesis was created with.

I would like to thank all of the friends I have made in the Department, especially in the research labs where I have worked. Having someone to talk to while you wait for a distillation or reaction to finish is a gift far greater than can be imagined. Also to all the members of the Taylor Research Group, thanks for your help and sympathy throughout this project, especially in the developmental stages of the BIPCON Suite, when the name of the system was considered more often than not, a swear word. For all the coffee breaks, long lab lunches, pub crawls, touch football games and especially "borrowed" glassware you have my ongoing thanks.

To the friends who have watched and waited for the completion of this thesis, thanks for the support and encouragement you have given me over the last few years. Especially to the guys from DBFC, your ongoing support, and the occasional soccer game have kept me smiling, and I appreciate it.

To my family, for putting up with having a perpetual student on your hands while I have been completing this project go me deepest thanks. You have shown me love and support at times when I needed it most and deserved it least, and I would have been unable to complete this without your love.

Finally, to Katherine, I just want to say "I love you."

## Chapter 1

### Introduction and Development of Hypothesis.

*Abstract:*

Historically, through the use of solvolysis, a greater understanding of the  $S_N1$  mechanism has been achieved. There have been multiple systems have been utilised as "model"  $S_N1$  substrates, in order to probe the effects of various conditions on the  $S_N1$  mechanism. For many years, the adamantyl system has provided a suitable "model" for these experiments. This system will now be used to investigate the effect of changes in the electron withdrawing nature ( $\sigma_I$ ) of a remote substituent on an  $S_N1$  system, on the response of the substrate to the ionising strength of the solvent (" $m$ ").

## 1.1 Introduction.

There has traditionally been significant interest in the elucidation of reaction mechanisms, not only to determine the reaction steps of the system observed, but to use this knowledge to predict the results of other related systems.

As with all fields of chemistry, advancement in mechanistic theory is crucial. The continual development of proposed mechanistic processes is essential to gaining a clearer understanding of the pathways by which chemical transformations occur. In seeking this understanding, much valuable information can be gained through an understanding of the kinetics of the reaction. Through an understanding of the kinetics of the reaction, we can observe the energetics of the reaction system, probe what species in the reaction mixture is participating, and determine the order of this participation in the reaction and use this information to determine likely outcomes for the reaction studied and others similar.

In this way, an understanding of the kinetics of a reaction can help categorise a reaction into a mechanistic type. For example, the kinetics involved with an  $S_N1$  or E1 reaction are clearly different from those of an  $S_N2$  or E2 reaction (Figure 1.1).

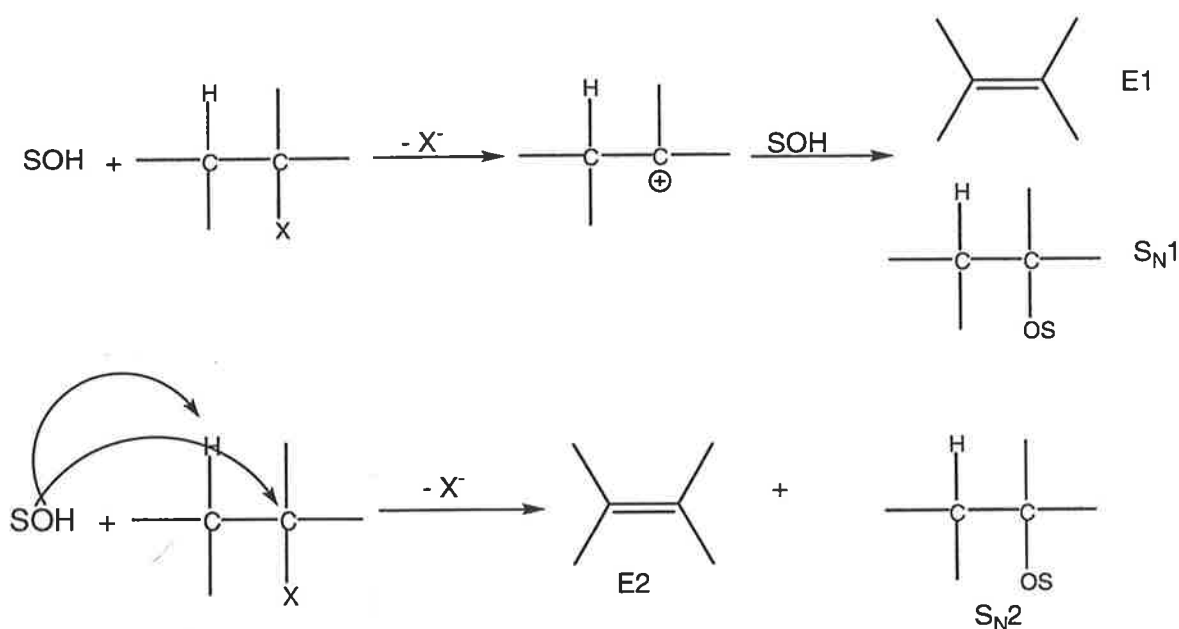


Figure 1.1: The traditional mechanistic description of the solvolytic process.<sup>1</sup>

The rate of reaction for the  $S_N1$  or E1 mechanisms would not be influenced by the concentration of the nucleophile, but only of the starting reagent. This

unimolecular ionisation would thus be easily differentiated from the bimolecular rate associated with the  $S_N2$  and E2 reaction types.

Kinetic experiments also allow us to probe the effect of steric hindrance, modification of the solvent system, leaving group stability, conformational isomers and other similar changes to the reaction that may alter the mechanism.

### 1.1.1 The $S_N1$ / $S_N2$ Reaction Classification.

Of particular importance to this body of work has been the classification of the  $S_N1$  and  $S_N2$  reactions (Figure 1.2).

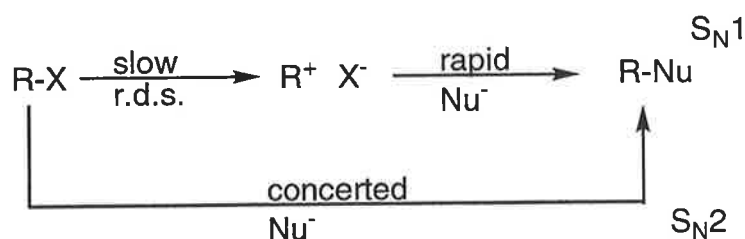


Figure 1.2: The traditional view of the  $S_N1$  and  $S_N2$  processes.

Through an understanding of the available rate data, significant insights into the mechanistic pathways involved with these reactions could be made.<sup>2</sup> Subtle changes to the solvent system, concentration of nucleophiles present, substitution patterns on the reagent or the leaving group would allow us to elucidate considerable information regarding the mechanistic pathway of the reaction.

If the reaction was following an  $S_N1$  mechanism, then structural features that would stabilise the formation of the carbocation would accelerate the rate determining ionisation step. Thus, modification of electron withdrawing nature of any substituents on the system will significantly effect the rate of an  $S_N1$  reaction. However, changes in the concentration of nucleophile present in the reaction mixture will have no effect on a pure  $S_N1$  reaction. The presence of sterically hindering groups on the substrate would have little effect on the rate of an  $S_N1$  reaction, as compared to the  $S_N2$  process, as the carbocation would approach a planar formation, reducing the effect of these groups on the trapping by the nucleophile.

For an  $S_N2$  reaction, changes in the electron withdrawing nature of any substituents will have very little effect on the rate, as these reactions proceed with little or no charge build up. The concentration of nucleophiles present in the reaction mixture will, however, have a direct effect on the rate, as it is the rear side attack of a nucleophile to the system with the concerted loss of a leaving group that defines an  $S_N2$  reaction. Further, sterically hindering groups would significantly reduce the rate of the reaction, as the nucleophile would be prevented from approaching the rear face of the substrate for attack.

Thus, these two reaction mechanism could be easily differentiated through their kinetic response to modification of the reaction conditions.

### **1.2 The Solvolytic Reaction.**

A favoured approach for probing the  $S_N1$  mechanism has been to conduct solvolyses. A solvolytic reaction is one where the ionisation occurs in a solvent which provides the nucleophile. In this way, the concentration of the nucleophile can be assumed to be constant, and thus allows us to observe pseudo-first order kinetics.

This is particularly important, as categorising reactions as  $S_N1$  or  $S_N2$  can be fraught with danger, as in solution many reactions fall between the two extremes that define these mechanistic types noted in text books. A more accurate picture of the reaction is shown below (Figure 1.3).

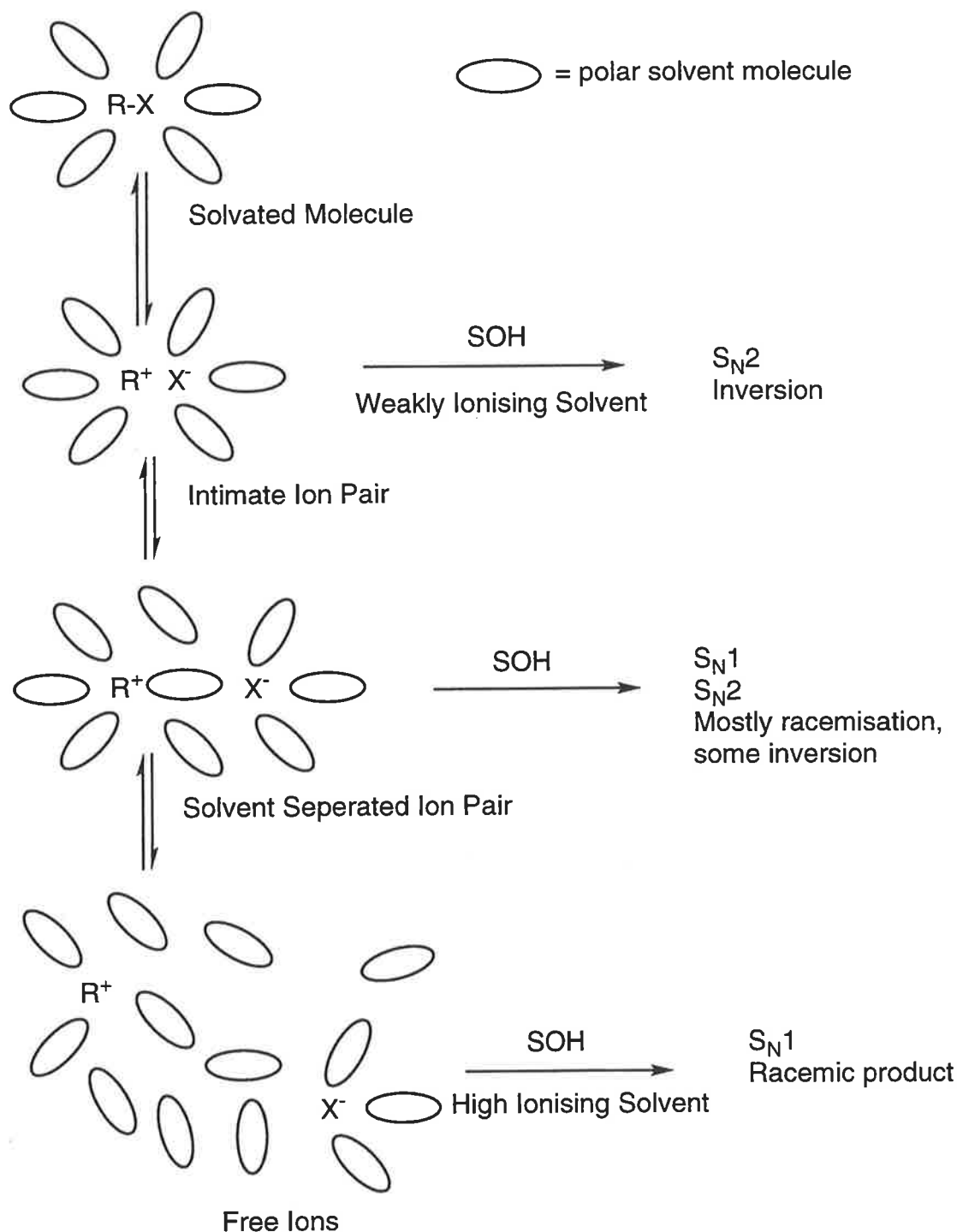


Figure 1.3: "Species proposed as intermediates in solvolysis reactions."<sup>2</sup> Figure adapted from "Perspectives on Structure and Mechanism in Organic Chemistry."<sup>2</sup>

In a solvolysis reaction the substrate undergoes ionisation followed by trapping with a solvent molecule. The products and their stereochemistry are determined by the extent to which the ionisation occurs. At the formation of a tight ion pair, the close interaction of the ions results in the only available approach for the nucleophile to the carbocation is from the rear face, which results in the formation

of the stereochemically inverted products associated with an  $S_N2$  mechanism. However, if this tight ion pair becomes separated by a solvent molecule, the interaction between the ions pair is reduced. This reduced influence between the ions allows the cation to be trapped from all faces, however, the presence of the anion will result in a slightly higher proportion of the inverted product in the mixture of stereoisomeric products. Further ionic separation prior to trapping of the cation would result in the formation of free ions, where the ions no longer have any influence on each other. With the formation of free ions, trapping of the cation will result in a completely racemic mixture of stereoisomers traditionally associated with an  $S_N1$  mechanism.

For a given substrate, modification of the solvent ionising strength and nucleophilicity can be used to probe which pathway the solvolysis of the substrate and the intermediates involved, will follow. The use of binary solvent systems, based on either aqueous ethanol or aqueous 2,2,2-trifluoroethanol mixtures, provides the ability to control the extent of the solvents ionising strength or nucleophilicity. As described in further detail later in this chapter, through modification of the amount of water in these binary solvent systems allows us to monitor the effect of changes in either the nucleophilicity or the ionising strength of the solvent alone, which provides significant insights into the kinetics of the reaction, and consequently the mechanism.

The use of substituent effects, especially the electron withdrawing nature of substituents on the substrate also allow us to probe this transition between the  $S_N1$  and  $S_N2$  mechanisms. Through the construction of Hammett relationships between the rate of solvolysis of the substrate and the electron withdrawing nature of its substituent ( $\sigma_I$ ) it is possible to observe if changes in the substituent effect the rate, and whether this effect is consistent across a range of substituents. Through modification of the reaction conditions in this way, it is possible to drive the reaction through particular mechanistic pathways, which allows us to ascertain the extent to which the substrate undergoes these solvolytic processes in various reaction environments.



### 1.2.1 Significant Developments Elucidated Through the Analysis of Solvolytic Reactions.

Historically analysis of solvolytic reactions have been used to probe the effect on the mechanism of multiple structural characteristics of the substrate systems, including strain energy, hyperconjugation and inductance, remote substituent effects, deuterium isotope effects, resonance and fragmentation, steric hindrance about the cation centre and leaving groups effects.<sup>2-6</sup> Through the study of these effects, a greater understanding of the relationship between the mechanism of the reaction and its kinetics was established. However, as many of these effects were not directly investigated in this project, they will not be discussed in significant detail in this thesis, except where appropriate.

### 1.2.2 The Grunwald-Winstein Correlation

It was through the analysis of the solvolysis of *t*-butyl chloride (1) that Grunwald and Winstein developed their description of the effect of solvent ionising strength on the rate of solvolysis.<sup>7</sup>

From this study, the authors developed the "Y" scale of solvent ionising power. The rate of the solvolysis of *t*-butyl chloride (1) was measured in the solvent of interest, and compared to the rate observed in the binary solvent mixture 80% ethanol in water (80E). In this way "Y" could be expressed (Equation 1.1).

$$Y = \log(k^{t\text{-Bu-Cl}} / k_0^{t\text{-Bu-Cl}})$$

Y = solvent ionising strength.

$k^{t\text{-Bu-Cl}}$  = rate of solvolysis of *t*-Bu-Cl in the solvent of interest at 25°C.

$k_0^{t\text{-Bu-Cl}}$  = rate of solvolysis of *t*-Bu-Cl in 80E at 25°C.

Equation 1.1: The relationship used in the development of the scale of solvent ionising strengths, based on the solvolysis of *t*-butyl chloride (1).

Through the development of this scale, further analysis of other reactions was made possible. The solvolysis of any other substrate could be described utilising this scale of solvent ionising strength (Equation 1.2).

$$\log (k_s/k_0) = m Y_s$$

$Y_s$  = solvent ionising strength of solvent  $s$ .

$k_s$  = rate of solvolysis of the substrate in solvent  $s$ .

$k_0$  = rate of solvolysis of the substrate in 80E.

$m$  = the response of the substrate to the ionising strength of the solvent.

Equation 1.2: The Grunwald-Winstein equation: Relationship between the rate of solvolysis of any substrate and the solvent ionising strength ( $Y$ ) based on the solvolysis of *t*-butyl chloride (1).

Grunwald and Winstein later expanded their description of these solvolytic processes with the inclusion of a description of the solvent nucleophilicity and its effect on the substrate (Equation 1.3).<sup>8,9</sup>

$$\log (k_s/k_0) = l N_s + m Y_s$$

$N_s$  = solvent nucleophilicity.

$Y_s$  = solvent ionising strength of solvent  $s$ .

$k_s$  = rate of solvolysis of the substrate in solvent  $s$ .

$k_0$  = rate of solvolysis of the substrate in 80E.

$m$  = the response of the substrate to the ionising strength of the solvent.

$l$  = the response of the substrate to the nucleophilicity of the solvent.

Equation 1.3: The expanded Grunwald-Winstein equation: Relationship between the rate of solvolysis of any substrate and the solvent ionising strength ( $Y$ ) and the nucleophilicity ( $N$ ) based on the solvolysis of *t*-butyl chloride (1).

The authors based this relationship on the solvolysis of *t*-butyl chloride, for which they assumed that the rate was solely due to the ionising strength of the solvent. Consequently for *t*-butyl chloride (1) " $m$ " was given the value of unity, and " $l$ " the value of zero, since the tertiary structure of the precursor was expected to preclude totally the possibility of any  $S_N2$  character. Any other substrate systems could then be related to *t*-butyl chloride (1) by their values for " $m$ " and " $l$ ". All  $S_N1$  reactions could be expected to have " $m$ " values close to unity and an " $l$ " value

of zero. The “*m*” value would be seen to decrease as the amount of S<sub>N</sub>2 character in solvolysis increased, while the “*l*” value would increase.

### 1.2.3 Refinement of the Description of Solvolytic Processes.

With the expansion of their equation, Grunwald and Winstein provided the first description of solvolytic processes in a quantitative fashion. This allowed considerable advances in the understanding of how the properties of the precursors and intermediate structures as well as the nature of the solvent medium influenced the kinetics of organic reactions.

There were however discrepancies observed when comparing the rates of solvolysis in strongly nucleophilic solvents.<sup>6,10,11</sup> Shiner had observed that the rate of solvolysis of *t*-butyl chloride (1) was unexpectedly accelerated with an increase in the nucleophilicity of the solvent, when carried out in 2,2,2-trifluoroethanol based binary solvent mixtures.<sup>6</sup> Schleyer and co-workers also noted that when compared to the solvolysis of polycyclic alkanes that were also identified as “model” S<sub>N</sub>1 substrates.<sup>12</sup> *t*-butyl chloride (1) exhibited an accelerated rate of solvolysis in nucleophilic solvents.<sup>10,11</sup>

From the solvolysis of 2-adamantyl tosylate (2), Schleyer noted that the “*m*” value for *t*-butyl chloride (1) elucidated from this new model system had a value of 0.5. This value, significantly removed from the value of unity anticipated for a unimolecular solvolysis, provided evidence of the participation of nucleophilic assistance during the ionisation of *t*-butyl chloride (1).<sup>5</sup> For comparison, the solvolysis of methyl tosylate (3), known to undergo bimolecular solvolysis, was also carried out. The “*m*” value associated with this “model” S<sub>N</sub>2 substrate was determined to be 0.3, indicating that the ionising strength of the solvent was still important in the solvolysis of S<sub>N</sub>2 substrates,<sup>5</sup> however, the rate was strongly dependant on the nucleophilic strength of the solvent.

Raber and Harris postulated that through analysis of the rate of solvolysis of any substrate in a range of solvents, which provided a spectrum of ionising and nucleophilic strengths, the extent of nucleophilic assistance occurring during solvolysis could be observed. If the assumption that a unimolecular solvolysis would provide an “*m*” value close to unity, while a pure S<sub>N</sub>2 solvolysis would show an “*m*” value  $\leq 0.3$ , then analysis of the “*m*” value for a solvolysis reaction

would provide information concerning the effect of the nucleophilicity of the solvent on the solvolysis.<sup>1</sup>

In order to prepare the solvent systems required to investigate this proposed correlation, ethanol (E) and 2,2,2-trifluoroethanol (TFE) were utilised. "Aqueous TFE and aqueous ethanol are quite different solvent systems. Ethanol and water are both highly nucleophilic, but water has a much greater ionising power; consequently, for aqueous ethanol increasing ethanol content produces a sharp decrease in ionising power accompanied by essentially unchanged nucleophilicity. In contrast, water is far more nucleophilic than TFE, although both solvents have high ionising power; consequently, an increase in TFE content in aqueous TFE produces a sharp decrease in the nucleophilicity accompanied by essentially unchanged ionising power."<sup>1</sup> (Figure 1.4).

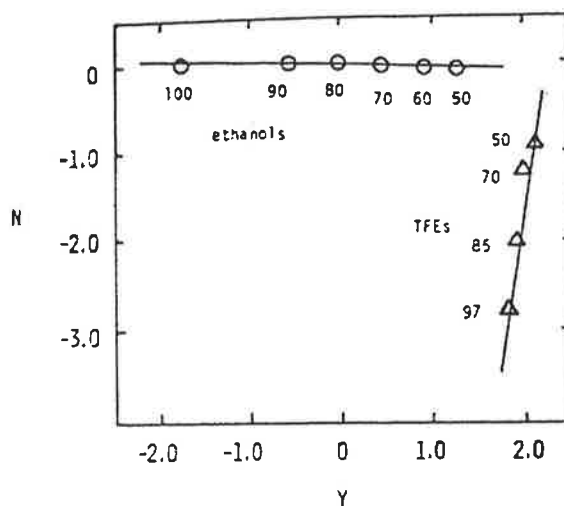


Figure 1.4: "A plot of solvent nucleophilicity (N) against solvent ionising power (Y, based on 2-adamantyl tosylate (2)) for aqueous ethanol and aqueous 2,2,2-trifluoroethanol. The numbers near the points refer to the percentage of nonaqueous component in the solvent mixtures". Figure and description from reference.<sup>1</sup>

The authors noted that for the solvolysis of a range of suitably substituted polycyclic substrates, the logarithmic plot of the rate of solvolysis of the substrate, versus the logarithmic plot of the rate of solvolysis of 1-adamantyl bromide (4), produced a single linear correlation. The slope of this line, which equated to the "m" value for the solvolysis, was observed to be close to unity for these model S<sub>N</sub>1 substrates. However, with the solvolysis of 2-propyl brosylate (5), or any other

substrate effected by the solvent nucleophilicity, the resulting Raber-Harris plot was seen to fragment (Figure 1.5).

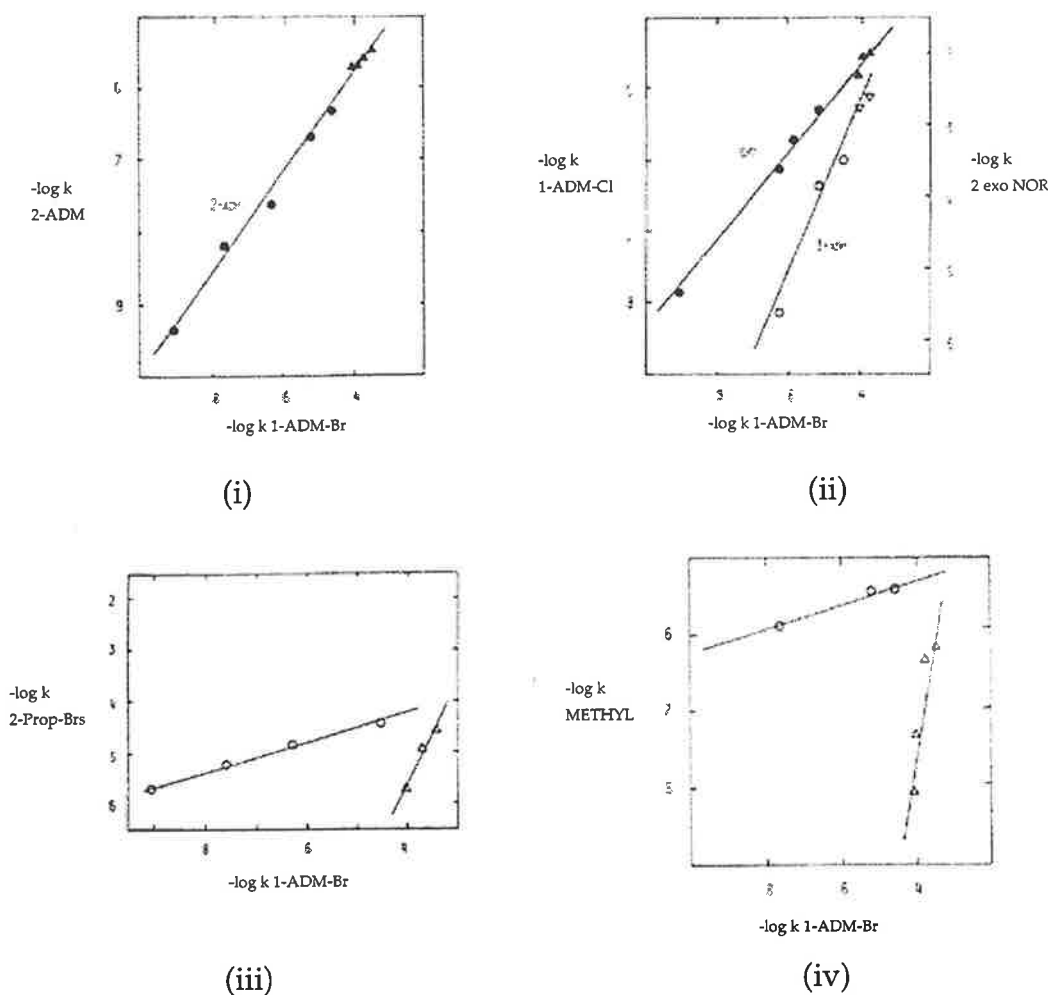


Figure 1.5: (i) Raber-Harris plot of 2-adamantyl tosylate (2) versus 1-adamantyl bromide (4).

(ii) Raber-Harris plots of (open symbols) 1-adamantyl chloride (6) and (closed symbols) *exo*-2-norbornyl tosylate versus 1-adamantyl bromide (4).

(iii) Raber-Harris plot of 2-propyl brosylate (5) versus 1-adamantyl bromide (4).

(iv) Raber-Harris plot of methyl tosylate (3) versus 1-adamantyl bromide (4).

Figures and text from adapted from reference.<sup>1</sup>

Consequently, it was possible, through the construction of a Raber-Harris plot of the rates of solvolysis for any substrate in a range of solvents to observe the extent of nucleophilic assistance in the solvolysis. The authors described an  $S_N1$  solvolysis as one where, the slope and intercept obtained from both ethanol and 2,2,2-trifluoroethanol based solvents were equal, and the slope (" $m$ ") close to unity. For an  $S_N2$  solvolysis, the observed slope and intercept from the ethanol

based solvents, should be less than those observed for the 2,2,2-trifluoroethanol based solvents, and consequently give a fragmented graph.<sup>1</sup>

#### **1.2.4 Identification of the S<sub>N</sub>2 Nature of the Solvolysis of *t*-Butyl Halides and the Development of Additional Scales of Solvent Ionising Strength.**

While the solvolysis of *t*-butyl chloride (1) was acknowledged as anomalous by previous authors, the solvent ionising scales developed by Grunwald and Winstein remained in use. It had been assumed that the accelerated rate of solvolysis of the *t*-butyl halides was due to rate-limiting elimination,<sup>6,12</sup> however, investigation by Bentley and Carter questioned this assumption. They found that through manipulation of the solvent systems, the effect of the solvent nucleophilicity on the *t*-butyl system could be closely monitored.

They confirmed that the adamantyl system was "insensitive to solvent nucleophilicity,"<sup>13</sup> and as such would be "very good models for S<sub>N</sub>1 behaviour."<sup>13</sup> The adamantyl system was also favoured as it further simplified the investigation of remote substituent effects on the mechanism, through the exclusion of elimination products, being disfavoured due to ring strain. Additionally, classical S<sub>N</sub>2 processes are not possible due to the polycyclic nature of the substrate.

1-Adamantyl chloride (6) was thus, used to generate a scale of solvent ionising power, designated Y<sub>Cl</sub>. A direct comparison of Y<sub>Cl</sub> to the classical Y scale of Grunwald and Winstein yielded an interesting result (Figure 1.6)

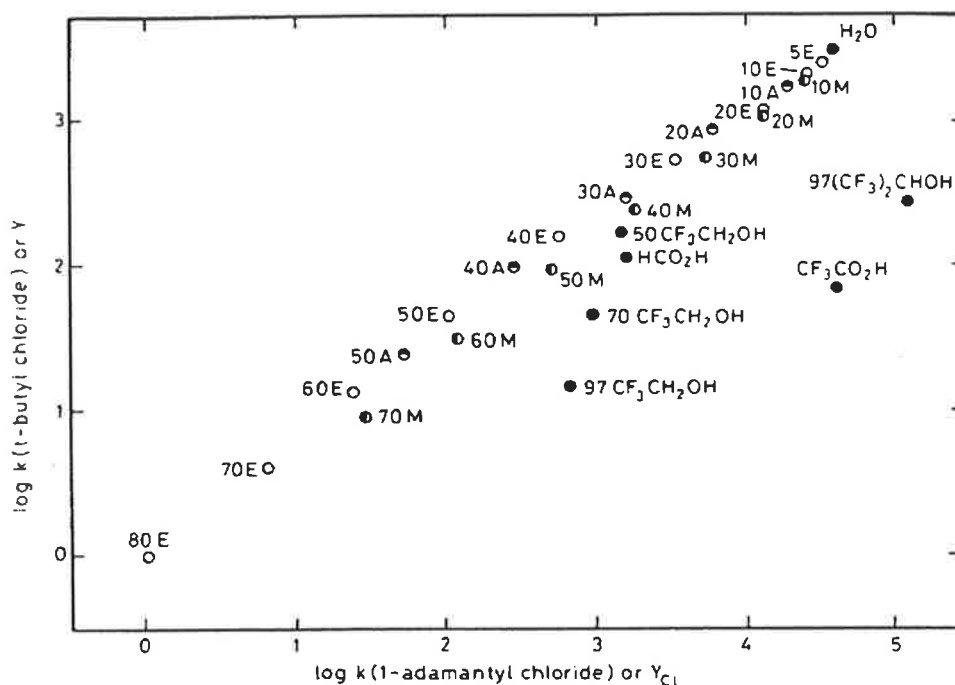


Figure 1.6: "Correlation of logarithms of solvolysis rates for 1-adamantyl chloride (6) vs. *tert*-butyl chloride (1) at 25°C." Figure and description from reference.<sup>13</sup>

From this comparison, it was observed that in the presence of nucleophilic solvents, the solvolysis of *t*-butyl chloride was three thousand times faster than in non-nucleophilic solvents. This clear sensitivity to nucleophilicity, allowed the authors to conclude that all available evidence led to the interpretation of the solvolysis of *t*-butyl chloride (1) via a nucleophilically assisted ionisation mechanism.<sup>13</sup>

Through their investigation, Bentley and Carter also identified the need to generate solvent ionising scales appropriate to the leaving group of interest. Changes in the solvent effects on the leaving group could significantly skew the interpretation of the results if an inappropriate Y scale was utilised. The authors detailed solvent ionising scales based on 2-adamantyl tosylate (2) ( $Y_{OTs}$ ), 1-adamantyl bromide (4) ( $Y_{Br}$ ) and 1-adamantyl chloride (6) ( $Y_{Cl}$ ),<sup>5,13</sup> and there have been further scales prepared by other researchers since.

### 1.2.5 The Effect on the Rate of Solvolysis of the 1-Adamantyl System with Substitution at the 3-Position.

The 1-adamantyl system had been shown to solvolysis via an  $S_N1$  mechanism for all leaving groups studied. Grob and co-workers were interested to see if this  $S_N1$  character of the solvolysis was consistent throughout a range of substitutions at the 3-position.<sup>14,15</sup> Through analysis of a wide range of 3-substituted 1-adamantyl tosylates, Grob observed a linear Hammett relationship between the rates of solvolysis of these substituents in 80E and the  $\sigma_I$  values of their respective substituents (Figure 1.7).

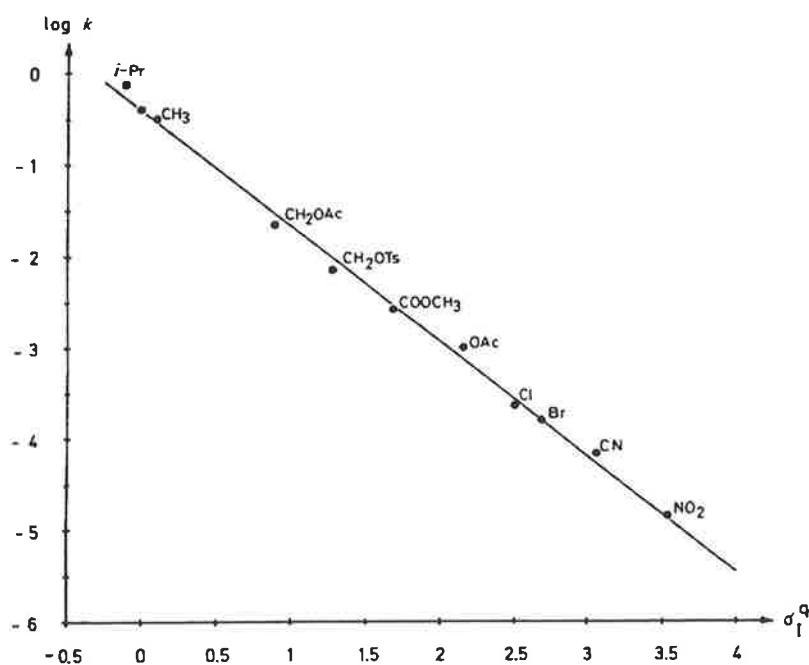


Figure 1.7: "Plot of  $\log k$  for 3-substituted 1-adamantyl toluenesulfonates vs. inductive substituent constants  $\sigma_I^q$ " in 80E at 25°C. Figure and description from reference.<sup>14</sup>

As anticipated, there was a proportional decrease in the rate of solvolysis with an increase in the electron withdrawing nature of the substituent. This linear relationship provided clear evidence that the mechanism of solvolysis for these substituted adamantyl tosylates was consistent, regardless of the substitution, and that the rate of solvolysis controlled by the withdrawing nature of the substituent ( $\sigma_I$ ) alone.



The combination of this finding, and those of Raber and Harris, allowed for the confident assignment of  $S_N1$  character to the solvolysis of these 3-substituted 1-adamantyl tosylates. Further confirmation came through the analysis of the solvolysis of these 3-substituted 1-adamantyl tosylates in 97T, which again showed a linear relationship when plotted against the  $\sigma_I$  values for the substituents (Figure 1.8).<sup>16</sup>

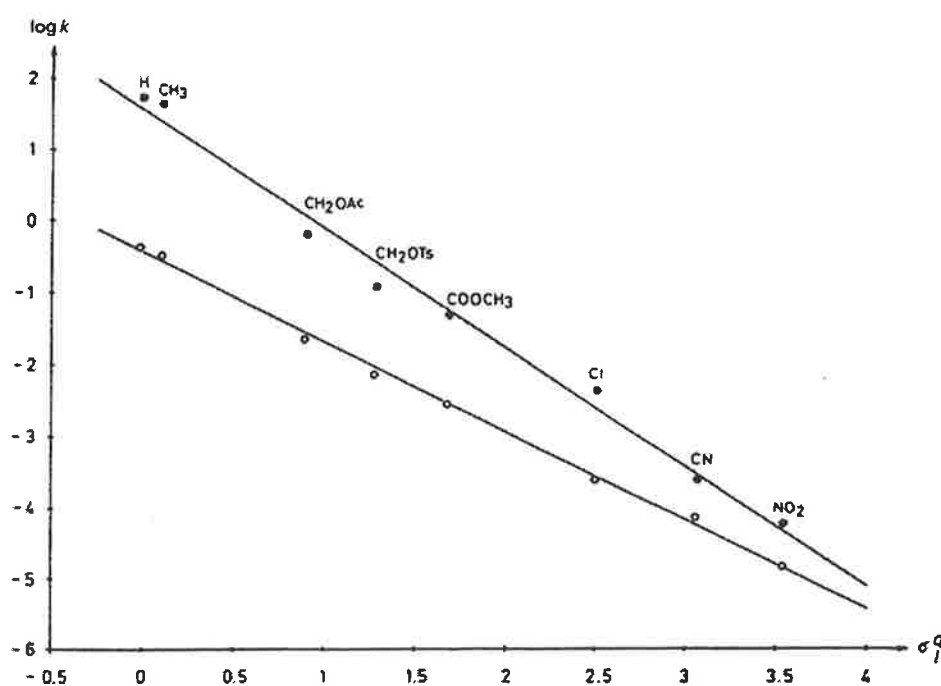


Figure 1.8: "Plots of  $\log k$  for 3-substituted 1-adamantyl *p*-toluenesulfonates in 97% TFE (filled circles) and 80% EtOH (open circles) vs.  $\sigma_I$ ." Figure and description from reference.<sup>16</sup>

This linear correlation, indicated that in both 80E and 97T, the solvolysis of the 1-adamantyl substrates proceeded via the same mechanism, regardless of the substitution at the three position. However, the authors did not comment on the significance of the change in slope of the two plots, in changing from a nucleophilic to a non-nucleophilic solvent system.

### 1.3 Comparison to Other Polycyclic Alkanes.

With the development of the use of the 1-adamantyl system as the model  $S_N1$  substrate for the description of solvolytic processes, the investigation of other polycyclic alkanes were carried out by a range of research groups. These polycyclic alkanes, due to their caged shape were expected to exhibit similar

results to the solvolysis of the 1-adamantyl system, as their caged structure would once again prevent rear side nucleophilic "attack" by the solvent, and the strain energy associated with the cage would discourage elimination process. The solvolyses of a large range of polycyclic alkanes has been carried out. In the vast majority of cases, it has been found that the solvolyses of these systems was reliant solely on the ionising power of the solvent. The differences in the rate of solvolysis for these systems could be directly correlated with the strain energy associated with the formation of a non-planar carbocation, as shown in independent studies by Müller and Della.<sup>3,17-23</sup>

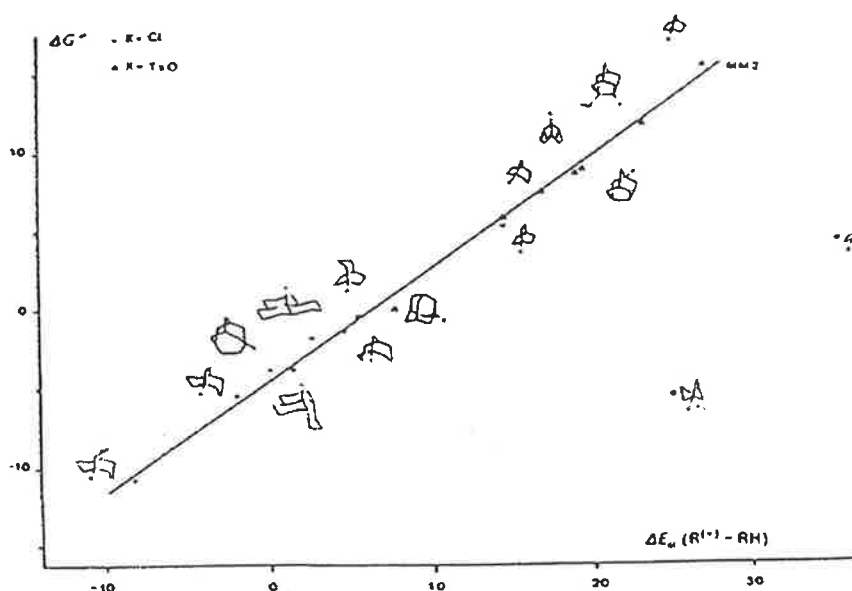


Figure 1.9: "Plot of the free energies of solvolysis versus the MM2 calculated strain energy difference ( $\Delta E_s(R^+-RH)$ )."<sup>4</sup> Figure and description from reference.<sup>4</sup>

While this correlation held for most of the polycyclic alkane systems studied, the [n,1,1]bicyclo alkanes (n=1,2,3) showed an unexpected acceleration in their rate, based on strain energy alone. This behaviour resulted in significant, and ongoing interest into the solvolysis of these systems, as discussed further in chapter six. It was through the solvolysis of some bicyclo[1.1.1]pentanes that Taylor observed an interesting effect of remote substitution on the solvolysis.<sup>22</sup> Following the solvolysis of a series of 3-substituted bicyclo[1.1.1]pentyl bromides in a range of binary solvent systems, the generation of Raber-Harris plots yielded linear correlations for these solvolyses when compared to that of 1-adamantyl bromide (4) (Figure 1.10).

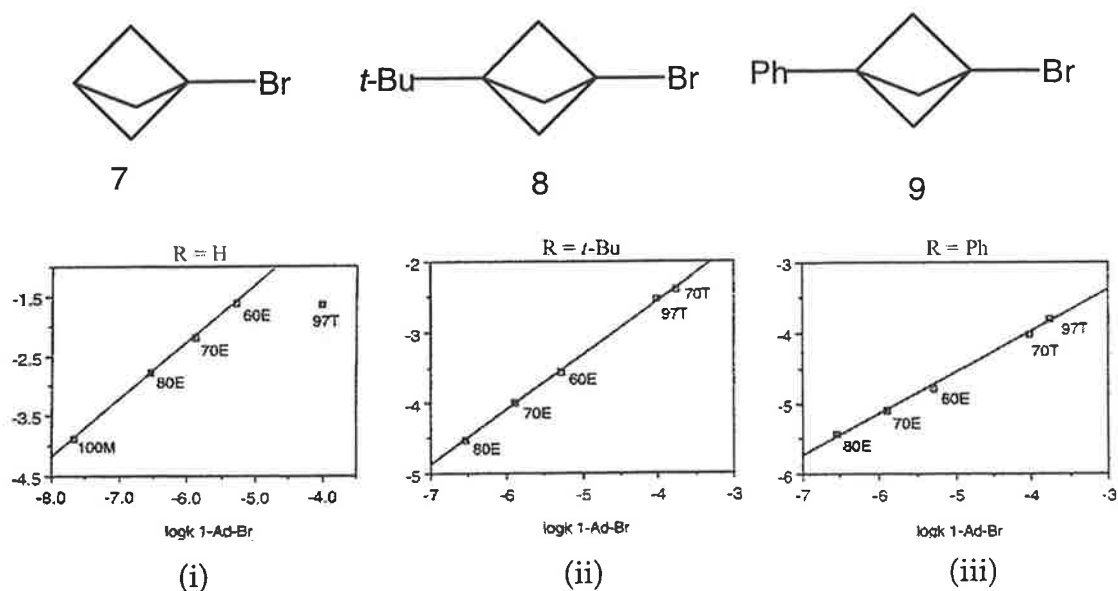


Figure 1.10: Plot of  $\log k$  of solvolysis of (i) 1-bromobicyclo[1.1.1]pentane (7), (ii) 3-*tert*-butyl bicyclo[1.1.1]pentyl bromide (8) and (iii) 3-phenyl bicyclo[1.1.1]pentyl bromide against  $\log k$  for solvolysis of 1-adamantyl bromide (4) in various binary solvents. Figures from reference.<sup>22</sup>

The “ $m$ ” values associated with these plots were, however, found to be lower than anticipated. While, for the parent system, 1-bromo bicyclo[1.1.1]pentane (7), the “ $m$ ” value obtained was 0.97, close to the value of unity anticipated, the “ $m$ ” value obtained from the solvolysis of 3-*tert*-butyl bicyclo[1.1.1]pentyl bromide (8) was, however, found to be 0.77. And further, the “ $m$ ” value obtained for 3-phenyl bicyclo[1.1.1]pentyl bromide (9) was found to be 0.59. Although not commented upon at the time of publication, this trend in the reductions of “ $m$ ” value seemed to correlate with the increase in the electron withdrawing nature of the substituent.

#### 1.4 Establishment of Hypothesis.

This unexpected observation led to our re-evaluation of the convergence of the Hammett plots constructed by Grob, for the 3-substituted 1-adamantyl series (Figure 1.9). We hypothesised that the change in slope between the two Hammett plots could be indicative of a reduction in the “ $m$ ” value proportional to the increase in the electron withdrawing nature of the substituent, similar to that observed in the substituted bicyclo[1.1.1]pentyl system.

If such a correlation was found to be present, then it would provide a significant step in the understanding of the kinetics of these systems, and allow researchers to carry out solvolytic experiments with a far greater understanding of the full effect of the system of interest. Furthermore, should this correlation be able to be described mathematically, then such an equation could be utilised in the prediction of novel rate data with improved accuracy over the current predictive procedures. It could be envisioned that if a correlation between " $m$ " and  $\sigma_I$  could be established, then through the measurement of the measurement of the rate of solvolysis of two differently substituted substrates, both in two significantly differing solvents, such as 97T and 80E, then the rates for all other substitutions could be extrapolated, significantly reducing the time and expense involved with the kinetic description of a substrate system. Furthermore, this data could then be expanded to provide kinetic information for the solvolysis of these substrates in any solvent for which the  $Y$  value was known, through substitution into the Grunwald-Winstein correlation.

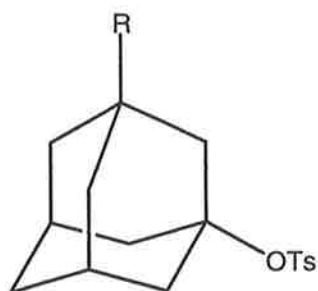
#### **1.4.1 Choice of Kinetic Substrates.**

In order to explore the possibility of this correlation between  $\sigma_I$  and " $m$ ", the solvolytic study of a series of polycyclic alkanes was envisioned. The known literature provided many possible substrate systems, as many solvolyses of these polycyclic alkanes had been previously observed by other researchers. We felt, however, that the initial study would be best served through the examination of the solvolysis of 3-substituted 1-adamantyl tosylates.

Many examples exist in the known literature of the preparation of 3-substituted 1-adamantyl systems which would provide us with several useful approaches to the substrates necessary for this investigation. Further, through the use of these 3-substituted 1-adamantyl substrates, the direct comparison with the known rate data for this system could be made. We felt that the establishment of this hypothesis on the system used to model  $S_N1$  character was necessary, prior to attempts to expand the scope of the investigation.

The choice of the *p*-toluenesulfonyl (tosyl) leaving group, was made as the known kinetic data for 1-adamantyl tosylates indicated that we would be able to carry out the vast majority, if not all of our experiments at 25°C, thus avoiding the need to extrapolate in order to determine the rate data.

Thus the synthesis of a series of 3-substituted 1-adamantyl tosylates, that would provide a spectrum of  $\sigma_I$  values would be necessary for this study (Figure 1.11).



R	$\sigma_I$
H	0.00
CH <sub>3</sub>	-0.01
Ph	0.12
CH <sub>2</sub> OAc	0.15
CH <sub>2</sub> OTs	0.23
CO <sub>2</sub> Me	0.32
OAc	0.38
Br	0.47
CN	0.57
OTs	0.58

Figure 1.11: The proposed 3-substituted 1-adamantyl tosylates to be prepared, and their associated  $\sigma_I$  values.

Once prepared, the solvolysis of these substrates would then be observed in a range of binary solvent systems, based on ethanol and 2,2,2-trifluoroethanol.

### 1.5 Establishment of the BIPCON Suite.

In order to investigate the effect of the electron withdrawing nature ( $\sigma_I$ ) of substituents on the 1-adamantyl tosylate group, on the "*m*" of their solvolyses, a large number of solvolytic experiments would need to be carried out, with both high efficiency and high accuracy. In order to generate a Raber-Harris correlation for one substrate in five solvents, with each solvolysis carried out in triplicate, fifteen independent kinetic experiments would be required, (Figure 1.12), the figure would be more if all solvolyses in each binary mixture could not be conducted at the same temperature.

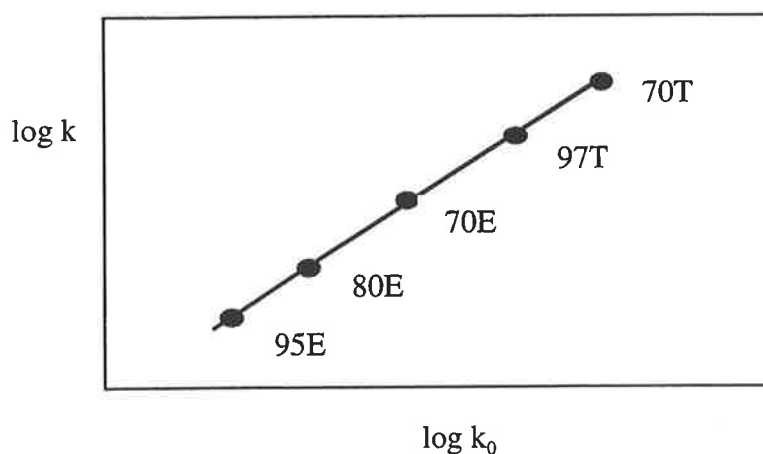


Figure 1.12: Theoretical Raber-Harris plot for a substrate in five solvent systems. Each point would be generated from the average rate determined through the observation of the solvolysis of the substrate in that solvent in triplicate.

Consequently, in order to observe the solvolysis of the ten proposed substrates, one hundred and fifty kinetic experiments would need to be carried out. Unfortunately, many of the traditional methods of carrying out solvolytic studies were not compatible with the number and frequency of experiments required for this project to be completed within a reasonable time scale.

Classically the majority of work carried out in this field had relied upon either titrimetric<sup>7,10,13,24</sup> or conductometric<sup>1,3,5,6,12,14</sup> monitoring of the solvolysis process. Other methods, including chromatographic and spectroscopic monitoring of the reaction are also known, however, their use is less common.

### 1.5.1 Kinetic Data Determined by Monitoring Solvolyses by Titration.

The widely favoured titrimetric technique, observing changes in the pH of the reaction mixture as the solvolysis reaction occurs, has been shown to be almost universal in its application, and can be applied to most systems for which kinetic data is required. However, the use of titration to determine rate constants for large kinetic studies is problematic. The titrimetric process is extremely time consuming and laborious, as at each time interval an aliquot of the reaction mixture must be collected, quenched and stored, awaiting titrimetric analysis. Consequently, the solvolytic reaction needs to be of a sufficiently large scale to allow for the sequential loss of a given volume at each required data point.

Furthermore, a high degree of care must be taken to ensure that each aliquot is handled in the same way to ensure the results are comparable.

As the reaction conditions of the solvolytic reaction need to be maintained throughout the kinetic experiment, it becomes difficult to analyse reactions with short half lives, as the ability of the researcher to take sufficient data points, with significant spacing becomes challenging. The only solution is through temperature manipulation, which unfortunately often leads to the introductions of error through the extrapolation of the data.

### **1.5.2 Kinetic Data Determined by Monitoring Solvolyses by Chromatography.**

A similar method to that above employs HPLC or GC to observe changes in substrate/product concentrations over time during the solvolytic process. In either case analysis of the aliquots would allow the researcher to observe the increase of the products of the solvolysis, with a proportional decrease in the starting substrate. This again has the difficulties associated with the accumulation of aliquots. The handling of the aliquots however, needs not to be as exacting, as internal standards can be utilised to more accurately determine the extent of reaction. Unfortunately, the cost associated with the set up of a chromatographic study, as well as the necessity to prepare specific protocols for each substrate and solvent system, make the use of these techniques unsuitable for large scale kinetic studies. In addition, only substrates visible by UV spectroscopy would be identifiable by these processes, reducing the number of substrate types that can be monitored.

### **1.5.3 Kinetic Data Determined by Monitoring Solvolyses by Spectroscopy**

The use of spectroscopic methods, involving either NMR or IR observation of kinetic experiments has been carried out with considerable success by Müller and others.<sup>25,26</sup>

The advantages in utilising spectroscopic techniques to follow a kinetic experiment are through the ability to sample the reaction products as the reaction continues without affecting the reaction conditions. However, due to the requirement of these experiments to be carried out in the spectrometer reduces the scope of the potential experiments. Accurate, prolonged modification of the temperature within the spectrometer is almost impossible, reducing the number of

reaction types that can be observed. Furthermore, the use of systems visible to the spectrometer is necessary in order to follow the reaction. This again reduces the range of systems that can be analysed through these techniques. The equipment requirements for these studies further disadvantages their expanded use. As all kinetic experiments require multiple runs to ensure accuracy, the use of spectroscopic methods would require either multiple spectrometers, or up to triple the time required to carry out a kinetic study.

#### **1.5.4 Kinetic Data Determined by Monitoring Solvolyses by Conductometric Methods.**

The method of following kinetic experiments that has shown the greatest adaptability to changes in the reaction conditions between experiments has been the conductometric method. The kinetics of a solvolytic reaction can be observed through the change in the resistance of the reaction solution as the substrate ionises.<sup>27</sup> This change in resistance over time can be measured through taking measurements of the resistance between electrodes in the reaction mixture and recorded as a continuous plot from the impedance bridge.<sup>5</sup>

This data plot can then be manipulated to give the requisite kinetic data. Unfortunately, the process requires the manual extraction of data from the resistance plot, which can lead to the entry of significant errors into the rate calculations. Further, due to the cost and spatial requirements in establishing a conductometric analysis array, the simultaneous operation of multiple kinetic experiments is prevented, once again, increasing the time required to carry out a solvolytic experiment through the need to triplicate the kinetic experiments.

#### **1.5.5 Automation of the Collection of Kinetic Data Through Conductometric Techniques.**

From the inception of the use of conductometric analysis of kinetic experiments, there has been an ongoing desire to improve the technique. Shiner and co-workers significantly advanced the field of conductometric kinetics through the progressive development of the techniques used. Murr, working in collaboration with Shiner provided an accurate mathematical description of the changes in the resistance of the solution as the solvolysis progressed.<sup>28</sup> This description allowed for the development of the first automated conductometric apparatus by the



Shiner group. The device was named BIPCON, from its use of the bi-polar pulsed technique, described by Jones and Josephs,<sup>29</sup> and shown in 1970 by Johnson and Enke to be able to be used to measure resistance.<sup>30</sup>

The development of the BIPCON system continued through the work of the Shiner group, culminating in the modernisation of the system by Tilley in 1996 as part of his Ph.D. research.<sup>27</sup> This system, based around a current Intel based CPU provided sufficient computing power to allow the BIPCON system to undertake multiple simultaneous data acquisitions. Consequently, this system provided the advantages of using conductometric analysis, while allowing multiple simultaneous experiments, and collecting and analysing all data electronically.

The advantages provided through the use of a BIPCON system were immediately apparent. There were however, no analogous systems in the Southern Hemisphere. We felt that in order to achieve the aims of this particular project, the development of a BIPCON suite was essential.

While the components required to assemble the BIPCON hardware were available, the development of the suite was not found to be an easy task. Through nearly 50 years of development at the University of Indiana, the Shiner group had maintained and operated the BIPCON system following techniques developed in house. While many of these were covered in the material available on the BIPCON system,<sup>27</sup> a great deal of information concerning the environmental, spatial and electronic requirements was not covered, as in many regards was considered common knowledge within the Shiner group.

A significant portion of this research project was to establish the development of a BIPCON suite at the University of Adelaide, and is described within Chapters 2 and 3, with Chapter 3 providing what we believe to be the first comprehensive manual for the use of the BIPCON suite.

## 1.6 Anticipated Results from the Kinetic Study.

Following the synthesis, and solvolytic analysis of the substrates highlighted previously (Figure 1.11), the correlation between the rate of solvolysis and the  $\sigma_I$  values will be determined. We anticipate that the results of Grob will be replicated, again showing convergence of the appropriate Hammett plots (Figure 1.8).<sup>16</sup> Reber-Harris plots for each substituent will then be generated, and the " $m$ " values determined.

It was anticipated that, in a similar fashion to the 3-substituted bicyclo[1.1.1]pentyl bromides studied by Taylor,<sup>22</sup> a decrease in the " $m$ " values of these 3-substituted 1-adamantyl tosylates would be seen, with an increase in the electron withdrawing nature of the substituent. If this is the case, we postulate that a correlation between " $m$ " and  $\sigma_I$  may exist, and that this correlation manifests itself in the ratio of the separation of the Hammett plots for significantly different solvent systems, such as 80E and 97T.

If this is the case, then from analysis of the plots generated by Grob,<sup>16</sup> an estimate of the decrease in " $m$ " value could be determined. On the assumption that the separation of the plots for the parent system 1-adamantyl tosylate (10) represents an " $m$ " value of unity, then extrapolation would give an approximate " $m$ " value for the 3-cyano substituted system of 0.2.

The ramifications of an " $m$ " value of this low a magnitude for an 1-adamantyl substrate are substantial. This extrapolated value falls well into the range typically associated with an  $S_N2$  solvolysis, when the 1-adamantyl system has been shown and assumed to be solely  $S_N1$  in character.

Regardless of the determination of mechanistic character of the solvolysis of these substrates, a finding of a correlation between  $\sigma_I$  and " $m$ " would allow the prediction of rate data from a much smaller subset of kinetic experiments. The potential of this work as a predictive tool will also be investigated.

### 1.7 Further Investigation of Other Substrates of Interest.

Upon the determination of any correlation between  $\sigma_I$  and "m" for the 1-adamantyl series, other systems of solvolytic interest will be investigated. Significantly, the synthesis of some novel 1,3-disubstituted [1.1.1]pentanes will be attempted, as their synthesis would provide not only systems of solvolytic interest, but also provide valuable information concerning the mechanism via which these systems are produced (Figure 1.13).

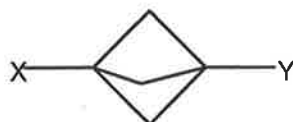


Figure 1.13: 1,3-disubstituted bicyclo[1.1.1]pentanes of interest (X and/or Y = I, Br, Cl, N<sub>3</sub>, OH)

**Development of the BIPCON Suite at the Department of Chemistry, the University of Adelaide.**

*Abstract:*

Although many methods are known for the kinetic study of solvolytic reactions, few of these methods are suitable for carrying out studies involving a large number of solvolyses. The BIPCON system, originally developed by the Shiner group, from the University of Indiana, USA, was designed specifically to be utilised for such large scale kinetic studies. As this system would provide accurate, consistent and reliable kinetic data from any solvolytic system, we felt that the development of a BIPCON suite was imperative to the success of the proposed kinetic study.

## 2.1 Development of the BIPCON Suite

The essential components required for a BIPCON suite were brought together at the Department of Chemistry of the University of Adelaide. These components were either specially purchased or designed and manufactured within the Department. The development of the suite constituted a considerable portion of the research time for this project.

### 2.1.1 The BIPCON System

The heart of the BIPCON suite is the BIPCON system itself that was purchased from the Shiner group from the University of Indiana, Bloomington Indiana USA. The system consists of two discrete components, a computer which houses the circuit boards that control the measurement of the analogue resistances and an external chassis which houses the boards that select the cell and measure resistance values. The system is controlled by the BIPCON software written and developed especially for these instruments.

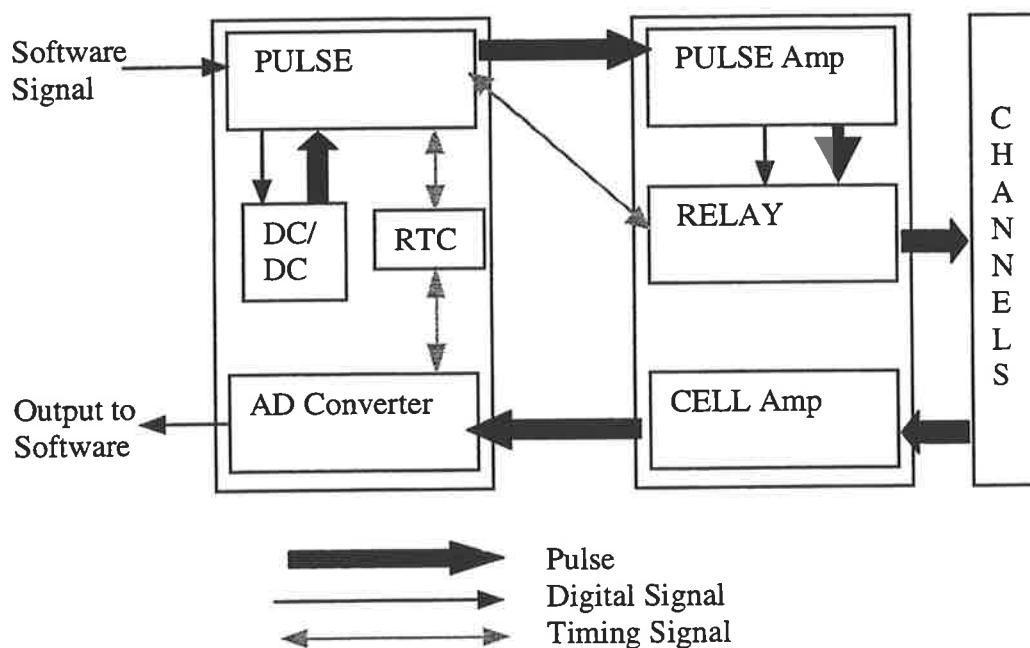


Figure 2.1. A simplified diagram of the BIPCON system showing the relationship of the various components.

The computer responsible for running the system is a 120MHz 486DX IBM compatible PC with a 387 math co-processor chip, running DOS 6.22, and a specially customised set of BIPCON software. The circuit boards that are housed

within the computer mini tower are the pulse generation board (PULSE), the analogue to digital converter (AD Converter) and the 32 bit real time clock (RTC), as well as a +/- 15 volt DC/DC converter. The external chassis houses the pulse amplification board (PULSE Amp.), the relay boards (RELAY) and the cell amplification board (CELL Amp.).

### **Pulse Generator Board (PULSE)**

The pulse generator board, in combination with the DC/DC converter produces the voltage pulse used through the system in the resistance calculations. Through synchronisation with the real time clock (RTC), the two on board digital to analogue converters provide simultaneous positive and negative voltage pulses, producing the bipolar pulse. As the pulse is generated a signal is sent to the analogue to digital converter to synchronise the system to read the voltage at the end of the pulse, and a second signal sent to the relay board specifying the channel to be measured and the feedback resistor to be used.

### **Pulse Amplification Board (PULSE Amp.)**

The pulse sent from the pulse generation board is passed through the pulse amplifier which ensures that the pulse maintains its square wave shape through the system to prevent signal loss and reduce noise.

### **Relay Board (RELAY)**

The relay board contains the hardware for selecting the channel and feedback resistor to be used in each measurement and ensures that the pulse is sent to the correct channel. This selection is controlled through a signal sent from the pulse generator board with the timing controlled through the real time clock (RTC).

### **Cell Amplification Board (CELL Amp.)**

The cell amplification board contains the hardware for carrying out the actual resistance measurement from the cell through measuring the voltage across the cell at the end of the pulse. From this voltage, ( $V_m$ ), the cell resistance ( $R_c$ ) can be determined using the equation detailed below (Figure 2.2).

$$R_c = R_f \{V_p / V_m\}$$

$R_c$  = cell resistance       $V_p$  = generated pulse voltage

$R_f$  = feedback resistance       $V_m$  = measured pulse voltage

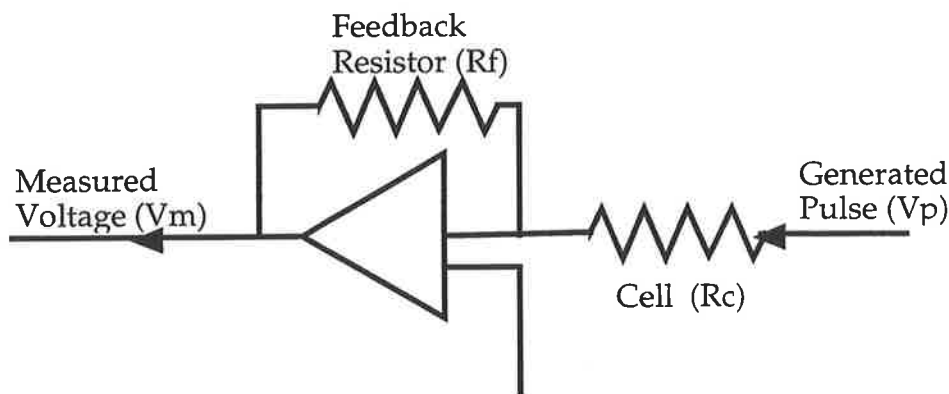


Figure 2.2: Equation detailing the measurement of a resistance point, and the schematic diagram of this resistance measurement.

The system contains four feedback resistors, that can be used in the determination of the cell resistance. In this way a calibration function can be employed by the software in choosing the known best fit within a particular resistance range. This calibration is achieved through the BIPCON software, the use of which will be discussed in detail further in this thesis.

### **Analogue to Digital Converter (AD Converter)**

The analogue to digital converter receives the signal from the cell amplification board and converts it into a digital data stream that can be interpreted and used by the computer to determine the rate constants.

### **Real Time Clock (RTC)**

The RTC provides to the nearest one hundredth of a second synchronisation between all of the BIPCON circuit boards and provides the timing of the system which allows for the accurate running of the instrument.

The design and manufacture of the custom hardware contained in the BIPCON system was carried out by the Shiner group and is discussed in greater detail in publications by them from which this simplified description was adapted.<sup>27</sup>

### **2.1.2 BIPCON Software**

All of the BIPCON measurements carried out by the hardware discussed above are controlled by the BIPCON software, which has been constantly redeveloped and rewritten by members of the Shiner group, most recently by Dr. Leon Tilley. There are many programs that are used in the control of the BIPCON suite and in his PhD thesis, Tilley provides a great deal of information concerning the development and evolution of these programs.<sup>27</sup> A listing of the programs required to control the BIPCON system is included in the following chapter which discusses the use of a BIPCON suite.

Throughout the evolution of the BIPCON system, the programs have been adapted to many areas of interest. While we are interested in utilising the suite for conductometric analyses, the software can also analyse data from other kinetic studies, such as polarimetric, UV spectroscopy or any kinetic data directly proportional to concentration to calculate first order rate constants.

While there are many programs required for the complete control of the BIPCON system, only three are employed manually by the user when carrying out a kinetic study with the BIPCON system. BIPREAD provides the interface to the system for setting up and running the experiments, TRANSHDR which adjusts the output from the BIPREAD program to account for the calibration data and converts the data to a form usable by KINPROG which carries out the calculations to determine the rate constant. The following chapter of this thesis will discuss the use of these programs to carry out conductometric analysis, however, the actual software design and function will not be discussed in any detail, except where adaptations to the software have been made.

### **2.1.3 The Conductance Cells**

The conductance experiments were carried out in specially constructed glass cells containing a pair of platinum electrodes. We employed cells obtained from a variety of sources to optimise the functionality of the BIPCON system including Philips PW 95 series quick-fit probes housed in 10 ml conical flasks (cell type i), a kinetic cell constructed by the Shiner group (cell type ii) and cells designed by the Taylor group and constructed within the Department of Chemistry (cell types iii, iv).





Figure 2.3: Cell types (i) The Philips PW95 series cell, (ii) cell designed and constructed by the Shiner group, The University of Indiana, (iii) cell designed and constructed by the Taylor group, The University of Adelaide, including a stirrer bulb and (iv) simplified cell design from the Taylor group, The University of Adelaide.

The cell design was very flexible as the prerequisites of the cell were only that it housed two platinum electrodes and that the cell could be adequately sealed to prevent solvent contamination and evaporation. The latter is especially important when conductance measurements are taken at elevated temperatures. This gave us a large amount of freedom in designing and manufacturing cells in order to overcome any difficulties we experienced in using cells from other sources, such as inadequate seals, inconvenient volumes and less than ideal construction methods.

The Philips PW 95 series cells (cell type i above), were used for many of the initial experiments in the preparation phase of the BICPON suite development and were constructed from a Philips probe that held the electrodes in a glass support fitted with a quick-fit joint that allowed us to complete the cell with a 10 ml quick-fit conical flask.

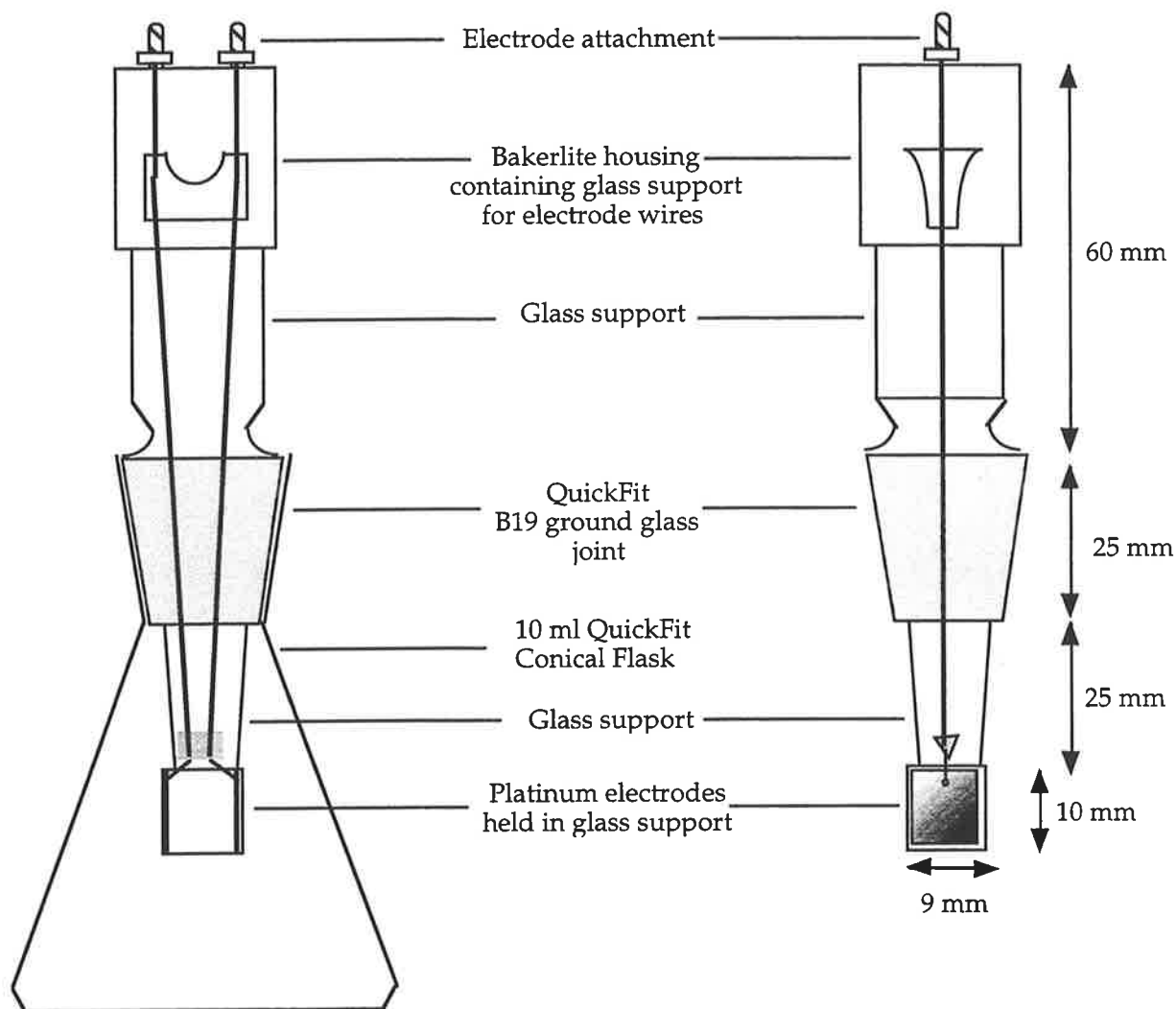


Figure 2.4: The Philips PW 95 series cell.

This cell design was not ideal for our system, as its construction required the probe to be removed from the cell for washing, drying and cell preparation and we found that the glass electrode support was not designed for such constant handling and was damaged easily. Furthermore, the cells required a Teflon sleeve in the neck of the conical flask to ensure that a complete seal was made around the electrode. This sleeve had to be replaced after each run to prevent cross contamination, which was not ideal for long term studies.

We did however, continue to use the Philips cells throughout the study to some extent as their volume, requiring only 10 ml of solvent for each run, was preferable for the 2,2,2-trifluoroethanol (TFE) based solvent system studies, due to the cost of purchasing TFE.

Another cell that we also utilised throughout our early investigations was

designed and constructed by the Shiner group (cell type ii above) which was provided to us with the BIPCON system.

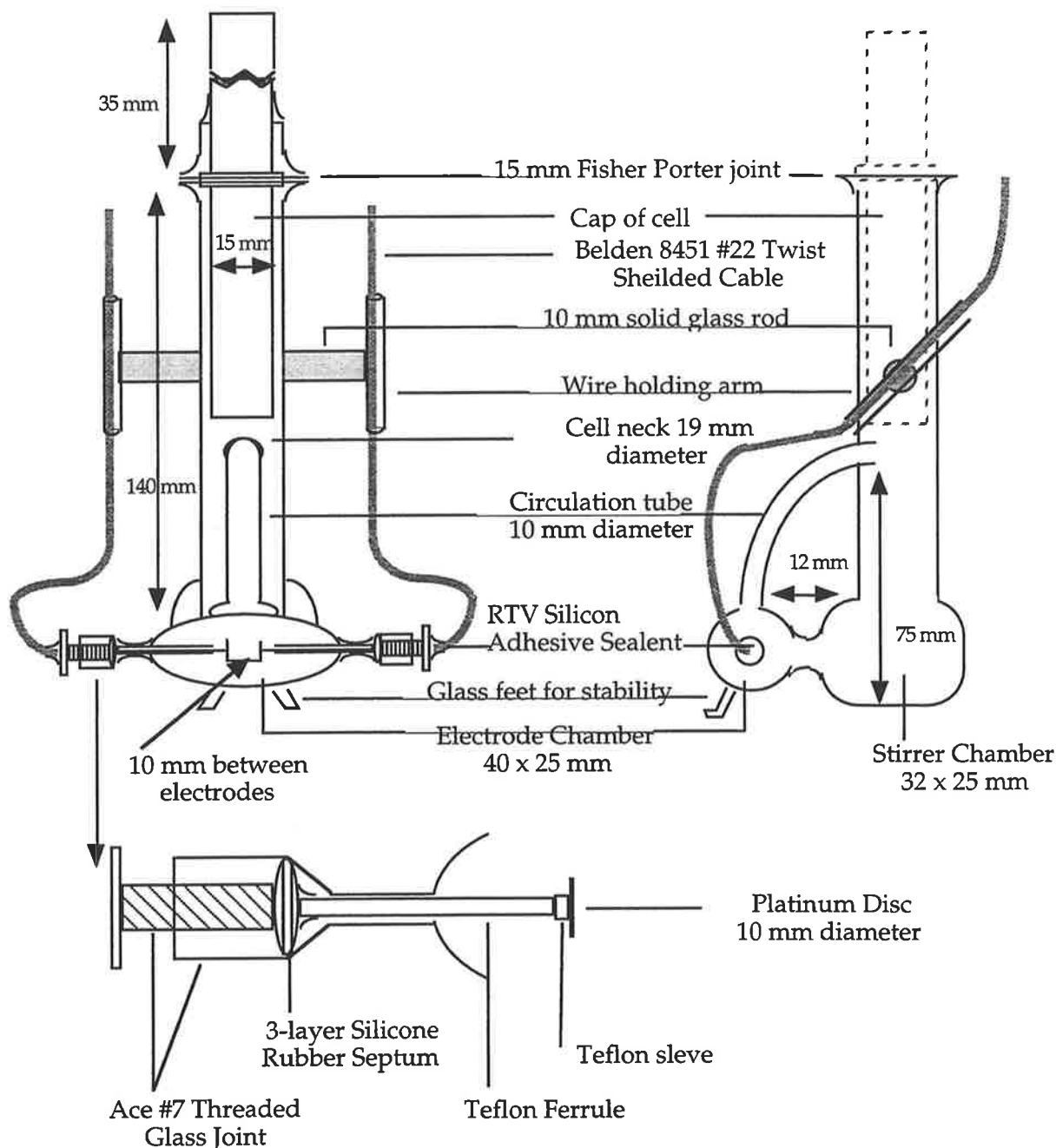


Figure 2.5: The Shiner cell.

This cell provided the inspiration for our first cell design. It incorporated the electrodes into the cell structure itself, thus reducing the chance of damage to the electrodes or their glass support when preparing and using the cell. The difficulty in producing cells of this nature is in ensuring that there is an adequate seal around the electrode wires where they protrude from the glass cell. If adequate

seals are not made then when the cell is immersed in the oil bath, contamination of the cell by the oil will occur. The Shiner group, having had difficulties in producing a direct glass to platinum seal due to the differences in the expansion coefficients of the Pyrex glass and the platinum wires, experimented with various sealant methods. The method that they used for their final cell construction consisted of running the electrode wire through a threaded glass joint tap produced to accommodate a 2 mm wire and filling the gap with silicon adhesive sealant. Further sealing was achieved through the use of a Teflon sleeve and ferrule around the electrode wire as it ran through a narrowed length of glass tubing to create a seal between the platinum and the glass of the cell.

While this technique successfully sealed the cell, the procedure for manufacture of the cells was very complicated and in the event of damage to the cell, the disassembly of the cell for repair would be considerably difficult. It was also important that we had multiple cells available so that we could carry out numerous synchronous runs, enabling us to maximise the throughput of the BIPCON system.

Therefore our early attempts at cell construction focussed on forming seals between the glass and platinum wires that were not as labour and time intensive to produce. We experimented with direct glass to platinum seals that we were led to believe would be possible using the electrodes that we had had manufactured by Englehard - Clal of Melbourne, Australia. However, we were unable to create adequate seals around both electrodes, while the first electrode would seal successfully, our attempts to insert the second electrode did not yield a usable seal while maintaining the first as the glass and platinum wire expanded at different rates, and as they re-cooled would produce leaks around the wire. A solution to this was to use an intermediary glass to form the seal around the platinum, which had a closer expansion coefficient to the wire and then seal this glass bonded wire into the Pyrex cell. However, if this solution was to be employed, then there would be great difficulty in removing the electrodes from the cell at a later time for maintenance or repair and so we postulated another sealant method that could be used in the cell manufacture. The solution that we decided on was to employ telfon young taps, custom bored to accommodate the electrode wire in a similar configuration to the original Shiner cells. We anticipated having to use a telfon paste or similar sealant around the wire to ensure a seal, however, in a trial system where the electrode was inserted through the young tap and the tap incorporated

into a high vacuum manifold, there was a sufficient seal around the electrode wire to hold a high vacuum, from which we concluded that this sealant method would be more than adequate for use in our cells (cell types iii and iv).

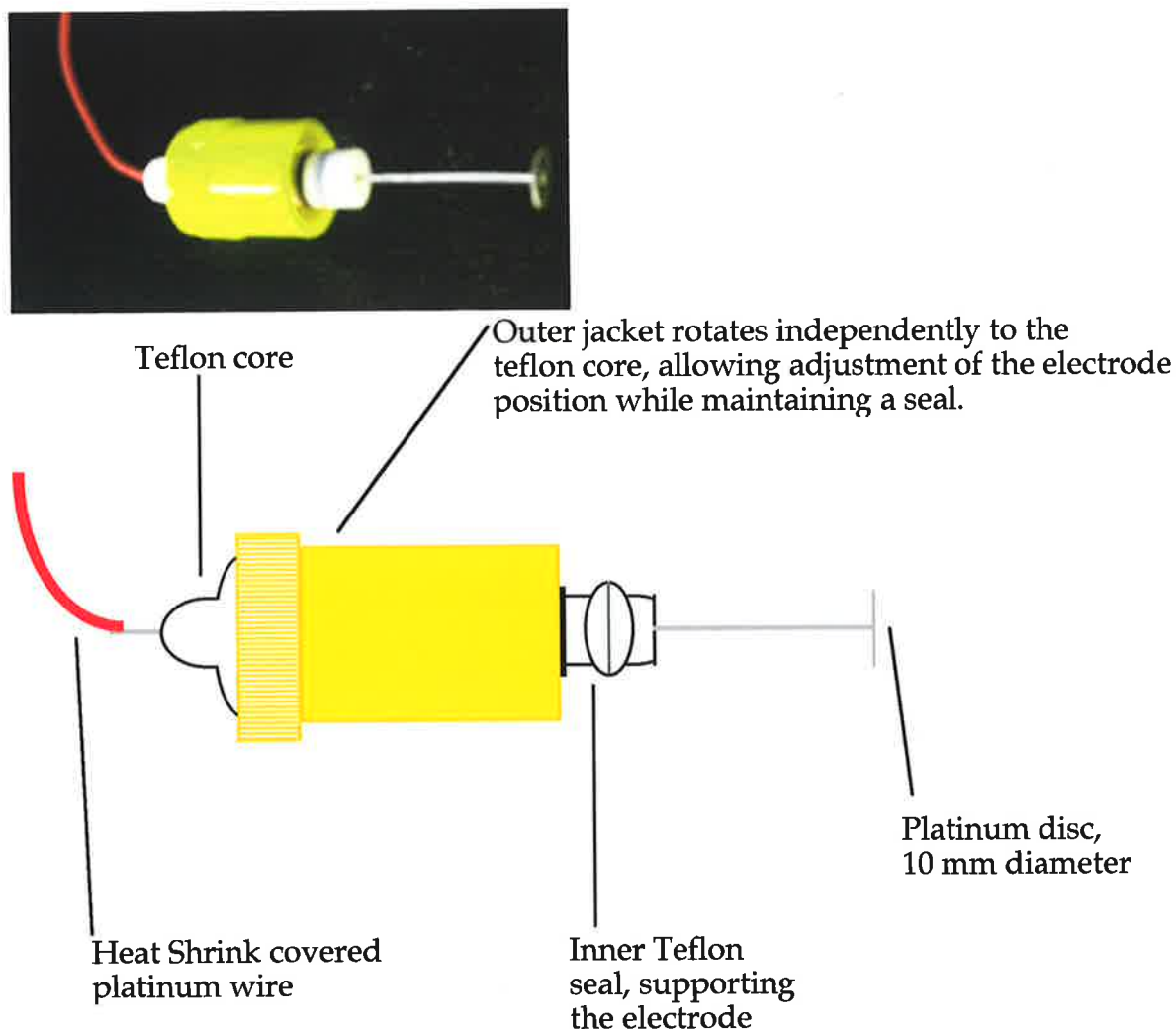


Figure 2.6: The electrode housing constructed from a modified Young Tap, used in the cells constructed at The University of Adelaide.

The use of these seals made the manufacture and maintenance of the cells significantly easier, as the electrodes could be removed from the cell completely, which simplified the manufacture of the cells as the complication of incorporating soft metal components into the Pyrex was eliminated and allowed for an easier firing process in the cell construction. In addition, it also made it easier to clean and dry the cells between experiments, as now the electrodes could be removed and the cell baked dry ensuring the complete removal of any solvent on the cell walls. The current cost of a pair of platinum electrodes is AU\$1,800 and is the major contributing cost to the cell construction.

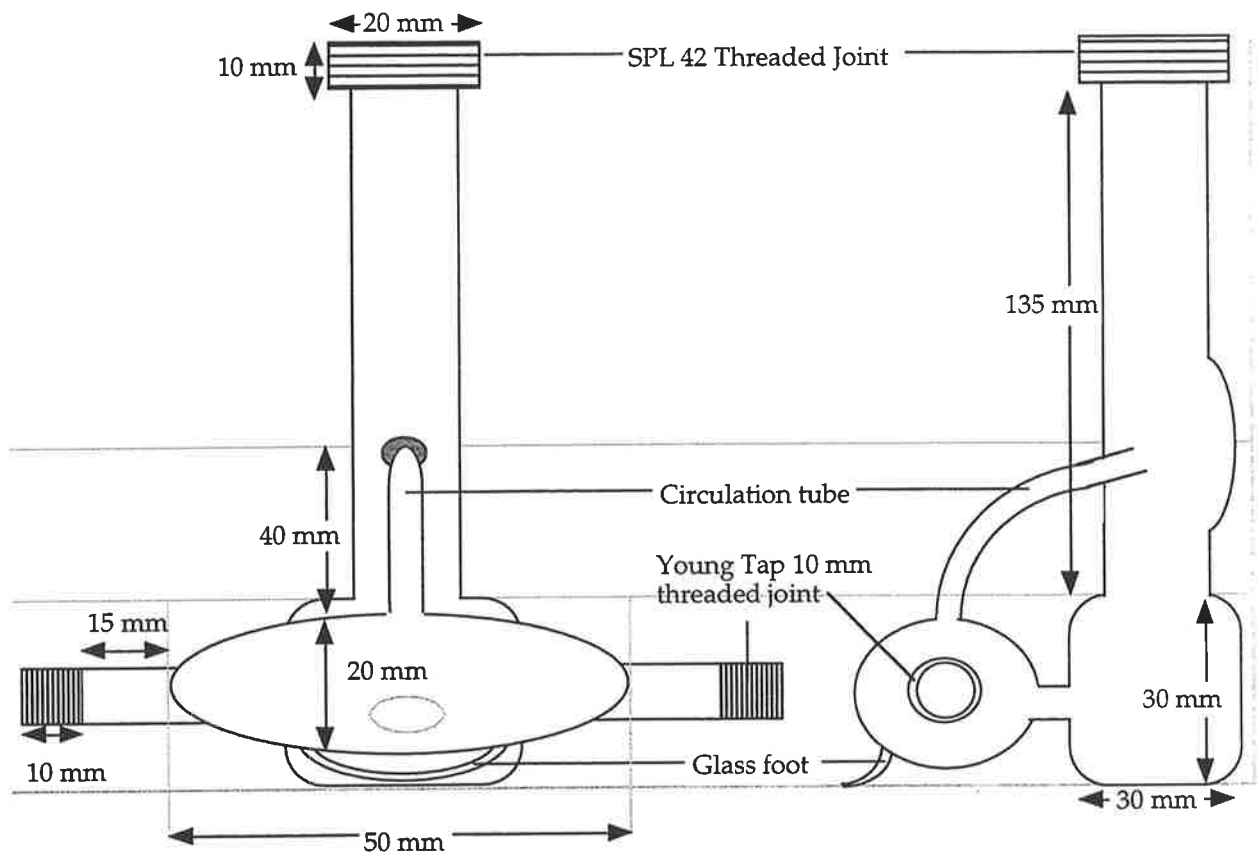


Figure 2.7: Cell design constructed at The University of Adelaide.

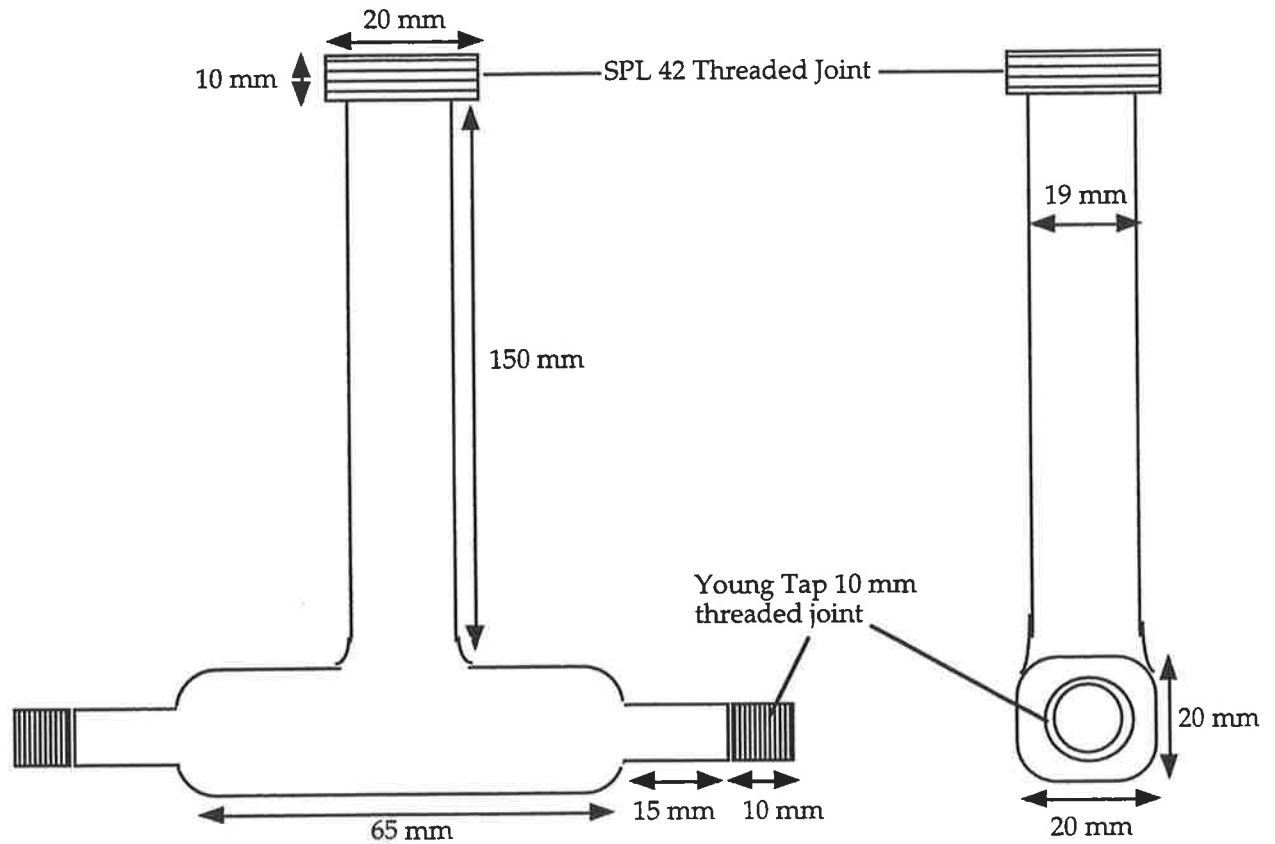


Figure 2.8: The simplified cell design, constructed at The University of Adelaide.

The improvement in the glass to platinum seal was not the only cell development that we undertook. The original Shiner design that we based our original cell design on, utilised a teflon plug that sealed the neck of the cell with a pair of O-rings, and incorporated a second chamber for stirring of the solution. We constructed two cell types, one that incorporated this stirring chamber, and also a simplified design using only a single chamber to reduce the solvent needed for each run. On both cell types we made use of SPL bored caps (701-42) and flanges (701-11) to create screw top seals for the cell necks, which eliminated the need for O-rings or Teflon sleeves which we found became contaminated with the solvent system / solvolytic products and required frequent replacement. These SPL seals were also able to withstand a higher vapour pressure, which would allow us to carry out experiments at higher temperatures without the fear of solvent loss during a solvolytic run.

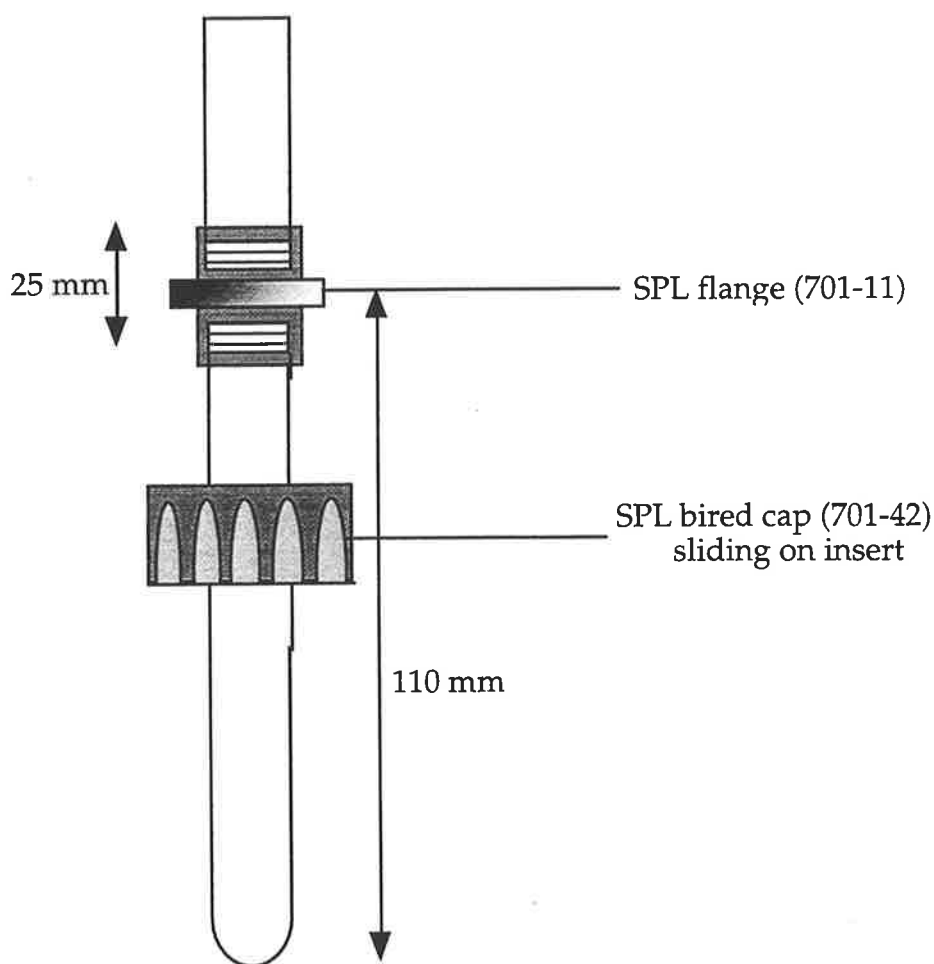


Figure 2.9: The insert for the Adelaide cells, utilising the SPL seals.

#### **2.1.4 Temperature Control**

In order to have comparable and consistent kinetic data, accurate temperature control and stability was essential. To provide this for the BIPCON suite we employed the use of a Julabo<sup>®</sup> F34-MD Refrigerated Circulator oil bath. This was chosen as it could provide a wide range of temperatures at high stability and accuracy from a single oil system (-40°C through to 110°C, with a setting resolution of 0.1°C, which was stable to  $\pm 0.001^\circ\text{C}$  when calibrated).

#### **2.1.5 Other Components**

The other components of the BIPCON suite include the solvent systems, that were prepared by literature methods as discussed in the preparation section further in this chapter and in more detail in the experimental chapter, a "dial-an-ohm" resistance box obtained from General Resistance Inc, Branford CT, USA which is necessary for the calibration of the BIPCON hardware and software and finally the establishment of a BIPCON Remote Access Terminal (BRAT) which could be utilised to analyse experimental data from completed runs or large volumes of Kinetic data without the requirement of stopping Kinetic data accumulation. The BRAT that we initially established utilised a 120MHz 486DX IBM compatible computer, although any PC compatible computer capable of running DOS 6.22 could be employed with the appropriate BIPCON software installed. We found that through use of PC emulation software (Virtual PC<sup>®</sup>) on a Power Macintosh gave us the greatest degree of functionality, as while the software PC handled the BIPCON functions, the functions of the more modern operating system could be employed for tasks such as screen capture, multitasking and other calculations.

The BRAT software is a specially customised BIPCON software set, designed especially for data analysis on a remote terminal, and significantly increases the automation of the analysis of multiple Kinetic data sets. Through the use of an analysis terminal, the productivity of the BIPCON suite was therefore optimised, allowing for simultaneous data collection and analysis, which is not possible from the use of just the BIPCON.

While many of the essential components of the BIPCON suite were purchased, the further developments and customisations of the system which were made during



these studies, especially in the areas of software automation, user interface, overall BIPCON stability and cell design, result in what we believe to be one of the most efficient, accurate and robust conductometric analysis suites in the world.

## **2.2 Set-up of the BIPCON Hardware.**

With the initial phase of purchase and manufacture of the essential components for the BIPCON system complete, the next stage was to set up and prepare the system for kinetic studies. At first, as a matter of convenience, the BIPCON system was set up in an available instrument room on the top floor of the Badger Laboratories close to the research laboratories.

### **2.2.1 Radio Frequency Shielding.**

However, our early attempts to calibrate and run the BIPCON system (as described in further detail later in this thesis) were haunted by large errors in the calculated resistance values obtained through the system, resulting in our inability to obtain any useful data. After a complete check of the BIPCON hardware for faults and multiple unsuccessful attempts to carry out software calibrations of the BIPCON system, we started investigating the possibility of external sources of error. Our early investigation focussed on the arrangement of the components of the system as it had been noted in some experiments from the Shiner group<sup>31</sup> that radio frequency (RF) interference between the components could cause errors in the reading of the resistance values. We found that there was a certain level of interference resulting from the component configuration, however, we were experiencing sporadic errors which occurred regardless of the system configuration, leading us to look for external causes of RF interference.

Our investigation was frustrated by our inability to isolate any apparent cause for the errors. As the errors would be present one day and apparently removed the next, we were often led to believe that we had removed the source of our problems. We considered many possible sources within the Department, such as the NMR facilities, the use of mobile phones, and the running of other instruments in the instrument room, however, the pattern of interference did not match with the periods and frequency of use of these and many other believed sources. Having exhausted all of the possibilities within the Department, our investigation of RF sources focussed outside the Department. We rapidly realised that through

the placement of the BIPCON suite on the top floor of the Badger Laboratories caused the system to pick up the transmissions of the University Radio Station. The observed errors, caused from these transmissions had appeared random as the broadcast schedule altered depending on the day of the week.

In an attempt to overcome the effects of this RF radiation, we experimented with using the BIPCON system within a Faraday cage. We found that the cage significantly improved the stability of the BIPCON, however, operation of the system from within the cage was highly problematic due to space limitations.

The Shiner group had made use of a copper lined room at the University of Indiana to prevent errors of this nature,<sup>31</sup> however, as we did not have access to such a facility at The University of Adelaide, we experimented with placing the BIPCON in a laboratory in the centre of the newly renovated Johnson Laboratories, where we had noted that because of the position of the building and the thick stone and brick walls there was little radio reception.

We immediately noted an improvement in the BIPCON stability, however, we now encountered errors of a different nature in the resistance readings. Previously, when running a calibration on the BIPCON system, the errors were noted through the whole spectrum of resistances measured (1000000 Hz through to 1 Hz) however, the errors that we experienced while running the BIPCON suite in this second location occurred more sporadically and over relatively short parts of the resistance spectrum. We were able to determine, after several calibration runs, that the errors were not restricted to any particular bands of resistance readings but the areas of error were all of the same approximate width in the resistance spectrum, indicating that there was some outside influence that was occurring sporadically that effected the BIPCON readings significantly. Our investigation of the laboratory conditions over several weeks yielded several potential causes of error that were eliminated as best we could.

### **2.2.2 Temperature Maintenance.**

The first area of error we noted resulted from fluctuations in the room temperature. Due to the sensitivity of the BIPCON hardware to electromagnetic interference, the second mini tower containing the majority of the BIPCON boards was not fitted with a cooling fan. Consequently if the room temperature exceeded

28°C the BIPCON was unable to vent the heat built up while running and would start to experience a larger number of errors in its readings. Several solutions to this were attempted, the most efficient being the running of a pedestal fan to provide a flow of air over the BIPCON boxes allowing for the dissipation of the built up heat. However, we did not believe that this was the cause of the sporadic errors that we had initially experienced, as the errors resulting from excessive room temperature had a broader effect over the entire resistance spectrum.

### **2.2.3 Electrical Isolation.**

With the removal of room temperature as the source of the error, we began to investigate other effects that could be causing the noted intermittent errors. Although the exact means of action are unclear, we determined that the most likely cause of these errors was through spikes in the power supply, caused by the power drawn by other major appliances. The original BIPCON system was manufactured in the USA and thus was designed and built to run on 110V AC. While it is possible to easily change the power supply to accommodate the 240V AC used in Australia it was advised against as it was unknown if the internal power supply would have the stability to ensure that the custom expansion cards used in the BIPCON system would not be overloaded. The solution was to use a large external, dedicated 240V to 110V transformer that ran the 110V BIPCON components. Due to a restriction in the number of electrical services provided to each lab, we had inadvertently connected the BIPCON system to the same power line as the large drying oven and the laboratory refrigerator. We determined that a large proportion of the errors that we were experiencing were coinciding with when one of these larger devices was either starting up or shutting down, as controlled by its thermostat. The resulting change in the electricity flow was causing the transformer to work harder to provide a stable flow to the BIPCON system and either provided an inconsistent flow or produced sufficient RF radiation to effect the measurement of the resistances until the electricity flow stabilised. We realised that the only way to avoid this problem was to have a dedicated power line for the BIPCON system

### **2.2.4 Ideal Physical Location.**

It was decided to attempt to find a location that would allow us to accommodate the conditions required for the BIPCON suite with as little restructuring as

possible. The lab space available in the Johnson laboratories was restricted through the requirements of other research groups, and thus alternative locations were scouted within the Department. The primary requirements for the BIPCON suite were sufficient space to place the components and RF shielding from external radiation, as the other variables, temperature and isolated power supply, could more easily be adjusted.

It was found that the basement of the Johnson building had excellent shielding from external RF radiation and provided a sufficiently large open area that we could use to set up the suite for our experiments. Unexpectedly, but fortuitously the basement was also naturally thermally stable, with several temperature studies carried out over the summer showing that the temperature reached a maximum of 25°C on days where the outside temperature was between 35°C and 40°C. The installation of two isolated electrical lines, allowed us to completely separate the BIPCON system from the other electrical components of the suite and completed the requirements for what we believed would be the ideal BIPCON environment.

We were careful in the placement of the components of the suite in this final location, having previously seen the importance in reducing the RF radiation picked up by the BIPCON system, and were able to minimise the effects of the various sources of RF interference on the BIPCON system and have not noted any significant errors in the BIPCON runs that could be attributed to RF signal interference.

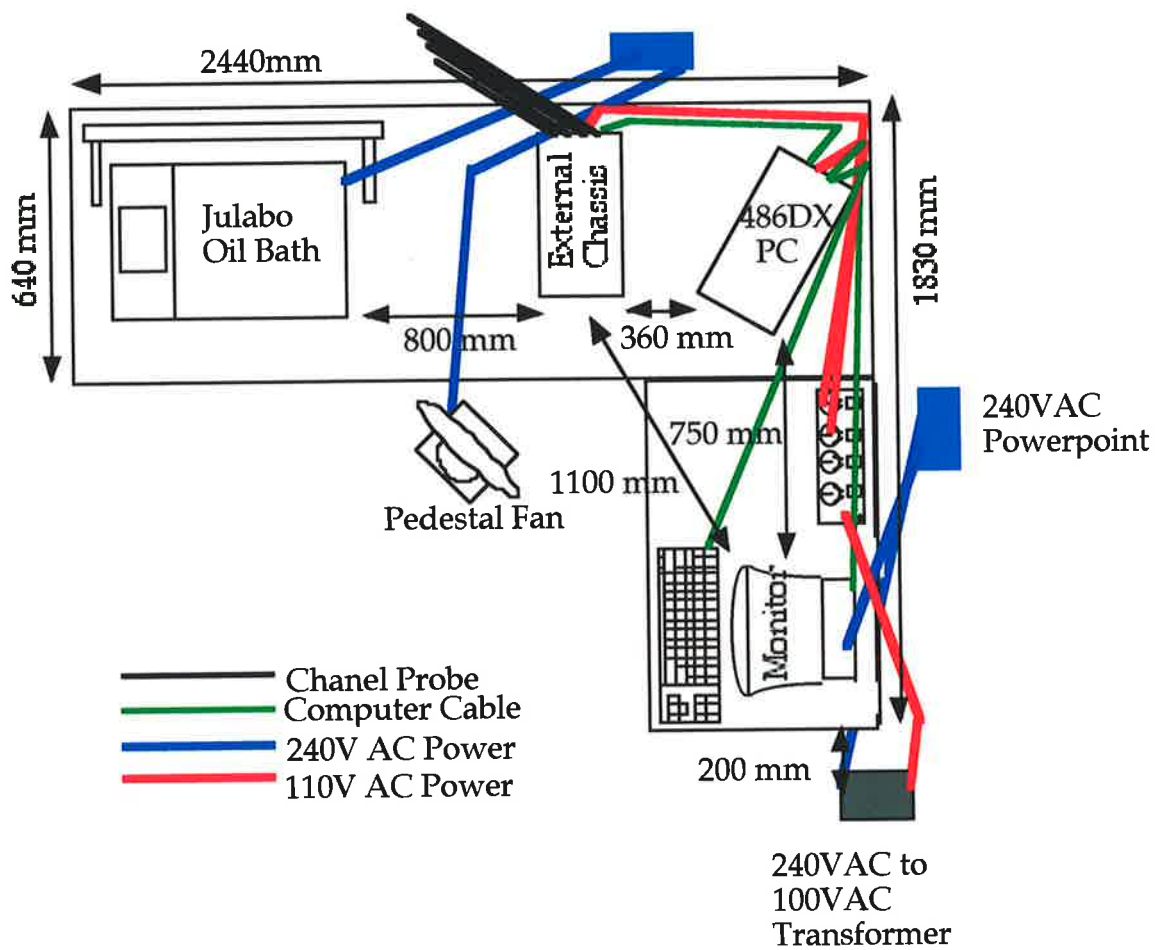
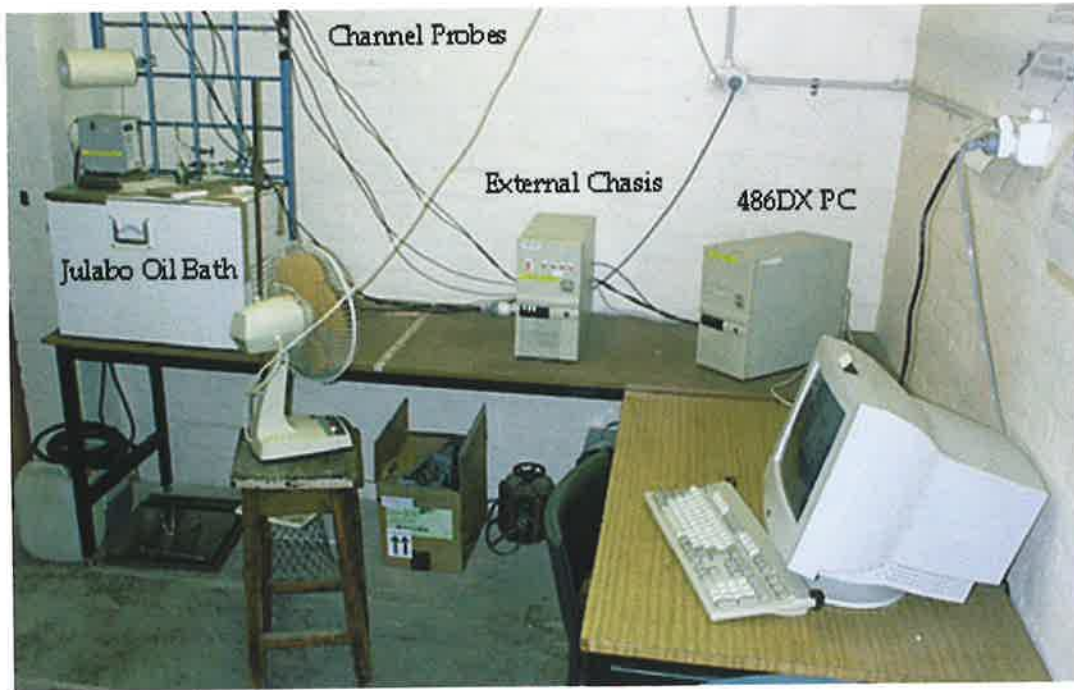


Figure 2.10: Photographic and schematic representations of the BIPCON suite at The University of Adelaide.

The current BIPCON suite set up at The University of Adelaide has been shown to be extremely stable, more so in fact than expected. The anticipated stability of the system between calibrations has previously been determined at approximately six months<sup>27,31</sup>, however, we have noted that our system has remained stable for more than eighteen months. Importantly, care must be taken to ensure that this stability is maintained. The system should therefore be calibrated at least every six months, as should the temperature stability of the bath. It is also highly recommended that the components of the suite are not moved or jolted, if possible, as this can affect the functioning of the suite, through not only changing the environment that the suite is working in, but also in jarring the computer boards in the BIPCON system, causing the system to freeze, miscalculate resistances or damage the boards.

### **2.3 Preparation of the BIPCON Suite for Conductometric Experiments.**

The preparation of the BIPCON suite involved the calibration of the various components, preparation of the binary solvent mixtures and the preparation of the conductometric cells for use.

#### **2.3.1 Calibration of the BIPCON Suite Components.**

With the suite set up and stabilised, the components were prepared and calibrated for use in the kinetic experiments. The BIPCON system was calibrated using the calibration software within the BIPREAD program. The calibration involves the sequential measurement of known resistances provided through the Dial-an-Ohm resistance box which are then compared by the system to the measured values stored in the APPROX.TAB file. This calibration is used in the data collection to determine which of the feed back resistors to use and then in the data analysis to ensure that the points are within the experimental tolerances of the system. It was found to be necessary to regenerate a new APPROX.TAB file whenever the BIPCON suite was used in a new environment, to ensure that the resistance values against which the calibration was carried out were still their true value. The generation of the APPROX.TAB and the calibration files is discussed in the next chapter.

The Julabo oil bath which made use of a special oil mixture that allowed for a temperature range of  $-40^{\circ}\text{C}$  through to  $100^{\circ}\text{C}$  from a single oil was prepared for use through heating the oil to  $95^{\circ}\text{C}$  for one hour to remove any water that may have been absorbed. The bath was then calibrated against an accurate mercury thermometer (error  $\pm 0.01^{\circ}\text{C}$ ).

Initially this calibration was carried out by suspending the high accuracy mercury thermometer into the bath while it was running. However, the results from several kinetic experiments, (substrate studied not important), showed a lower than expected rate for the solvolysis of the substrate. The discrepancy between the expected value and the experimentally determined value was very consistent which indicated the source of the error was a single factor. Through the experiments many of the areas we suspected to be the cause of this error, such as solvent system, substrate and impurities on the glassware had been adjusted which allowed us to eliminate them as potential sources of error. This led us to investigate the internal temperature of the solution, using a pseudo cell constructed from a corked test tube containing approximately 10 ml of Milli-Q reagent grade water. The thermometer was inserted through the cork and the temperature measured over an hour. This showed that the internal cell temperature was  $0.15^{\circ}\text{C}$  lower than the surrounding oil temperature, which accounted for the reduced rate. This discrepancy was corrected for, using the accurate temperature calibration (ATC) routine within the Julabo software. It was also noted that in this and in several repeat experiments that the solution required a minimum of 20 minutes to come to complete temperature equilibration, which would be required in order to reduce error in the kinetic data.

Moreover, using a digital probe at various positions around the bath indicated, as we suspected that there were hot and cold spots within the oil due to the placement of the cooling coils and the heating element within the bath. We found, however, that the effect of these zones on the cells could be minimised if the cells were positioned towards the centre of the bath. Further temperature stability was attained through the use of a styrofoam cover through which the cells were suspended, preventing surface cooling of the oil which reduced the amount of heating required to maintain the bath temperature and in turn reducing the size and frequency of the hot and cold spots. With the temperature now corrected to allow for the change between the interior of the cell and the oil and with improved temperature stability, the accumulated rate data was found to fall into correlation

with the expected data from the literature for our trial substrate pinacolyl brosylate in 97T.<sup>27</sup>

### **2.3.2 Binary Solvent Mixtures.**

These solvent mixtures were prepared via literature techniques from purified AR grade solvents and stored under nitrogen in Schlenk flasks. The purification of these solvents is discussed in the experimental chapter of this thesis. The 2,2,2-trifluoroethanol (TFE) based solvent systems, 97% aqueous 2,2,2-trifluoroethanol (97T) and 70% aqueous 2,2,2-trifluoroethanol (70T) were prepared using weight for weight, 97T being a ratio of dry TFE (97g) to water (3g), and 70T being a ratio of dry TFE (70g) to water (30g). The measurement of these solvents was carried out using a Mettler BasBal balance in the laboratory with the solvents stored and transferred under dry nitrogen. The ethanol based solvent systems, 95% aqueous ethanol (95E), 80% aqueous ethanol (80E) and 70% aqueous ethanol (70E) were prepared volume for volume, with the numerical value indicating the percentage of ethanol, for example 80E is composed of a ratio of ethanol (80ml) to water (20ml). In order to ensure the purity of the solvents and to keep them under nitrogen, the solvent volumes were calculated from their mass at a known temperature using the density tables from the CRC handbook of Chemistry and Physics.<sup>32</sup>

As an example, the preparation of 70E was carried out by distilling dry ethanol under nitrogen into a pre-tarred Schlenk flask. The ethanol was left over night to equilibrate to room temperature (22°C) under dry nitrogen and the mass of ethanol determined to be 579.00 g at 22°C, which equates to 735.74 ml. In order to make a 70E solution, 314.32 ml of degassed Milli-Q reagent grade water was then added via syringe under dry nitrogen, which at 22°C equates to 314.63 g.

The nitrogen that the solvents were stored and handled under was dried through activated silica beads and calcium chloride in a 0.5 metre drying tube.

### **2.3.3 Cell Preparation.**

The conductometric cells used for the solvolytic experiments were prepared and the cell constant determined using the following techniques. Initially all cells were soaked in Milli-Q reagent grade water for several days, with the water replaced



daily to leach out any salts that may have been present on the glass surface from its manufacture. Before use, the cells were also washed with acetone (x3), a dilute lutidine solution, Milli-Q water (x3) and finally rinsed with AR grade acetone (x2) to ensure that they were completely clean and free from proton sources on the glass, as we had noted that acid accelerates the decomposition of some of our test substrates, thus leading to artificially high rates. The cells were dried by a variety of methods depending on the cell construction. For the cells manufactured within The Department of Chemistry, drying was achieved through the removal of the platinum electrodes and baking the cell for a minimum of thirty minutes at 130°C and then allowing the cell to cool under vacuum in a desiccator. For the Philips cells, the conical flask was baked at 130°C and allowed to cool under vacuum, and the quickfit electrodes were dried under a dry nitrogen stream. The cell constructed by the Shiner group was dried over night on a dry nitrogen line, as the construction did not allow for the cell to be baked dry. The washing technique outlined was followed between each run with the cell to ensure that there was no contamination from previous runs.

Once the cells were cleaned and dried their cell constant (cell k) was determined. This constant is used by the BIPCON software to ensure that resistance measurements between cells produce consistent results. An accurate cell constant value is also needed for the determination of the solvent parameters  $\sigma_1$  and  $\Lambda_0$  employing either gravimetric or kinetic methods described by Shiner.<sup>6</sup>

Determination of the cell constant (cell k) was carried out using the BIPCON suite, through the determination the solvolytic rate of a standard compound, pinacolyl brosylate (1)<sup>27</sup> in 97T, for which its rate data was accurately known.

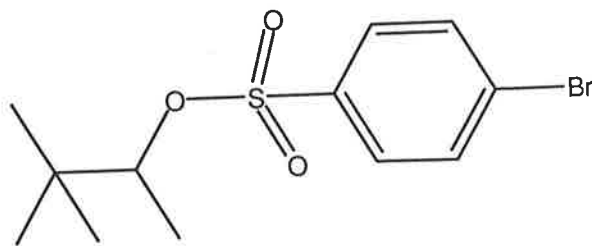


Figure 2.11: Pinacolyl ( 2,2-dimethyl-2-butyl) brosylate (12)

Details of the synthesis of pinacolyl brosylate (12) are covered in the experimental section of this thesis (Chapter 7). The procedure for determining the cell constant

(cell k) was to prepare a known concentration, of the pinacolyl substrate (approximately 1 mM) in 97T which was then analysed through a BIPCON run.

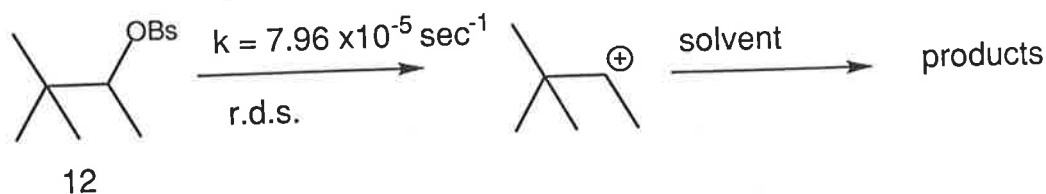


Figure 2.12: The solvolysis of pinacolyl brosylate.

The setup parameters of this run were provided with an initial cell constant (cell  $k_{int}$ ). Generally a value of 0.5 was used if no previous data on the cell constant was known. During the analysis of the data using the KINPROG program, the cell  $k$  value was adjusted until the calculated infinity concentration matched the known concentration of the solution.

Following thorough cleaning of the cell a repeat run was carried out, using the cell  $k$  value determined from the averaged values of the initially predicted cell constant (cell  $k_{int}$ ) and the previously experimentally determined value. The output from this new run was then analysed using the KINPROG program, and the cell  $k$  value again adjusted until the correct infinite concentration was attained.

This process was repeated until the cell constant (cell  $k$ ) value that correlated to the correct infinite concentration in the KINPROG program stabilised over several runs, giving the expected first order rate constant.

We were also able to ensure that the oil bath temperature was correct through this procedure, as, if when a stable cell constant was determined, which provided the correct concentration, then the rate constant determined from the analysis should equal the known value. If the experimentally determined value was found to not correlate well with the known value, and other sources of error had been excluded then the temperature of the bath needed to be re-examined for potential deviation from the calibrated value.

#### 2.3.4 Development of the BRAT and Other Software Improvements.

An integral part of the BIPCON suite is the software that controls the collection

and analysis of the data. While the software that controls the system was left essentially unchanged, the user interface was improved and some of the default values set in the analysis software were altered to facilitate ease of use and increase throughput on the BIPCON suite by reducing the amount of the data manipulation that was essential in the original programming in order to carry out a complete analysis of the BIPCON output data. Through the use of DOS menuing systems, the BIPCON interface was upgraded to provide the user with an automated setup, customised for either data collection or data analysis, which prepared the system and initiated the appropriate software. Furthermore, the BIPCON analysis software was adapted for the use in a separate analysis suite, which became known as the BIPCON Remote Analysis Terminal or BRAT. This computer was set up with a customised set of the BIPCON software designed specifically to allow the user to analyse data from the BIPCON saved onto a floppy disk from within the BIPREAD program, and with no further file manipulation carry out a full analysis of the data.

The development of the BRAT was essential to the optimal use of the BIPCON system. In order to make best use of the system, whenever possible, as many of the BIPCON channels should be in use simultaneously. However, because the rates of reaction for the various substrates and solvent systems to be investigated vary vastly, without a separate analysis terminal, channels would have to lie dormant awaiting the completion of the slowest run before analysis of the data could be initiated. The BRAT allows constant use of the BIPCON with simultaneous analysis while awaiting further runs to complete.

A full explanation of the use of the BIPCON software suite follows in the next chapter, including a description of the differences between the BIPCON and the BRAT and how best to optimise a BIPCON analysis.

## *Chapter 3*

### **Development of a Complete BIPCON Suite Users Manual**

#### *Abstract:*

The following chapter discusses the use of the BIPCON suite, developed here at The University of Adelaide. In order to best describe the use of the instruments that comprise the BIPCON suite, much of this chapter will be presented in the form of a user manual. We felt that as there had not previously been a user manual available for the BIPCON system, that it was both relevant and necessary to spend time preparing this documentation.

### **3.1 Set Up of the Components of the BIPCON Suite.**

As described earlier, the BIPCON suite requires careful preparation and set up to ensure that the system will operate at its highest efficiency. Most importantly, temperature stability, low radio frequency (RF) interference and isolation of the BIPCON devices from other heavy electrical drawing sources should be considered if an alternative location for the BIPCON suite is required. Once set up in the desired location, the components of the suite should be left unmoved as much as possible, as excessive motion has been shown to disrupt the function of the system and can cause damage to the custom computer boards housed within the BIPCON. Care must be taken to ensure that the layout of the components reduces the interference between the components, as described earlier.

### **3.2 Turing On the BIPCON Suite.**

There are multiple components of the BIPCON suite that need to be individually activated. The two mini-towers that house the BIPCON custom computer cards and the 486DX computer that runs the system need both to be powered in order to use the BIPCON. It is strongly recommended that the power to both towers is confirmed prior to attempting any data collection with the BIPCON system, as there may be damage to the customised computer boards in the external chassis if they receive the pulse from the controlling box and are unable to divert it as they are unpowered. The Julabo<sup>®</sup> oil bath has two separate systems that need to be powered. The main control unit and the refrigerator/circulator. Unless both are active and working correctly, the bath will be unable to maintain a constant temperature, and may cause significant damage to the bath. The bath should be allowed to come to temperature equilibrium over at least an hour, with best results attained if allowed to stabilise for up to six hours. It is also of note that due to the lack of cooling fans within the external chassis of the BIPCON, an external cooling fan must be operative whenever the BIPCON is activated to ensure that the BIPCON readings are reliable as extreme temperatures can effect the efficiency and accuracy of the suite.

### **3.3 First Time Use.**

The BIPCON system uses the MS-DOS operating system. Many of the operations described in the following section require an understanding of the basic DOS commands. This thesis will by no means cover all of the possible functions of the DOS system, however, a small glossary of the commonly used commands will be included as an appendix. For further information on other DOS commands and functions, please consult either the on-line DOS help menu or books written on this subject.

Whenever the BIPCON suite has been moved to a new location, or has had significant modification to any of the components, it is advised that the next use of the instrument is treated as the "first time use" and the following procedures followed to ensure the ongoing stability and reliability of the suite.

The components of the BIPCON suite need to undergo software and hardware calibration prior to use. The Julabo<sup>®</sup> oil bath should be calibrated against a high accuracy thermometer housed in one of the conductometric cells to ensure that the solvolytic reactions will be carried out at the exact temperature desired. Through use of the inbuilt Accurate Temperature Calibration (ATC) function of the baths control unit, it is possible to adjust the bath thermostat in 0.01°C increments ensuring accurate and stable reaction temperatures. Further details on the procedure are outlined in the Julabo<sup>®</sup> manual. The conductometric cells must first be prepared for use through thorough soaking in reagent grade Milli-Q<sup>®</sup> water for at least three days, with regular replacement of the soaking solution, and are then calibrated, and their cell constants determined through analysis of known solvolytic reactions once the BIPCON suite has been stabilised and calibrated.

Once the suite has been activated, the user will be presented with the BIPCON Startup menu (Figure 3.1). The second option "Run BIPCON analysis software" should be chosen and the system will default to the BIPCON directory on the hard disk.

MS-DOS 6.22 Startup Menu

1. Run BIPCON data collection software
2. Run BIPCON analysis software

Enter a choice: 1

F5=Bypass startup files F8=Confirm each line of CONFIG.SYS and AUTOEXEC.BAT [N]

Figure 3.1. The BIPCON Startup Menu.

As this is the first use of the BIPCON instrument, it can be assumed that any APPROX.TAB file, which stores the known true resistance values for the system, present will not accurately indicate the current conditions. While not essential, it is advised that the old file (if present) be deleted, or moved to a new folder prior to the creation of a new APPROX.TAB file, to avoid any complications in later calibration of the instrument.

Once this has been done, the BIPREAD program should be activated and the user will be asked to input the date and time to calibrate the Real Time Clock (RTC). The system will then indicate that there is no APPROX.TAB file present, and allows the user to continue to the main BIPREAD menu (Figure 3.2). A full description of the functions of the BIPREAD program is covered later in this chapter

```

Current date: 05-10-2000 and time: 16:44:02      RTCTime: 4294963455
  Channel Run      Delay      Lifetime  Status  Defined      Resistance
  Number  Number      Time
=====
    0           0.00      0.00      0      0.00      SAvg% = 0
    1           0.00      0.00      0      0.00      SAvg% = 0
    2           0.00      0.00      0      0.00      SAvg% = 0
    3           0.00      0.00      0      0.00      SAvg% = 0

(U)pdate Run, (R)estart/Start Run, (S)ave Data, (C)opy To Floppy
(D)os Cmd, (Q)uit

```

Figure 3.2: The main menu of the BIPREAD program.

It is advised that all calibrations of the system are carried out on the same channel. In order to maintain this we used channel "1" for all calibrations of the BIPCON suite. The first stage of the calibration is the formation of a new APPROX.TAB file that will describe the true resistance readings for the environment of the suite. This is achieved by the sequential reading of accurate resistances from the Dial-an-Ohm resistance box through the calibration channel (Channel "1").

To achieve this, the user would choose to (U)pdate Run, from the main BIPREAD menu, select the channel from the list provided and choose (C)alibration (Figure 3.3).



```
Channel to update (0 - 3)? 1
Modes of Acquisition Supported
(N)ormal
(C)alibration
(S)ingle Point
(Z)ero Channel
Select Acquisition Mode ? █
```

Figure 3.3: The channel and acquisition mode selection menu.

Upon choosing to run a calibration, the user will be asked to input a file name for the calibration file in the format of "CALMondd.yy". For example, a calibration run on October 31<sup>st</sup> 1975 would be "CALOct31.75". In most cases the default setting should be chosen. Once a file name has been entered, the system enters the calibration program (Figure 3.4).

```

Enter '-' to redo previous reading, '/' to exit calibration and save data.
Enter '#' to exit calibration without saving data.
Please dial resistance to 990000 ohms.? █
Number of samples averaged: 100
Pulse width: 100000 microseconds.
Selected feedback resistor: 3 ( 535000 ohm feedback resistor ).
Applied voltage pulse: 9.796143 volts. [Offset in UPTAB = 0 (= 32100
)]
Measured voltage : -5.248892 volts. 535667.5 250.803
Dialed Resistance: 1000000
Approx. calculated resistance: 999900.8
? Deviation of approx calc resistance from dialed resistance: -1.92E-0
3

```

Figure 3.4: The calibration program within the BIPREAD software.

With the Dial-an-Ohm box connected to the calibration channel and grounded, the requested resistance (initially  $1 \times 10^6$  ohms) should be dialled in and return pressed on the keyboard. In a normal calibration, the system would read the resistance between the electrode of the calibration channel and compare it to the known resistance in the APPROX.TAB file, alerting the user with a beep if the read resistance was different from the known value by greater than 0.02%. However, as the APPROX.TAB file is not present, the approximate calculated resistance will be 0 ohms, causing the system to produce a warning message and beep for every point within the calibration run. These error messages can be ignored, however, particular care must be taken to ensure that the dialled resistances are correct, as this run will provide the true values for inclusion in a new APPROX.TAB file. If an error is made, it is possible to go back and repeat the collection of a data point through entering '-'. At any time the calibration program can be exited through

entering '/' to exit and save a partial calibration file or '#' to exit without saving any of the data.

At the completion of the calibration process, with the entering of the value of 1 ohm, the system will return to the main BIPREAD menu (Figure 3.2).

BIPEAD should then be exited, through (Q)uit followed by confirmation with (T)erminate and the user will be returned to the DOS prompt. To create an APPROX.TAB file, the calibration file should be copied to the main C:\BIPCON directory, renamed APPROX.TAB. and edited.

Eg. from the main directory C:\BIPCON directory the following would be typed  
copy C:\bipcon\calfiles\CALMONDD.YY

```
rename CALMONDD.YY APPROX.TAB
```

```
edit APPROX.TAB
```

The file opened in the DOS editor will consist of 3 lines followed by 67 lines of data indicating the dialled resistance values, starting under the heading of "RKNOWN" with 1000000-700000 and ending with 10-0. The three header lines should be deleted, as well as any raw data after the end of the 67 line data set. The APPROX.TAB file will now consist of only the 67 lines of regression data. This file should then be saved and the editor program exited.

BIPREAD can now be restarted and the warning message concerning the lack of APPROX.TAB file should no longer be presented. The calibration procedure should now be repeated as described above, in order to ensure that no errors were made in entering the resistance values in creating the APPROX.TAB file. At each point in the calibration process, the system will read the resistance across the calibration channel and compare it with the true value from the APPROX.TAB file. If an error greater than 0.02% is detected, a warning message and beep will occur, and the user will be able to choose to repeat the point after ensuring that the correct resistance has been dialled, or to continue. If large discrepancies are noted, it is possible that there were errors in the APPROX.TAB file. In this case, the new calibration file can be used as above to make a replacement APPROX.TAB file and the procedure repeated. While the majority of the points should fall within the

0.02% error range, discretion should be taken when assessing the need to repeat the point/entire run, especially at the extremes of the calibration process, and in particular with lower values as it is possible that the noise is significantly greater. Once calibrated the BIPCON instrument is ready for use in kinetic experiments. We have found that once the system is calibrated it will remain very stable, however, it is recommended to carry out a calibration at least once every six months to ensure that environmental differences do not effect the accuracy of the system.

### **3.4 Cell Calibration.**

Prior to the running of any kinetic experiments, the conductometric cells need to be calibrated and their cell constants determined. This is carried out through the running of a BIPCON run on a known standard, pinacolyl brosylate (12), for which the rate data is well known (rate constant in 97T at 25°C  $7.96 \times 10^{-5} \text{ sec}^{-1}$ ).<sup>27</sup> By preparing a known concentration of the substrate in 97T, and measuring its rate using the BIPCON, it is possible via a trail-and-error process altering the cell constant in the run set up parameter to gain an accurate calculation of the concentration of the solution as discussed earlier.

The average of several runs with good data fitting was used to give the final cell constant. This process also enables the user to confirm the temperature of the oil bath, as, if the bath is not accurately maintaining 25°C, the calculated rate constant will vary significantly from the true value.

### **3.5 Setting Up a New BIPCON Run.**

The following section describes, with examples the procedures that need to be followed in order to carry out a BIPCON run on the BIPCON suite at the University of Adelaide. The procedure is also outlined in the flowcharts found in the appendices at the end of this thesis.

#### **3.5.1 Preparation of the Cells for Conductometric Experiments.**

The first stage in preparing and setting up a new BIPCON run is in the preparation of the cell with the desired substrate and solvent mixture. Depending on the half life of the reaction, it may be advisable to pre-equilibrate the

temperature of the solvent system prior to preparing the reaction solution, as we have noted that a minimum of 10 minutes, with a recommendation of 20 minutes equilibration is required to ensure that the reaction mixture is at the desired temperature prior to beginning the kinetic experiment. For calibration purposes, when using pinacolyl brosylate in 97T, the half life of the reaction was sufficient that we were able to prepare the mixture in volumetric flasks, and transfer it to the cell for calibration without significant progression of the solvolytic reaction (half life of 8707 seconds, approximately equal to 2.5 hours).

Once the cell has been prepared and allowed to come to temperature equilibration in the bath, a series of single point resistances were taken to confirm that the solvolytic reaction was proceeding and that there were no adverse effects from inadequate dissolution of the substrate in the solvent system. These single point measurements can be carried out through the selection of the (U)pdate run option from the main menu, followed by the desired channel number and then the selection of (S)ingle Point. The system will determine a single resistance across the electrodes of the cell and provide the results in the main BIPREAD menu (Figures 3.2 and 3.3).

Once satisfied that the experiment was proceeding as anticipated, one final single point measurement was taken and reordered in order to determine the trigger resistance (dependant on concentration). The BIPCON run could then be implemented.

### **3.5.2 Entering Run Data.**

From the main BIPREAD menu, selection of (U)pdate run, followed by the channel that the experiment was being carried out on would provide the acquisition mode menu (Figure 3.3). To prepare a BIPCON run (N)ormal is chosen and a run number is requested by the system in the format [xxxx.uu] where the "xxxx" identifies the run and "uu" identifies the user, allowing for multiple users running experiments with the same numerical coding. As an example, as the primary user, the first run may be given the code 0001.01, indicating it is run 0001 for user 01.

Entering a new unique run number will take the user directly to the Run Set-up Menu (Figure 3.6) with blanks in all of the run parameters. However, if the run

number provided has been used previously, the user will be presented with options screen to decide how to proceed (Figure 3.5).

In this way, the data from a previous run can be used to create a template for the new run, reducing the amount of data that needs to be entered. If this is chosen, then a new run number is required. It is also possible to use the run, which is similar to creating a template in that all of the run set-up data is used as before, however, if this option is chosen, then all of the data saved from the previous run using this run number will be lost.

```
Run number 1234.10 already used.  You have the following options:

(S)elect new run number
(C)reate new run number using run number 1234.10 as template
(R)eturn to acquisition display

Select option from the list above? █
```

Figure 3.5: Previously used run number options.

It is worth noting that if the run number chosen is already loaded into one of the other channels, then the (U)se option is unavailable, however, it is still possible to create a new run using the other run as a template.

When the run number has been entered, the user will be presented with the Run Set-up Menu (Figure 3.6), through which the information required to carry out the run by the BIPCON is entered. These variables include the following, the run number, the operator, a space for compound information, the solvent, the cell number, cell constant(+), the solvent system constants Lambda 0(+) and S-alpha(+)<sup>27</sup>, number of points to be acquired – to a maximum of 400(\*), an approximate rate constant / half life(\*), number of half lives to be followed / percentage of reaction completion(\*), a space for comments and finally the trigger resistance(\*).

The items marked with an asterisk (\*) must be entered for each run while those marked with a dagger (+) are recommended. While the cell constant, S-alpha and Lambda-0 values can be entered in the KINPROG program during run analysis,

they will not be saved in the run info file. The others while not essential are recommended as it makes using the run data as a template for a future run far easier with all the information at hand. When entering numerical values into the system for the cell constant, Lambda-0, S-alpha and rate constant values, it is necessary to input the value including at least the first decimal point to ensure that the value is correctly read by the system.

```
New Run Number 1234.10 - no previous data available
Channel Number 1      Run Number 1234.10

( / ) Accept all values AS-IS

(1) Title: Run Number 1234.10
(2) Operator: Ian Milne
(3) Compound: Pinacolyl Brosylate
      1.0mM
(4) Solvent: 97T
(5) Cell Number: 5
(6) Cell Constant: .34
(7) Lambda0: 31.79
(8) SAlpha: 122
(9) Number of points to acquire: 400
(10) Rate Constant: .0000796
      Half Life: 8707.879
(11) Number of Half Lives: 2
      Percent Reaction: 75
(12) Comment:

(13) Trigger Resistance: 120000

Specify item number to change ( / to accept all values)? /
Percent Reaction = 75
TDel&( 1 ) = 23.62637263596199 Press return to continue ? █
```

Figure 3.6: Run set-up menu.

To change or enter a value, the user would type the number associated with the entry, and be prompted to enter the appropriate information. The half life / rate constant entries are merely alternative methods of describing the same value, and as such only one needs to be entered, and the system will calculate the other. The same is true for the number of half lives / percentage reaction.

When determining the resistance trigger, the rate of change of the resistance values from the single point calculations that were taken initially can be used to approximate the trigger used to provide a specified start point. This is particularly

useful if a temperature equilibration period is required, and will allow more flexibility in the run set up procedure. Alternatively for especially rapid reactions, it is possible to start the experiment immediately through the input of the '/' symbol as the resistance trigger. This will take the channel to an active status as soon as the run set-up is exited and will begin taking data points.

Once all of the parameters have been entered, the run set-up can be exited through inputting '/' the initial time interval (TDel(1)) will be displayed. If this value is less than the maximum sampling rate (approximately 0.42 seconds) then the set up should be re-edited to reduce the number of data points to be collected.

### **3.6 The Relevance of the S-alpha and Lambda-0 Values.**

The ability to measure the rate of solvolysis conductometrically has been known for over forty years. The rate constant is determined through an understanding of the relationship between the concentration of the ions in solution and the measured resistance. This relationship was originally believed to be linear,<sup>33</sup> however, this has since been shown not to be the case.<sup>34</sup>

In a pure water system, the error in the determined rate constant incorporated through this miscalculation is negligible. However, in ethanol based solvent systems, the deviation is quite pronounced.<sup>27</sup>

The true relationship between the concentration and the resistance can be described through an understanding of the equivalent conductivity ( $\Lambda$ ) (Equation 3.1)

$$L = \Lambda \cdot c$$

L = Specific conductivity.

$\Lambda$  = Equivalent conductivity.

c = The molar concentration of the solution.

Equation 3.1: The relationship between the specific conductivity and the concentration of the solution.



Fuoss described  $\Lambda$  in the Fuoss-Onsager equation (Equation 3.2).<sup>35,36</sup>

$$\Lambda = \Lambda_0 - S\alpha\sqrt{c} + E.c \ln(c) + Jc - F.\Lambda_0.c$$

$\Lambda$  = Equivalent conductivity of solution.

$\Lambda_0$  = Equivalent conductivity of solution at infinite dilution.

$S\alpha$  = The Onsager limiting slope.

$c$  = The molar concentration of the electrolyte.

$E$  is a function of  $\Lambda_0$  and the solvent properties.

$J$  is a function of  $\Lambda_0$ , the solvent properties and ion size.

$F$  is a function of the solute.

Equation 3.2: The Fuoss Onsager Equation.

It was found by Murr,<sup>28</sup> that for first order kinetics at low concentration ( $<10^{-3}$ ) that a simplified version of the equation could be used to provide an adequate description of the changes in resistance with changes in ionic concentration (Equation 3.3).

$$\Lambda = \Lambda_0 - S\alpha\sqrt{c}$$

Equation 3.3: A simplified version of the Fuoss Onsager Equation.

The  $S\alpha$  and  $\Lambda_0$  values used in this equation are solvent system and leaving group dependant. They can be determined either gravimetrically or kinetically, following techniques described elsewhere.<sup>6</sup>

This relationship was used in creating the necessary code in the BIPCON system for determining the rate constant from a given run. Consequently, the use of this software requires the input of both the  $S\alpha$  and  $\Lambda_0$  values for the substrate being studied. Fortunately, a large number of these constants have been determined previously, and we made use of the values listed in the Ph.D. thesis of Leon Tilley, where he had collated data from a several references and included some previously unpublished work.<sup>6,27,37-40</sup> This data has been reproduced below for convenience.

Table 3.1: Conductance parameters ( $S\alpha$  and  $\Lambda_0$ ) for kinetic rate constant measurements. The values shown are appropriate for experiments carried out at 25°C.

Solvent	Cl		OTs		OBs		OPms		OPf	
	$\Lambda_0$	$S\alpha$	$\Lambda_0$	$S\alpha$	$\Lambda_0$	$S\alpha$	$\Lambda_0$	$S\alpha$	$\Lambda_0$	$S\alpha$
100T										
97T	32.13	100.0	33.7	138.9	31.79	122.0	35.96	182.0	32.14	102.56
94T	35.6	95.0								
90T	42.4	93.2			41.05	112.5				
80T	64.1	90.2			54.7	110.83				
70T	79.83	89.0	78.3	75.53	78.17	71.59				
60T	106.8	84.0			106.803	8.146				
50T					145.026	33.34				
40T					230.0	55.0				
100E										
95E	48.62	113.0	45.0	145.0	37.45	102.62	42.5	143.4	46.8	129.0
90E	47.09	114.7	50.24	123.4	42.7	107.5	46.0	120.0	53.5	126.0
85E	55.0	113.0					55.62	119.6		
80E	71.64	112.0	62.7	98.6	55.2	90.0	62.9	109.6	69.6	105.8
70E	91.03	99.0	81.47	88.04	75.0	77.0			80.3	68.3
60E	113.57	87.0	102.3	70.43	97.0	65.0			93.68	51.83
50E	140.18	85.8	132.0	65.3	125.0	60.0			105.6	
40E			156.2	40.07						
Solvent	ONs		OMs		OTf		OTr		OHfb	
	$\Lambda_0$	$S\alpha$	$\Lambda_0$	$S\alpha$	$\Lambda_0$	$S\alpha$	$\Lambda_0$	$S\alpha$	$\Lambda_0$	$S\alpha$
100T										
97T	36.2	107.3	28.5	119.3	60.0	220.0	55.0	230.0	25	418
94T										
90T										
80T										
70T			72.7	113.5	106.0	172.0	105.0	118.0		
60T										
50T							175.0	80.0		
40T							250.0	90.0		
100E										
95E			55.0	220.0			60	168		
90E			58.9	217.3			65.0	170.0	53.08	398.0
85E										
80E			66.7	212.0	83.0	190.0	70.5	113.6	67.0	260
70E									99.79	86.16
60E			125.3	109.0	153.0	160.0	150.0	105.0		
50E							190.0	162.0		

The abbreviations used in Table 3.1 are:

OTs = tosyl = *p*-toluenesulfonate,

OBs = brosyl = *p*-bromobenzenesulfonate,

OPms = pemsylate = pentamethylbenzenesulfonate,

OPf = perflate = pentafluorobenzenesulfonate,

ONs = *p*-nitrobenzenesulfonate,

OMs = mesylate = methanesulfonate,

OTf = triflate = trifluoroethanesulfonate,

OTr = tresylate = trifluoroethanesulfonate,

OHfb = heptafluorobutyrate.

This data has been reproduced from the Ph.D. Thesis of Dr. Leon Tilley.<sup>27</sup>

### 3.7 Completion of the Run Setup.

All of the data from the run set up will be saved in a file in the c:\bipcon\runfiles directory named Rxxxx\_uu.inf (eg., for run number 1234.01 the information file would be R1234\_01.inf).

The system will then return to the BIPREAD main menu, and the channel will show the current run data (Figure 3.7). The status of the channel is also indicated with a numerical code (Table 3.2).

Table 3.2: Channel Status Numbers

-4	= Paused
-3	= Ready to start (run parameters defined, awaiting user activation)
-2	= Calibration Hold (awaiting user input to read calibration point)
-1	= Finish
0	= Inactive / Passive
1	= Run acquisition
2	= Awaiting Resistance Trigger to start run
3	= Calibration acquisition (acquire 1 point)
4	= Single point acquisition (acquire 1 point)

```

Current date: 11-30-2000 and time: 14:40:52      RTCTime: 4294963455
Channel Run      Delay      Lifetime  Status  Defined      Resistance
Number  Number          Time
=====
0         0         0.00       0.00      0        0.00      SAvg% = 0
1       1234.10     23.63     17415.99  -3        23.63      SAvg% = 0
2         0         0.00       0.00      0        0.00      SAvg% = 0
3         0         0.00       0.00      0        0.00      SAvg% = 0

(U)pdate Run, (R)estart/Start Run, (S)ave Data, (C)opy To Floppy
(D)os Cmd, (Q)uit

```

Figure 3.7: Channel 1 is loaded with the run data for run number 1234.01

### 3.8 Initiating the BIPCON Run.

Unless an immediate start was selected for the resistance trigger, the channel will show an activity status of “-3” which indicates that the channel is awaiting the start signal from the user (Table 3.2). If multiple simultaneous runs are being prepared, the run data entry can be repeated for each channel, and when ready, the runs can be initiated through entering the (R)un start command. The channel will change to a status of “2”, which indicates that it is awaiting the trigger resistance to start collecting data and the systems counts down a defined delay of three seconds or the first time interval, whichever is longer, before taking the first resistance measurement. When the trigger resistance is reached, the status is changed to “1” and the lifetime defined in the run set-up will start counting down and data points collected. If in the run set-up an immediate start was selected, then as soon as the user exits the run set-up menu, the channel will begin taking points.

### 3.9 Modifying a Run.

It is possible to modify a run that is in progress at any time. If the (U)pdate channel command is chosen the desired channel can be modified. If (C)alibration, (S)ingle point or (Z)ero channel are chosen the run will be terminated. However, if (N)ormal run is selected the user will be presented with a series of options (Figure 3.8).

```
Channel 1 is currently active (Status = 2 ). Do you want to

(K)ill the run
(R)eplace the run
(M)odify the run
(C)ontinue the run unchanged

Select option K, R, M, or C ? █
```

Figure 3.8: Run modification options.

The (K)ill the run option will terminate the current run. Choosing (R)eplace the run will also terminate the current run, and will ask the user for a new run number, allowing another run to be set-up for the channel. (C)ontinue the run unchanged will take the system back to the main BIPREAD menu and the run will be unaffected. The (M)odify the run option, however, will temporarily pause the acquisition of the run and allow the user to input modified data into the run set-up for that run and then immediately resume the run. This may be advantageous when studying compounds for which there is no known rate data as it allows for the user to use a subset of the data to determine a closer approximate value of the rate constant which can then be re-entered into the run set up while the run is proceeding.

### 3.10 Run Completion and Data Saving.

When the lifetime of the experiment has completed, the channel will transfer to a status of -1, indicating the termination of the run. The data will automatically be saved onto the hard disk into the file Rxxxx\_uu.dat in the c:\bipcon\runfiles directory (eg. for run number 1234.01 the data will be saved as R1234\_01.dat).

While the run is proceeding the data will automatically be saved every ten minutes to minimise losses due to power failure or in the event of a crash of the computer. It is also possible to manually save the data at anytime, either onto the hard disk using the (S)ave Data option from the BIPREAD main menu, or onto a floppy disk for analysis using the BRAT by selecting (C)opy to Floppy.

### **3.11 Other Commands For Channel and Data Manipulation.**

If the data in a channel needs to be cleared, either to allow the reassignment of the run number to another channel, or simply to clean-up the display, this can be achieved through the selection of (U)pdate run, followed by selection of (Z)ero channel for the desired channel number. This will remove all of the run status information, as well as any run data stored in memory for that channel and reset the channel to the default settings.

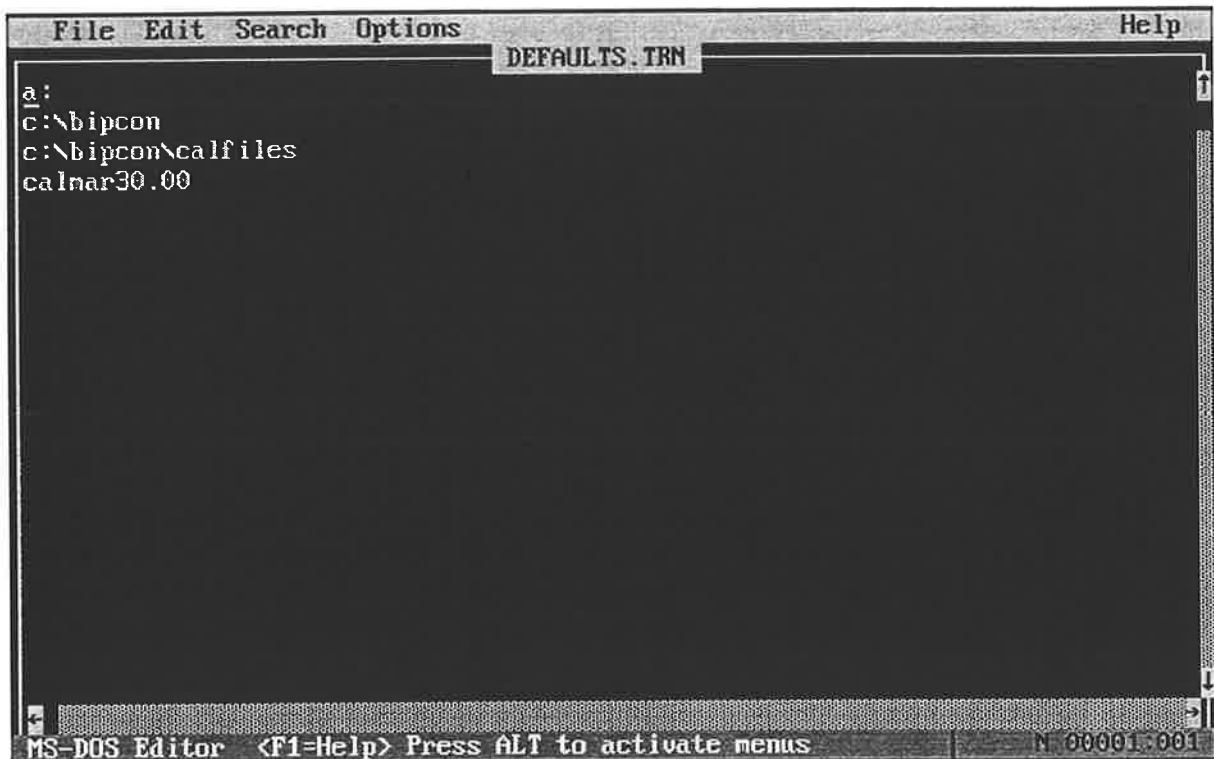
If at any time the DOS prompt needs to be reached while a run is proceeding, the user can enter (D)OS CMD from the main menu, and will be prompted to enter a single DOS command. At the completion of this command, the computer will return to the main menu and the acquisition will continue. If at the prompt the user hits return without entering a command, the DOS prompt will be displayed, and in order to return to BIPREAD, 'exit' must be typed into the DOS prompt. It is important to note that if this command is used, all runs in the BIPREAD program will be paused and data points will not be collected while the DOS command is active.

The final option available in the BIPREAD program is to (Q)uit the program and return to the DOS prompt. If the user enters the (Q)uit command, they will be asked to confirm that, as all run data saved in the channel memories will be lost and any active runs terminated. If the user wishes to continue out of the program (T)erminate should be entered. Any other key will return the system to the main menu.

### 3.12 Data Analysis.

The analysis of the run output data from the BIPREAD program is handled through two programs, TRANSHDR and KINPROG. TRANSHDR translates the raw output data [Rxxxx\_uu.DAT] and adjusts it for the information provided in the run info file [Rxxxx\_uu.INF] and against the calibration file [CALmond.yr] to give resistance/time data for regression. KINPROG then takes this output data [Rxxxx\_uu.ALL] and carries out an analysis of the data from which the rate constant, half life, number of half lives followed and concentration are given. The KINPROG program is able to analyse any time based system, and can be employed for kinetic analysis of output from UV/Vis, titrametric, HPLC or NMR studies as well as BIPCON runs. Details for translating the data from such experiments into a format compatible with the KINPROG program are available in a number of publications on the topic.<sup>27</sup>and references cited therein

Prior to using the analysis suite, it is recommended that the default settings of TRANSHDR are adjusted to look for the most recent calibration file. To do this the DEFAULTS.TRN file in the c:\bipcon directory should be opened with the DOS editor (Figure 3.9).



```
File Edit Search Options Help
DEFAULTS.TRN
a:
c:\bipcon
c:\bipcon\cal files
calnar30.00
MS-DOS Editor <F1-Help> Press ALT to activate menus N 00001:001
```

Figure 3.9: The defaults.trn settings as shown in the DOS editor.

Within this file are all of the default settings the TRANSHDR uses to find the files associated with a BIPCON run, and the location of the modified output file. While all of these settings may be changed, their current values indicate the optimal settings for ease of use of the BIPCON suite at The University of Adelaide. In order to update the calibration file data, the line containing the calibration file name should be updated to the most recent calibration file. It is important that if both the BIPCON and the BRAT are being used to analyse run data then both defaults files should be updated and a copy of the calibration file copied to the BRAT hard disk.

The analysis of the run data is identical to the user on both the BRAT and the BIPCON, however, there are slight differences in the file management between the systems. As these do not affect the actions of the user, they will not be detailed, but will be noted in the BIPCON/BRAT analysis flowchart (in the appendices at the end of this thesis), in order that the necessary adjustments can be made, should the software need to be re-installed onto either system in the future.

### **3.12.1 Data Translation.**

To carry out an analysis of BIPCON run data, the user should enter the TRANSHDR program from the c:\bipcon directory. They will be prompted to enter the run number that they wish to analyse [xxxx.uu]. TRANSHDR will then prompt the user for the locations of the run data and run info files, as well as the calibration file and the location to which the translated output file should be saved. The default settings should be used. The data will then be translated and saved into the c:\bipcon directory awaiting analysis with the KINPROG program. The user will then be asked if they wish to translate another run number. When all the runs that the user wishes to translate have been completed, the system returns to the DOS prompt.



```
C:\NBIPCOM>transhdr
Run Number (xxxx.xx)? 6061.01
Data file [a:\R6061_01.DAT]?
Information file [a:\R6061_01.INF]?
Output file [c:\bipcom\R6061_01.ALL]?
Calibration File to Use [c:\bipcom\calfiles\caljun05.00]?
Do you wish to translate another data set?
```

Figure 3.10: The TRANSHDR program.

### **3.12.2 Kinetic Data Calculation.**

The KINPROG program can then be used to analyse the translated output data and determine the rate constant. Upon initiation, KINPROG will ask if the user wants a long or short copy of the output. The short copy is usually sufficient, as the extra information provided by the long output is of more use in resistance maintenance studies. The user will then be prompted to enter the name of the input file, which is the file that was created by TRANSHDR [Rxxxx\_uu.ALL] and the option to create an output file is given.

It is often useful, especially when carrying out cell calibrations runs to create an output file. It is recommended that the following format is adopted in naming output files in order to simplify future reference to the files. As it is conceivable that through adjustments to the run constants within the KINPROG program, there will be a series of output files created for any given run. Thus, as KINPROG is unable to carry out a file re-write (should a previously used file name be given, the software will show an error to the user, and return to the DOS prompt), it is advised that the output files be saved in the format Rxxxx\_uu.OUi (eg, for run number 1234.01, the first output file created would be R1234\_01.OU1, the next R1234\_01.OU2 etc.). This will allow easy identification of the files for future reference, and provide a means of efficient file management should the data need to be shared with third parties.

```
DO YOU WANT A BRIEF COPY OF OUTPUT ? (Y/N) Y
INFILE = R1234_01.ALL
DO YOU WANT OUTPUT ON FILE (Y/N) Y
OUTFILE = R1234_01.OU1_
```

Figure 3.11: The opening information required by the KINPROG program.

KINPROG will then prompt the user for which details of the analysis they wish to have plotted in the output, either a plot of the percentage errors in the residuals versus point numbers, versus percentage reaction, both or none. As it was considered unnecessary, the BIPCON suite at The University of Adelaide is not equipped with printing capabilities. As such, it has not been desirable to choose to view either plot in the output in most cases. Information regarding the error in the final calculation is given with the final results, and this has been sufficient in all cases thus far.

KINPROG will then upload the input file information, and display an menu of the conductance parameters that will be used to determine the rate constant value (Figure 3.12).

```
THE MORE IMPORTANT EXTERNAL VARIABLES USED IN KPROG OPERATION ARE :
```

```
A: N          :250          G: IDSCD       : 2
B: NOPASS     :10          H: RATE        : .00000117
C: NPARAM     : 3          I: RIMF        : 68989.110
D: NOCAL      : 1          J: RZERO       :432571.500
E: INFOBS     : 1          K: TZERO        : 30116042.30
F: ISEQ       : 4          L: REJLIM      : .100

M: S ALPHA    :138.900000
N: LAMBDA 0   : 33.700000
O: CELL K     : .355000
P: K-SOLVENT  : .00000E+00
```

```
DO YOU WANT TO CHANGE A VALUE? (YES/NO) _
```

Figure 3.12: External variables can be modified from within the KINPROG program.

The values displayed indicate the original parameters that were part of the BIPCON run set-up, as well as other parameters that are set within the KINPROG software. Modification of the values can be achieved by inputting the letter corresponding to the value that the user wishes to change. The **S ALPHA** and **LAMBDA 0** values should be confirmed to be correct for the solvent system being used, as should the **CELL K** (cell constant) value if known. **N** (the number of data points) should not be altered, however, if the value for **N** is significantly lower than the value specified in the run set-up, then caution should be taken when considering this run for analysis as it indicates that there has been an error in the reading of data point values during the run.

The values for **NOPASS** (number of regression passes), **NPARAM** (process parameter function to determine output format), **NOCAL** (number of calculations to be done in the rate calculation subroutine), **INFOBS** (infinity resistance value guessed or observed), **ISEQ** (data sequencing information), and **IDSCD** (data examination control) should not be altered.

However, the **RINF** (estimated infinity resistance), **REJLIM** (point rejection limit), **RATE** (the estimated rate constant) and **K-SOLVENT** (solvent dissociation constant) can be adjusted to get a truer analysis of the data.

Modification of the **RINF** value can be useful when analysing data from runs in which only a short percentage of the reaction has been monitored, or for reactions for which the rate-constant is not known. Adjustment of the **RINF** value should be attempted if a math error occurs while the **KINPROG** software is attempting to perform the non-linear least-squares fit. A trial and error approach can be used to adjust the **RINF** value (usually to a lower value) until a complete analysis can be carried out. An alternate approach is to enter a value of '0' for the approximate rate constant. The system will then generate an approximate rate constant value prior to attempting analysis of the data. It is also possible at this point to enter a true value for the infinity resistance, if known. This value can be determined through taking a single point reading after a minimum of 10 half lives (99.902% completion).

Similarly, entering a known **RATE** value, may enable the system to more accurately determine values for the concentration of the sample. This can be important when determining cell constants and  $S$ -alpha and  $\Lambda_0$  values for new solvent systems.

The **REJLIM** value is used by the system to determine which points are to be discarded in the analysis. Any points whose calculated error is greater than an order of magnitude higher than the **REJLIM** value will be removed from the calculation, and not displayed in the plots of the residuals (if chosen). By default, the **REJLIM** value is defined as 0.1, however, this value can be adjusted if the number of points rejected by the system is unsatisfactory.

If the solvent system has a large dissociation constant, this may effect the results of the kinetic experiment. If the value of the solvent dissociation constant is known with a reasonably high degree of accuracy, then it can should be entered into the **K-SOLVENT** parameter, as this may result in a better fit of the data. However, this has not been necessary in any of the experiments carried out thus far on the **BIPCON** suite at The University of Adelaide.

Once the parameters have been entered and/or modified to the specifications of the user, the user will be asked to enter 'Ctrl-P' to start printing. As mentioned above, the suite developed at The University of Adelaide does not have on-line printing capabilities, and so 'Enter' should be pressed and the output will scroll up the screen rapidly. If at any time the user wishes to pause the output scroll 'Ctrl-S' can be entered and then re-entered to restart the scroll. As this is difficult to control, it is advised that the output be saved to a file and viewed in the DOS editor, as this gives better control over the scrolling.

The final values for the calculated zero, and infinity concentrations, half life, number of half lives followed and the rate constant will be displayed on the screen at the end of the calculations and will not scroll off.

```
THE HALF-LIFE IS .63067E+06 SECONDS, .10511E+05 MINUTES, .17519E+03 HOURS
THE NUMBER OF HALF-LIVES FOLLOWED IS .74589E+00
THE STANDARD DEVIATION IS .3518720E-02

THE FINAL VALUES OF THE PARAMETERS ARE
CONCENTRATION AT ZERO TIME .2730064E-04 ( .51330 %)
CONCENTRATION AT INFINITE TIME .1120294E-02 ( .59576 %)
RATE CONSTANT .1099059E-05 ( .76183 %)

*** EXIT ***
Stop - Program terminated.

C:\BIPCON>
```

Figure 3.13: The data shown at the completion of a KINPROG analysis.

It is possible to review the data from the calculations, if an output file was created, through using the DOS editor on that file. We have found this advantageous as in cases where the rate constant or cell constant is not known prior to starting the run, it is possible that a considerable number of points will be excluded through having too low a REJLIM value, which results in a falsely determined rate constant. If this is noted, KINPROG can be re-used with the same TRANSHDR

output file to recalculate the rate constant with modification to the parameters in the KINPROG set-up menu.

### **3.13 Preparation of the BIPCON Suite for a New Run.**

Prior to starting another experiment on the BIPCON, the cells need to be thoroughly cleaned and completely dried so as not to contaminate the proceeding runs. If the BIPREAD program has been running for a long period of time, it is advisable to re-start the program to ensure that the RTC has not lost its calibration. On a regular basis, at least once a month, the suite should be shut down and rebooted. This allows the system to resynchronise the computer boards within the PC tower and external chassis, which will ensure that the system is not effected by synchronisation errors when analysing the data.

In addition to this, regular maintenance of the oil bath, and ensuring that the calibration of both the BIPCON system and the Julabo<sup>®</sup> oil bath are regularly updated are necessary in preserving the accuracy and efficiency of the BIPCON suite.

## Chapter 4

### **Synthetic Approaches to Precursors of Kinetic Interest.**

*Abstract:*

The synthesis of the substrates required for the proposed kinetic study is discussed, with reference to the methods chosen, and any subsequent synthetic modifications to improve either yield or more importantly purity of the desired tosylates.

#### 4.1 The Preparation of the Substrates Used for Calibration.

During the preparation of the BIPCON suite for kinetic studies, the cells needed to be calibrated (Chapter 3), which was carried out utilising the traditional standard, pinacolyl brosylate (3,3-dimethyl-2-butyl brosylate) (**12**).<sup>27</sup> The requisite brosylate was prepared through the reaction of pinacolyl alcohol (**13**) (3,3-dimethyl-2-butanol) and brosyl chloride (**14**) (4-bromobenzenesulfonyl chloride) at room temperature for six days (Figure 4.1).

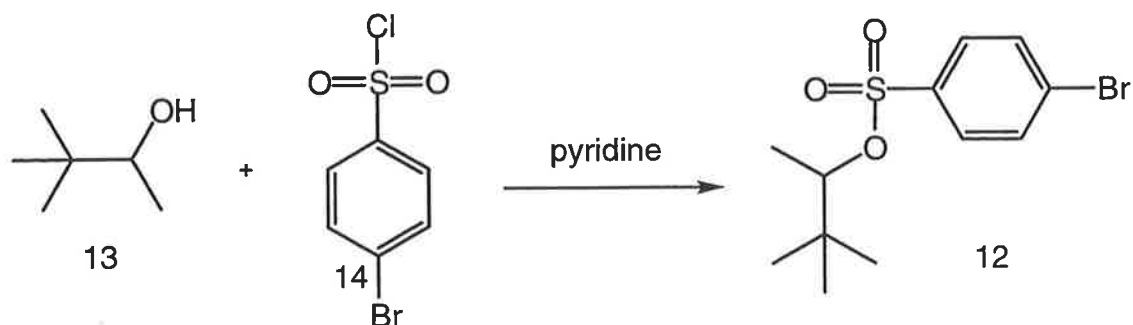


Figure 4.1: The synthesis of pinacolyl brosylate (**12**).

The isolated yield was consistently high (80-90%), however, it was found that the brosylate (**12**) would decompose rapidly, catalysed by the presence of acid. It was further found that the effects of this decomposition could be reduced if the product, after purification was taken up in pentane, and allowed to crystallise out at  $-4^{\circ}\text{C}$ , and kept in the mother liquor at this temperature until required.

#### 4.2 Synthetic Approaches Towards the 3-R-Substituted, 1-Adamantyl Tosylates.

As described in the opening chapter, we wish to investigate the effect of changes in the electron withdrawing strength of remote substituents on the adamantyl substrate, specifically on the response of the substrate to solvent ionising power (" $m$ ").

In order to observe this effect, a kinetic study of the solvolysis of a series of 3-substituted 1-adamantyl tosylates with a wide range of  $\sigma\text{I}$  values was envisioned. As shown below (Figure 4.2) the preparation of a series of ten substrates was



initially proposed to provide significant scope over the range of synthetically available  $\sigma_I$  values.

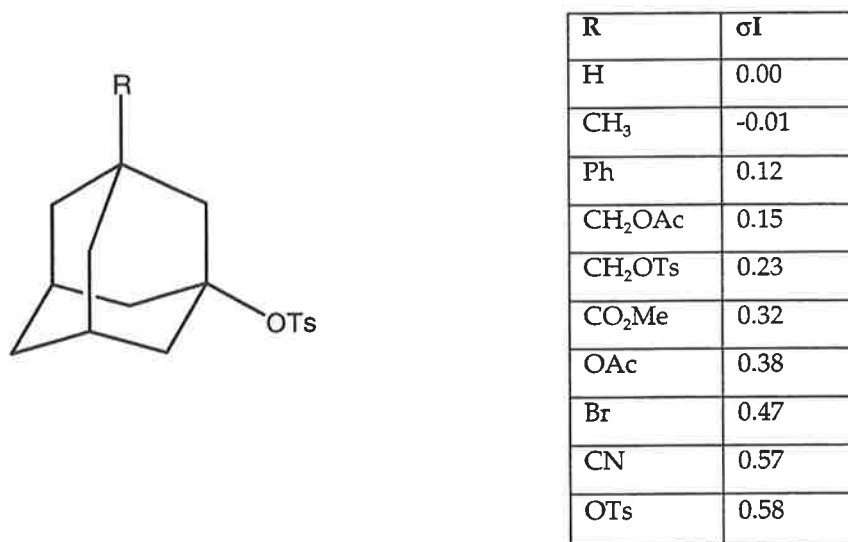


Figure 4.2: Proposed 3-R-substituted adamant-1-yl tosylates for the envisioned kinetic study.

It was envisioned that all the requisite substrates could be readily prepared from either commercially available adamantane or adamantane-1-carboxylic acid. The reactions are described in detail in the forthcoming section, but each approach would utilise the interconversion of an adamantyl alcohol or bromide to the relevant tosylate (Figure 4.3).

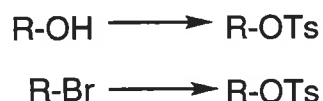
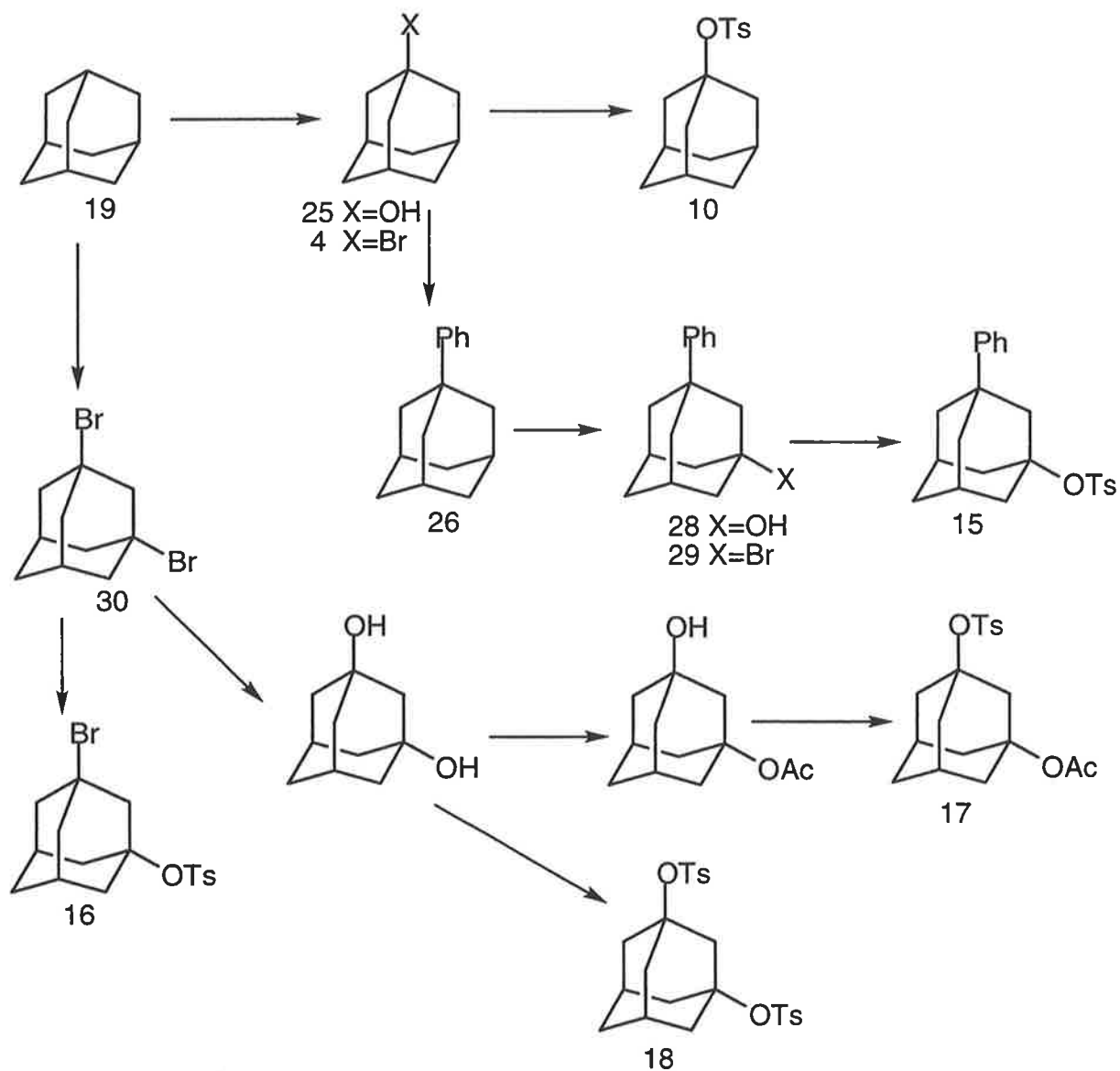


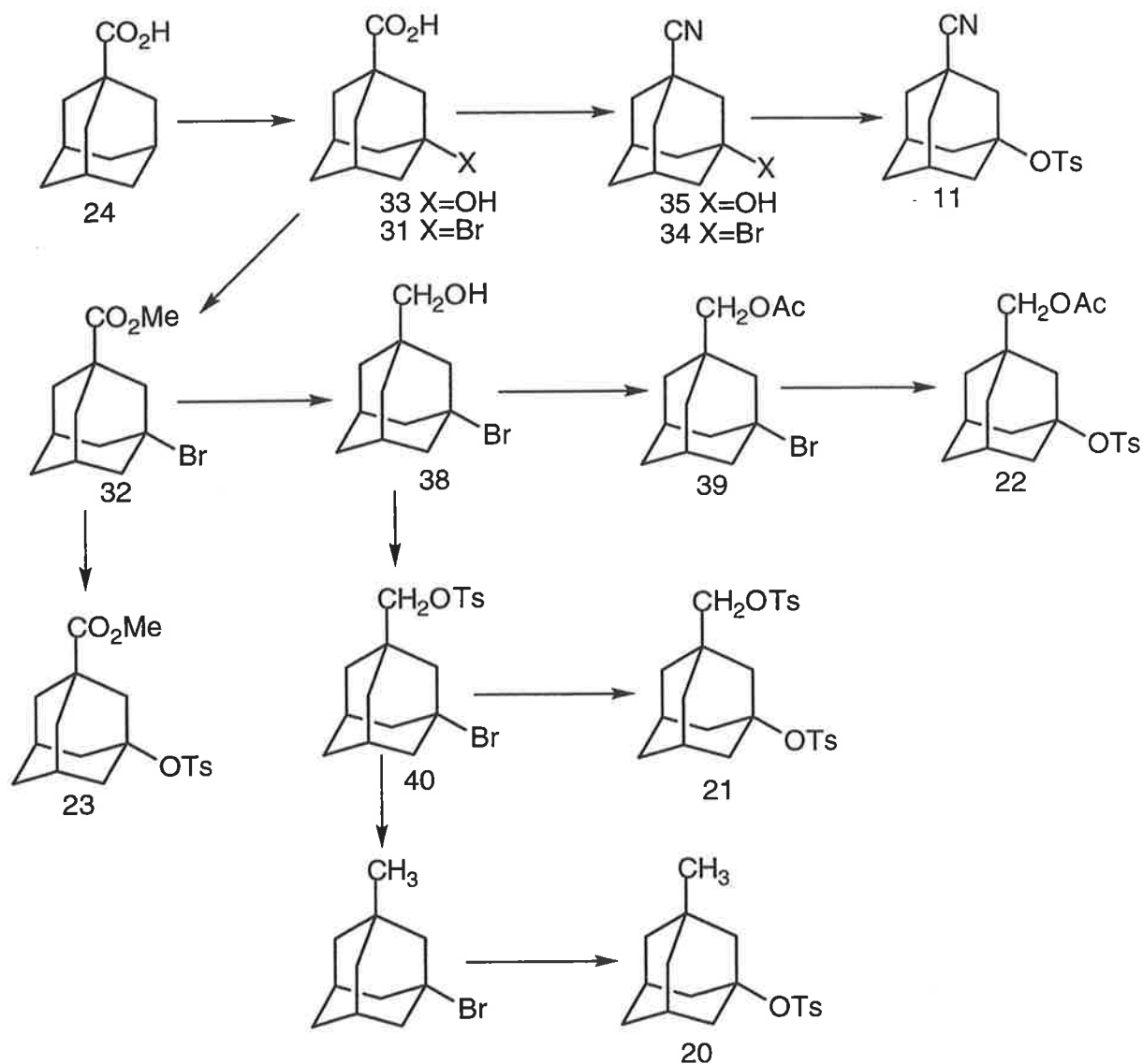
Figure 4.3: The main interconversions utilised in the formation of the requisite tosylates.

The synthesis of the 1-adamantyl (10), 3-phenyl 1-adamantyl (51), 3-bromo 1-adamantyl (16), 3-acetyl 1-adamantyl (17) tosylates as well as the adamantane 1,3-ditosylate (18) could be anticipated to proceed from adamantane (19) via a series of syntheses as outlined in Scheme 4.1.



Scheme 4.1: Simplified scheme of the proposed synthesis of the tosylates **10**, **15**, **16**, **17** and **18** from adamantane (**19**).

The remaining proposed substrates, namely 3-cyano 1-adamantyl tosylate (**11**), 3-methyl 1-adamantyl tosylate (**20**), (3-[(tosyl)oxy]-1-adamantyl)methyl tosylate (**21**), (3-[(tosyl)oxy]-1-adamantyl)methyl acetate (**22**) and methyl 3-[(tosyl)oxy]-1-adamantanecarboxylate (**23**) were to be synthesised from the adamantyl carboxylic acid (**24**), as indicated in Scheme 4.2.



Scheme 4.2: Simplified scheme of the proposed synthesis of the tosylates 11, 20, 21, 22 and 23 from adamantane carboxylic acid (24).

With the exception of the methyl substrate (20), the synthesis of all of the proposed substrates was attempted, with the majority being attainable providing the right approaches were utilised. The final approaches used were those for which the desired synthesis was able to be carried out in fair to high yield and most importantly, of high purity. Although we did not carry out kinetic experiments on all of the ten initially proposed substrates, those that were prepared and utilised provided a broad range of  $\sigma_I$  values, which was required for our results to have significant meaning, as outlined in the opening chapter.

### 4.3 Direct Tosylation of the Adamantly Alcohols Utilising *p*-Toulenesulfonyl Chloride.

The leaving group (tosyl) chosen for the kinetic experiments was able to be introduced through several different approaches. Traditionally, the use of tosyl chloride (*p*-toluene sulfonyl chloride) in pyridine has been highly successful for the conversion of an alcohol to the tosylate.<sup>41</sup> The rate, and success, of this conversion of an alcohol to the tosylate product has been shown to decrease from primary, secondary to tertiary alcohols respectively.<sup>41</sup>

We were fortunate to have a supply of adamantan-1-ol (25) available, and thus attempted the tosylation. However, despite multiple attempts, and varying the reaction conditions in regards to the base used to deprotonate the alcohol, the solvent system, the reaction time and temperature and the use of catalysts, in particular DMAP (di-methylaminopyridine) as outlined in Table 4.1, we were unable to isolate the desired 1-adamantyl tosylate (10).

Table 4.1: Reaction conditions and yields for the interconversion of adamantan-1-ol (25) to the parent tosylate (10).

Base	Solvent	Time/Temperature	Catalyst	Yield
Pyridine	Pyridine	Reflux / 16 hours <sup>i</sup>	-	0% <sup>i</sup>
Pyridine	Pyridine	Reflux / 5 hours <sup>i</sup>	DMAP	~15% <sup>ii</sup>
Sodium Hydride	DMF	Room Temp / 24 hours	-	0% <sup>iii</sup>
Sodium Hydride	DMF	Room Temp / 24 hours <sup>i</sup>	DMAP	0% <sup>iii</sup>

<sup>i</sup> Monitored by TLC.

<sup>ii</sup> Product unable to be isolated from complex reaction mixture.

<sup>iii</sup> No product isolated following work up.

Through monitoring the reactions by TLC we were able to observe the formation of the tosylated product, which was confirmed by <sup>1</sup>H NMR on the crude mixture. However, through attempting to push the reaction to completion it was noted that the tosyl product was further converted under the reaction conditions, to the respective chloride (6) (Figure 4.4).

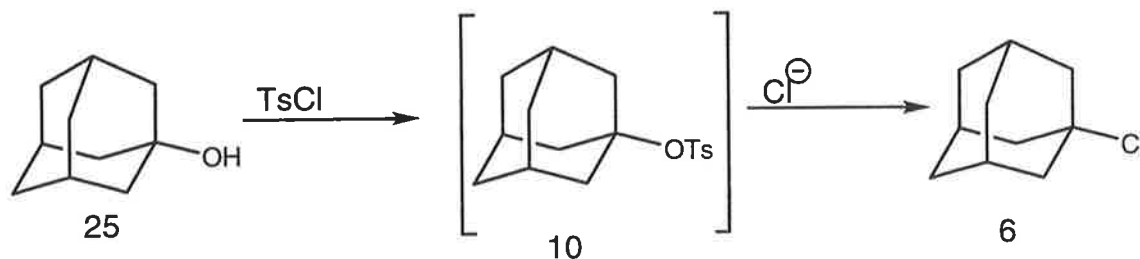


Figure 4.4: Attempted conversion of the alcohol 25 to the tosylate 10 utilising tosyl chloride, yielding the chloride (6).

Through careful monitoring of the reaction, we were able to quench the reaction at the point which we felt would yield the highest quantity of the desired product. We intended to then isolate the tosyl product through careful chromatography. Unfortunately, we found that the tosyl system was too sensitive for chromatographic separation to be performed and thus we were unable to isolate the desired material. Such sensitivity of the parent tosylate was also noted by Grob once the product (10) had been isolated.<sup>42</sup>

#### 4.4 Use of Silver Tosylate and the Corresponding Adamantly Bromides.

The difficulty in synthesis and purification of the parent tosylate and anticipating that this approach may be inappropriate for the remaining requisite tosylates, especially those with low  $\sigma_I$  values, which are more reactive, prompted us to explore alternative methods of preparation. An alternative method of tosylation is known in the literature and hinges on a halide to tosyl exchange, utilising silver tosylate (silver *p*-toluene sulfonate) (Figure 4.5).<sup>42</sup>

This tosylation technique had been shown by Grob and co-workers,<sup>42</sup> to be highly adaptable to many tertiary adamantane systems, providing many tosylates in good yields and excellent purity. The chief advantage of this approach, was the removal of the halide ion as it precipitates out of solution as the silver halide. The examples known in the literature proceeded with the greatest success when the adamantyl bromide was employed for the exchange. Although there were some examples of the tosylates we required for this project, the scope of the prior work gave us sufficient confidence that this technique could be adapted to all of the substrates that we were interested in. Consequently, the bridgehead bromides were required.

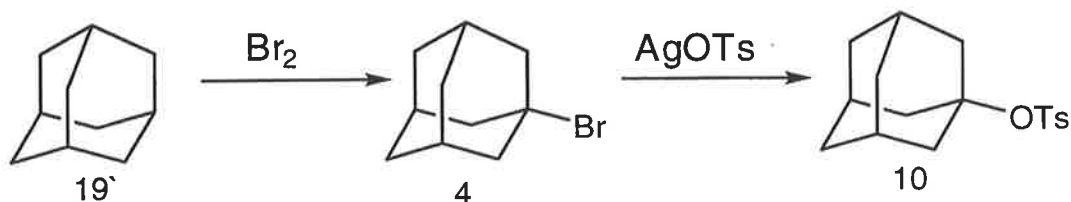


Figure 4.5: The conversion of adamantyl bromide **4** to the tosylate product **10** utilising silver tosylate.

Synthesis of 1-bromo adamantane (**4**) was achieved through the reaction of adamantane (**19**) with excess bromine under reflux for six hours, as previously reported.<sup>43</sup> Sublimation was utilised to purify the product, yielding the desired bromide (**4**) in excellent yield (85%). As we intended to use this 1-bromo adamantane in the synthesis of the 1-phenyl adamantane (**26**), the bromination reaction was attempted on a synthetically large scale, and found to be easily scalable up to 20 grams.

With the parent bromide in hand, we next trialed the halide tosyl exchange reaction (Figure 4.5). Thus, to the bromide (**4**) was added a slight excess of silver tosylate in acetonitrile at ambient temperature and the mixture allowed to stir for one hour. As the tosylation reagent was highly light sensitive, adequate precautions had to be taken to ensure that the reaction would go to completion by shielding the reaction vessel from light. In addition, the desiccation of the silver tosylate prior to reaction reduced the possibility of hydrolysis.

At the completion of the reaction, the silver salts were removed by filtration, and the solvent removed to yield the desired 1-adamantyl tosylate (**10**) in excellent yield (93%) and was found to be essentially pure (>95%) by <sup>1</sup>H NMR. This product was further purified by rapid sublimation to ensure 100% purity and then immediately used for the kinetic experiments, as it was found to be extremely sensitive to moisture upon prolonged storage.

#### 4.5 Friedel Crafts Arylation of the Bridgehead Bromide to Introduce a Phenyl Substituent.

With the parent tosylate (10) successfully synthesised and knowing that this would be the most sensitive substrate in terms of decomposition due to hydrolysis, it was felt that this approach to the required tosylates would be the most appropriate to pursue.

The 1-bromo adamantane (4) could be further interconverted to the 1-phenyl adamantane (26) through a Friedel Crafts arylation addition of benzene in the presence of ferric chloride. This reaction proceeded in good yield (75%) and the final adduct (26) was purified by rapid sublimation. This product (26) was found to be highly volatile, and thus to reduce losses through evaporation was stored at  $-4^{\circ}\text{C}$  until needed.

Oxidation of 1-phenyl adamantane (26) with chromium trioxide in a mixture of acetic acid / acetic anhydride introduced an acetate moiety into the 3-position of the adamantane, yielding (27),<sup>44</sup> which could then be hydrolysed with sodium hydroxide in methanol, producing 3-phenyl adamantan-1-ol (28),<sup>44</sup> in moderate yield after purification by sublimation (59%) (Figure 4.6).

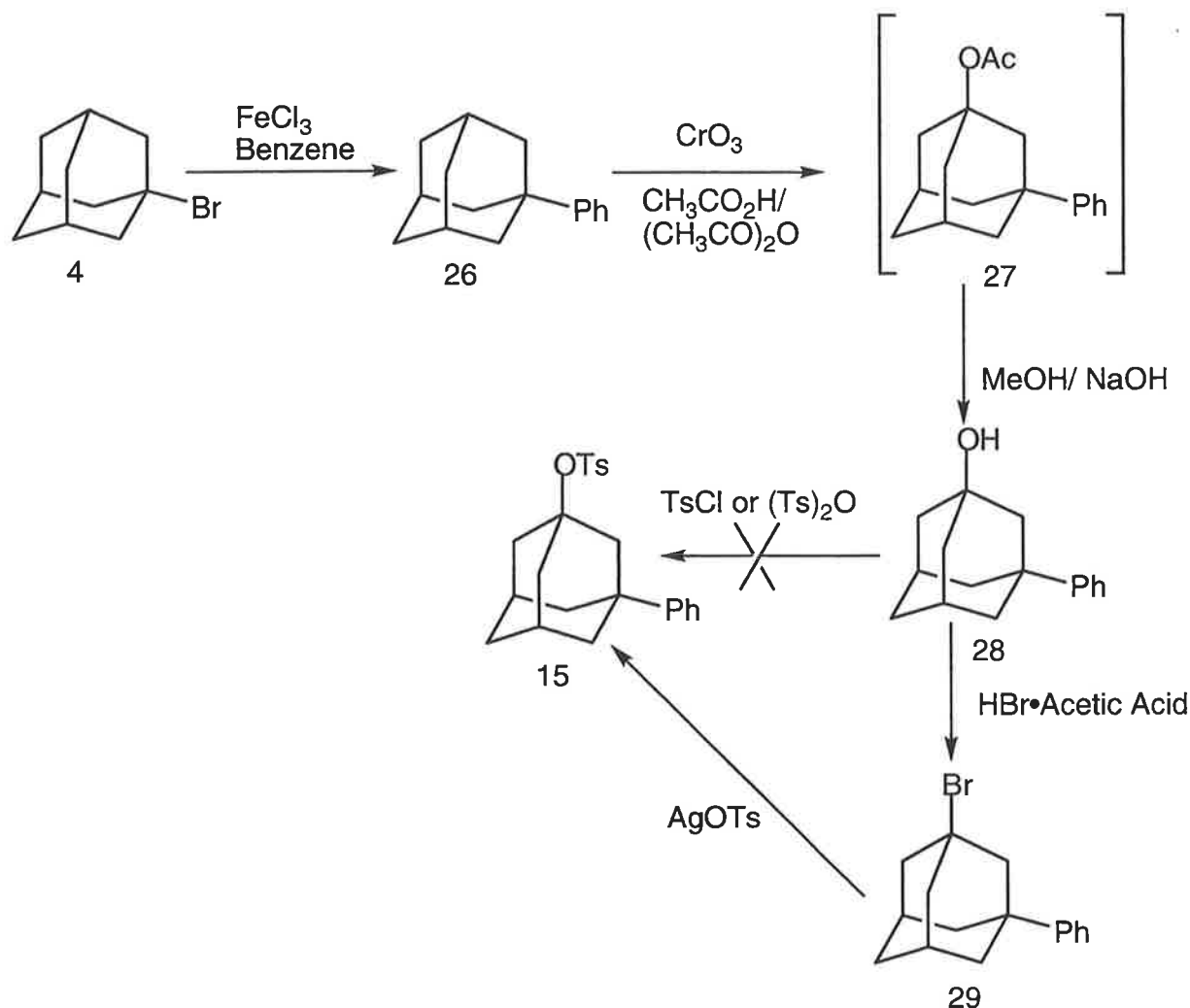


Figure 4.5: Interconversion of the bromide (**4**) to 1-phenyl adamantane (**26**), and sub sequential transformation to 3-phenyl, 1-adamantyl tosylate (**15**).

#### 4.5.1 Preparation of the Desired Tosylate (**15**).

As the alcohol (**28**) was readily produced, we attempted the tosylation directly . Tosylation with tosyl chloride was again unsuccessful, providing a low yield of the desired 3-phenyl 1-adamantyl tosylate (**15**) as evidenced by  $^1\text{H}$  NMR, which could not be isolated from the reaction mixture. We attempted the tosylation using tosyl anhydride (*p*-toluene sulfonyl anhydride) as the nucleophilic tosylating agent,<sup>41</sup> which resulted in a slightly better crude yield of the desired tosylate, however, once again isolation and purification on silica from the reaction mixture proved difficult. These complications and the inability to ensure absolute purity of the required tosylate prevented us from utilising this approach to the tosyl substrate (**15**).



As the tosyl halide exchange had been shown to be successful with the parent system (10), we felt that use of this method may be the most appropriate for all further tosylations. However, in order to utilise this reaction, the 1-phenyl adamantan-3-ol (28) was required to be converted to the corresponding bromide (29).

This could be achieved through the reaction with excess hydrobromic acid in acetic acid according to a literature procedure.<sup>44</sup> This transformation proceeded in good yield (75%) following purification by Flash column chromatography in hexane ( $R_f = 0.3$ ) and the resulting 3-phenyl, 1-adamtyl bromide (29), was tosylated using silver tosylate in acetonitrile to afford the desired 3-phenyl, 1-adamantyl tosylate (15) in good yield (71%) (Figure 4.6).

#### **4.6 Synthetic Approach to Other Required Substrates.**

The remaining substrates of interest were conceived to be synthesised from either 1,3-dibromo adamantane (30), or from further functionalisation of the commercially available adamantane-1-carboxylic acid (24).

The synthesis of the 3-bromo, 1-adamantyl (16), 3-acetyl, 1-adamantyl (17) tosylates and the 1,3-ditosyl, adamantane (18) were perceived possible through the transformation of 1,3-dibromo-adamantane (30) (Figure 4.7).

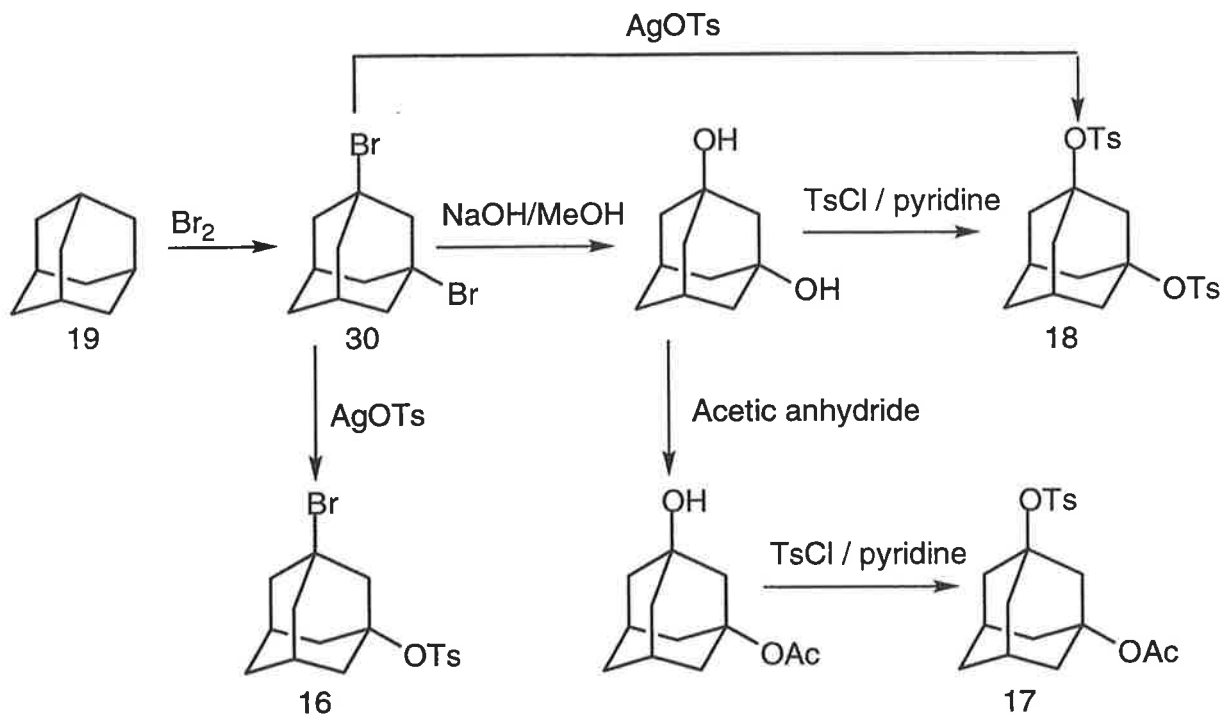


Figure 4.6: The synthetic approach to the synthesis of the tosylates 16, 17 and 18.

The attempted synthesis of 1,3-dibromo-adamantane (30) was carried out through the reaction of excess bromine with adamantane (19) in the presence of aluminium bromide under reflux for six hours, according to a literature procedure.<sup>45</sup> Although several replications of the reaction were carried out, and the reaction conditions modified to reduce the excess of bromine present, successful isolation of the desired dibrominated compound (30) was not achieved. The reaction inevitably yielded a complex mixture of polybrominated adamantanes, whose exact chemical composition was left undetermined.

#### 4.7 Synthetic Approaches from Adamantane-1-Carboxylic Acid.

Due to the difficulty in synthesising the starting precursor for the tosylates 16, 17 and 18, it was decided to instead focus on the synthesis of the remaining substrates of interest (11, 20, 21, 22 and 23). The  $\sigma_I$  values of these substrates would still provide significant scope for the proposed kinetic study. The synthesis of the remaining required tosylates was envisioned to be possible through the conversion of adamantane-1-carboxylic acid (24) (Figure 4.7).

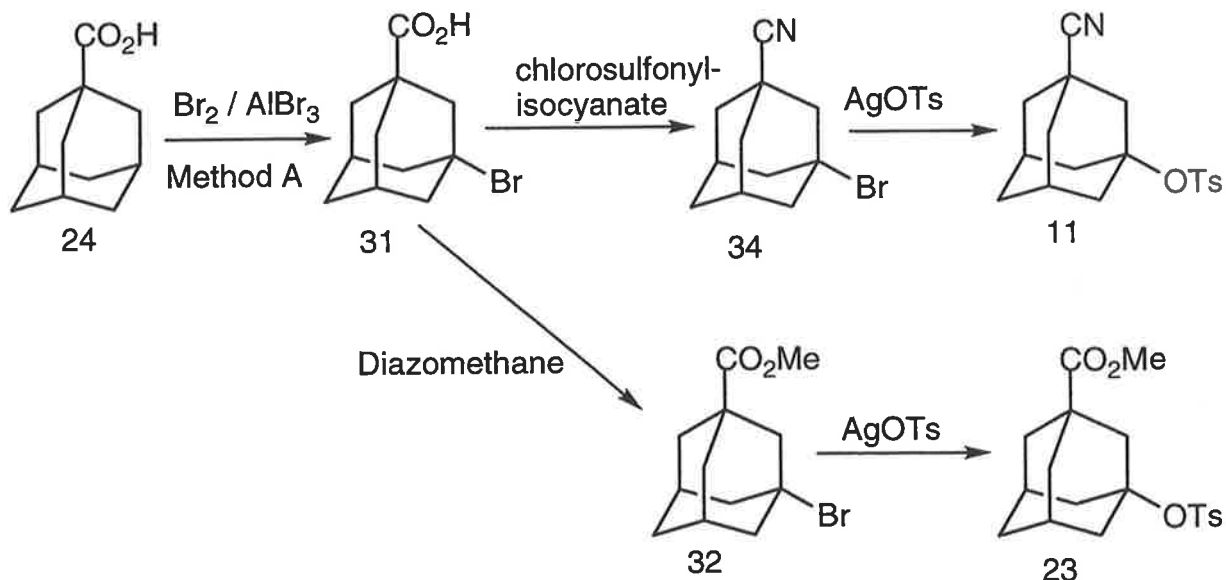


Figure 4.7: Synthetic approach to the required tosylates 11 and 23.

From the literature, bromination of the 3-position of adamantane carboxylic acid (24) would provide us with significant synthetic scope.<sup>46</sup> It has previously been shown in the literature that direct bromination could be achieved through its reaction with bromine in the presence of aluminium bromide, if the reaction conditions were stringently controlled.<sup>46</sup>

In order to reduce the synthesis of poly-brominated species, adamantane-1-carboxylic acid (24) was introduced to a stirring mixture of aluminium bromide in bromine, at a reduced temperature. The reaction was followed by TLC and crude  $^1\text{H}$  NMR analysis of micro-work up adducts. We were able to observe the formation of the desired brominated product (31), and when the reaction had reached greater than 95% completion, it was quenched with sodium metabisulfite. Isolation and partial purification from the reaction mixture was achieved through sublimation ( $120^\circ\text{C}$  @5 mmHg), giving the 1-bromo adamantyl-3-carboxylic acid (31).

#### 4.8 Introduction of a Methyl Ester Moity.

The 1-bromo adamantyl-1-carboxylic acid (31) was transformed into the respective methyl ester (32). For this reaction, the use of diazomethane as the methylating agent was found to be highly successful (Figure 4.7).

The safe use of diazomethane, when prepared *in situ*, and used immediately, could be carried out at up to a several gram scale. This methylating agent was found to be highly advantageous as, due to the reactivity of the diazomethane the reaction was seen to go to completion. In addition, the high volatility of this methylating agent resulted in easy isolation of the product (32) from the reactants, as any excess diazomethane would evaporate out of the reaction vessel if allowed to stand over night.

The desired product, methyl 3-bromo-1-adamantane carboxylate (32), was isolated as a white crystalline low melting point solid (34°C) and judged to be >95% pure by <sup>1</sup>H NMR. However, a small amount of methyl 3-hydroxy-1-adamantane carboxylate (33) could not be readily removed by sublimation due to the low melting point, or by chromatography as the ester was somewhat sensitive to silica.

#### 4.9 Alternate Approach to the Desired Ester (32).

While the previous synthesis yielded the desired product, it was essential to ensure the absolute purity of the final substrates prior to carrying out the kinetic studies. As the purification of the ester (32) was problematic from the previous approach, it was decided to attempt the synthesis through an alternate approach.

From the success of the use of hydrogen bromide in acetic acid as a brominating agent on 3-phenyl-1-adamantanol (28), led us to speculate that a similar approach may be possible for the synthesis of the desired 3-bromo-1-adamantane carboxylic acid (32) (Figure 4.8).

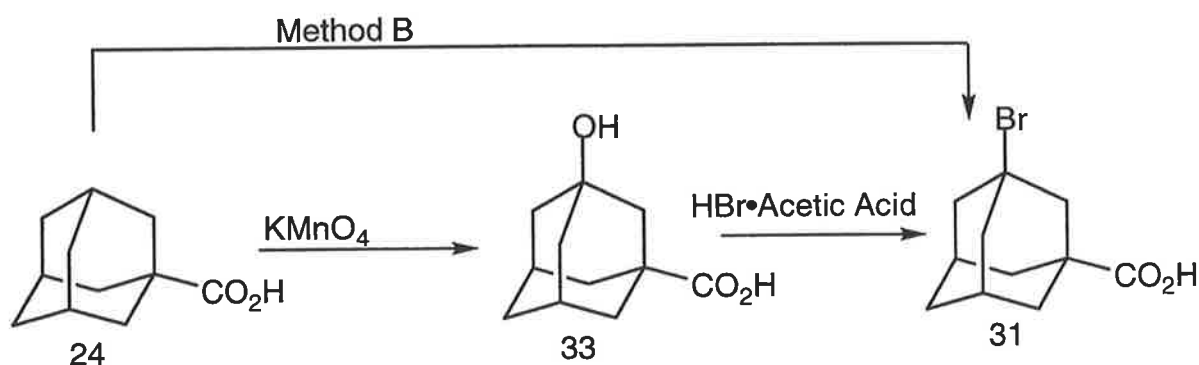


Figure 4.8: Oxidation of 1-adamantane carboxylic acid (24) followed by bromination to give the precursor 31 (via Method B).

As indicated above (Figure 4.8), the required precursor 3-hydroxy-1-adamantane carboxylic acid (33) was synthesised through the oxidation of the 1-adamantane carboxylic acid (24) with potassium permanganate in aqueous potassium hydroxide under reflux for three hours, following a literature procedure.<sup>47</sup> Isolation of the desired product (33) was achieved through continuous extraction of the aqueous solution with chloroform over 40 hours. Purification was achieved through recrystallisation from an acetone/water solution (90:10) providing the desired alcohol (33) in good yield (75%).

The alcohol (33) was then brominated, through reaction with an excess of hydrogen bromide in acetic acid under reflux for two hours. Following work-up and isolation of the desired bromide (31) purification was carried out utilising fractional sublimation, initially at high temperature (130°C, 0.005 mmHg), giving a rapid sublimation of the product and starting materials from any polybrominated impurities and then a second slower sublimation (70°C, 0.005 mmHg) to isolate and purify the desired product (31) in good yield (72%) (Figure 4.8).

As before, the 3-bromo-1-adamantane carboxylic acid (31) was then esterified, with diazomethane, to furnish the required methyl ester (32) in a near quantitative yield (Figure 4.8). In addition, this second approach allowed us to ensure the purity of the bromide (31) prior to esterification, and thus allowed us to synthesise the ester (32) in absolute purity, as observed by <sup>1</sup>H NMR, in 97% yield.

The ester (32) was then used in the synthesis of methyl 3-[(tosyl)oxy]-1-adamantane carboxylate (23) through tosyl halide exchange with silver tosylate (yield 86%), which was used for the kinetic studies (Figure 4.7).

#### **4.10 Introduction of a Cyano Group.**

In addition to the esterification reaction described above, the prepared 3-bromo-1-adamantane carboxylic acid (32) was also utilised as a precursor to the required cyano substrate. This was achieved following a literature procedure, which involved through allowing a portion of the acid (32) allowed to react with chlorosulfonyl isocyanate in dry dichloromethane under reflux for 3 hours, followed by the addition of triethylamine and a further 5 hours under reflux

conditions.<sup>48</sup> This yielded 3-cyano-1-adamanty bromide (**34**) as shown above (Figure 4.8).

<sup>1</sup>H NMR analysis of the crude reaction mixture indicated that the transformation of the carboxylic acid to the cyano group was greater than 95% complete at the end of the reaction time. Isolation and purification of the desired product (**34**) was, however, difficult as the product was prone to decomposition at temperatures greater than 60°C. Consequently, the use of slow, cold sublimation over several days, was required in this purification, which provided a fair yield (58%).

The synthesis of 3-cyano-1-adamantanol (**35**) was attempted, with the hope that on formation, isolation from the reaction mixture would be easier than that of the bromide (**34**) (Figure 4.9).

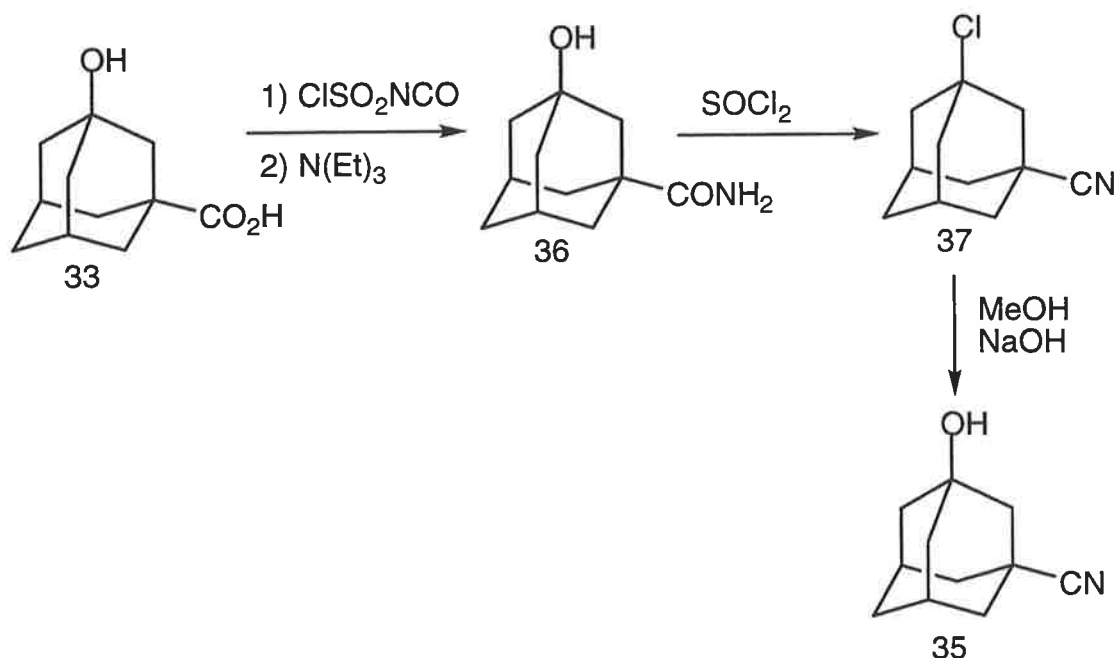


Figure 4.9: Approach to 3-cyano-1-adamantanol (**35**).

The reaction between 3-hydroxy-1-adamantane carboxylic acid (**33**) and chlorosulfonyl isocyanate yielded an insoluble brown mixture (60%). Crude IR analysis led us to believe that the solid contained 3-hydroxy-1-adamantane carboxamide (**36**). An attempt to dehydrate this mass was made, using sulfonyl chloride under reflux over night. Following the removal of the excess sulfonyl chloride, 3-cyano-1-adamantyl chloride (**37**) was isolated from the reaction

mixture in fair yield (48%). This chloride was then hydrolysed with sodium hydroxide in aqueous methanol, and the desired 3-cyano-1-adamantanol (35) was isolated and purified by sublimation (37%). The yield of the entire synthesis was unfortunately low (11%) and consequently this approach was not further elaborated.

Consequently, following slow sublimation, the 3-cyano-1-adamantyl bromide (34) was converted to the respective tosylate (11) through tosyl-halide exchange.<sup>42</sup> Due to the thermal instability of the bromide (34), the exchange reaction was limited to a temperature range maintained below 60°C. Subsequently, the reaction time required for this exchange was 1 week. After this time, the reaction was quenched, and the desired tosylate (11) was isolated and purified by flash chromatography (100% dichloromethane,  $R_f = 0.35$ ). While the isolate yield of this exchange reaction was poor (35%) we were able to isolate sufficient quantities of the analytically pure tosylate (11) to carry out the required kinetic experiments (Figure 4.7).

#### **4.11 Synthetic Approaches to Other Substrates Through Reduction of the Ester (32).**

The synthesis of the remaining tosylates of interest could be achieved through the reduction of methyl 1-bromo, 1-adamantane carboxylate (32). This reduction, carried out through the use of lithium aluminium hydride in dry ether under reflux for 2 hours, provided a good yield of (3-bromo-1-adamantyl) methyl alcohol (38) after purification by recrystallisation from hexane (62%) (Figure 4.10).<sup>44</sup>

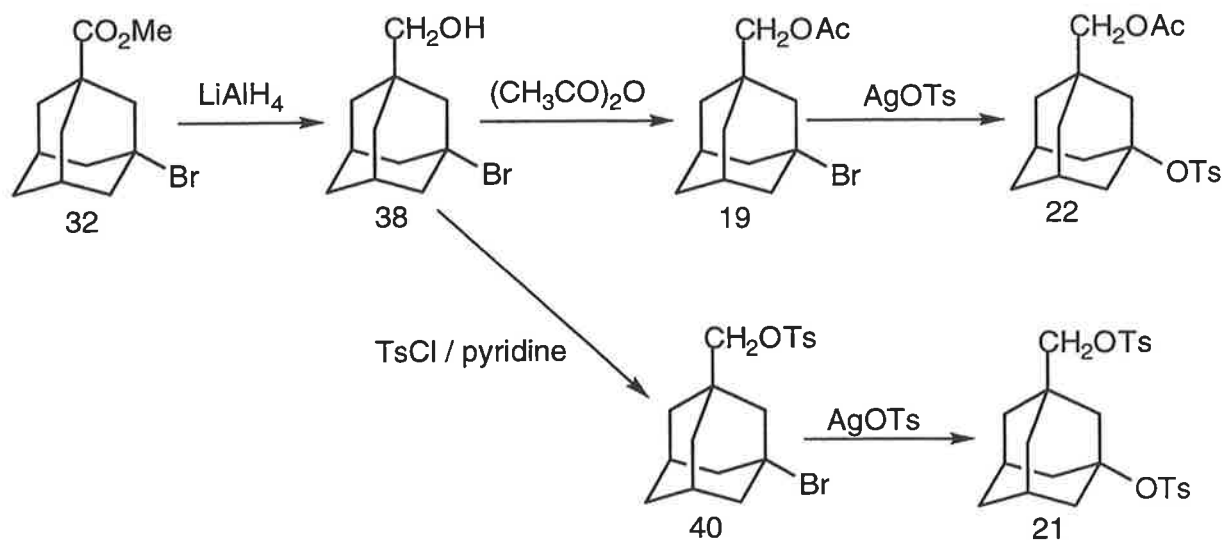


Figure 4.10: Reduction of the ester **32** to give the primary alcohol **38**, and further transformation to the desired substrates **21** and **22**.

With the primary alcohol (**38**) in hand, we were able to further convert the system, and introduce either an acetate or a tosylate at this primary site, giving (3-bromo-1-adamantyl) methyl acetate (**39**) or (3-bromo-1-adamantyl) methyl tosylate (**40**) respectively (Figure 4.10).

#### 4.12 Introduction of Primary Acetate Functionality.

An acetate group was introduced to the primary alcohol of (3-bromo-1-adamantyl) methyl alcohol (**38**) through its reaction with acetic anhydride in triethylamine with a catalytic quantity of DMAP (dimethyl aminopyridine), stirred at room temperature for sixteen hours. The desired product (3-bromo-1-adamantyl) methyl acetate (**39**) was isolated as a yellow oil in good yield (78%). It was found by  $^1\text{H}$  NMR that this oil did not require further purification, and was transformed to the required (3-[(tosyl)oxy]-1-adamantyl) methyl acetate (**22**) substrate, through a halide tosylate exchange with silver tosylate in good yield (79%) (Figure 4.10). The tosylate (**22**) was then used in kinetic experiments.



#### **4.13 Introduction of Primary Tosylate Functionality.**

Similarly, a primary tosylate grouping was introduced to (3-bromo-1-adamantyl) methyl alcohol (38) through its reaction with tosyl chloride and triethylamine in dichloromethane with a catalytic quantity of DMAP. The reaction was monitored by TLC over 48 hours. With the observation that the alcohol (38) was all consumed, the reaction was quenched. Following work-up, the desired tosyl ester (40) was isolated in low yield (30%) (Figure 4.10).

While low yielding, the isolated product (40) was isolated in excellent purity, and was further converted to (3-[(tosyl)oxy]-1-adamantyl) methyl tosylate (21) through tosyl halide exchange with silver tosylate. Which was purified by recrystallisation from diethyl ether, in moderate yield (47%) and used to collect kinetic data (Figure 4.10).

#### **4.14 Tosyl-Halide Reaction Conditions.**

The tosyl halide substitution reactions which were used in the formation of the final substrates, were carried out under various conditions, depending on the reactivity of the precursor. As summarised below (Table 4.2), the conditions ranged from room temperature to 60°C, and reaction times of from two hours to one week.

Table 4.2: Reaction conditions for the tosyl-halide exchange reaction of the precursor bromides (4, 23, 29, 34, 39 and 40) with silver tosylate.

3-R substituted 1-adamantyl bromide	Number of equivalents of silver tosylate	Reaction temperature.	Reaction time.
R = H (4)	1.5 equivalents	Room temperature	2 hours
R = Ph (29)	1.5 equivalents	60°C	2 hours
R = CH <sub>2</sub> OAc (39)	1.5 equivalents	50°C	3 hours
R = CH <sub>2</sub> OTs (40)	1.5 equivalents	40°C	18 hours
R = CO <sub>2</sub> Me (23)	1.2 equivalents	45°C	6 hours
R = CN (34)	1.7 equivalents	60°C	1 week

## Chapter 5

### **Kinetic Study of the Adamantyl System, and the Mechanistic Implications of the Results.**

#### *Abstract:*

With the successful synthesis of the desired 3-substituted 1-adamantyl tosylates, the systems were studied under solvolytic conditions. From these studies, in a range of solvent systems that provides a spectrum of solvent ionising strengths and nucleophilicities, we were able to determine the effect on the response of the system to solvent ionising strength (" $m$ ") with changes to the electron withdrawing nature of the substituent ( $\sigma_I$ ).

## 5.1 Conductometric Analysis.

With the successful preparation of the 3-substituted 1-adamantyl tosylates required to carry out the kinetic study proposed in the opening chapter, these substrates were now solvolysed in a range of binary solvent systems.

Through these kinetic experiments, carried out using the previously described BIPCON suite, we hoped to observe the effect of changes in the electron withdrawing nature of the substituent on the kinetics of the solvolysis, specifically the response of the substrates to the solvent ionising power (" $m$ ").

As described earlier, Taylor's investigation of the solvolysis of 3-substituted bicyclo[1.1.1]pentyl bromides showed an unexpected decrease in the slope of the Raber-Harris correlations for their solvolysis.<sup>22</sup> It was observed that as the electron withdrawing nature of the substituent increased, the slope of the Raber-Harris plot decreased, indicating a reduction in the " $m$ " value of the solvolysis.

Although this finding was not elaborated upon at the time of publication, we have postulated that this decrease in " $m$ " can be attributed to a subtle change in the mechanism of the solvolysis as the substituent becomes more electron withdrawing. In essence, the solvolysis is moving away from a pure  $S_N1$  mechanism towards a more  $S_N2$  like solvolysis, even though these caged systems prevent rear-side "attack" as known for a traditional  $S_N2$  mechanism.

Investigation of the known literature was unsuccessful in identifying this phenomena in other polycyclic alkane systems. However, in a series of solvolytic studies by Grob and co-workers, on 3-substituted adamantyl, 7-anti-substituted 2-exo norbornyl and 7-anti-substituted 2-endo norbornyl tosylates (Figure 5.1), the effect of changes in solvent nucleophilicity and ionising power on the solvolytic rate (ionisation) of these substituted systems, could be indirectly observed.<sup>16</sup>

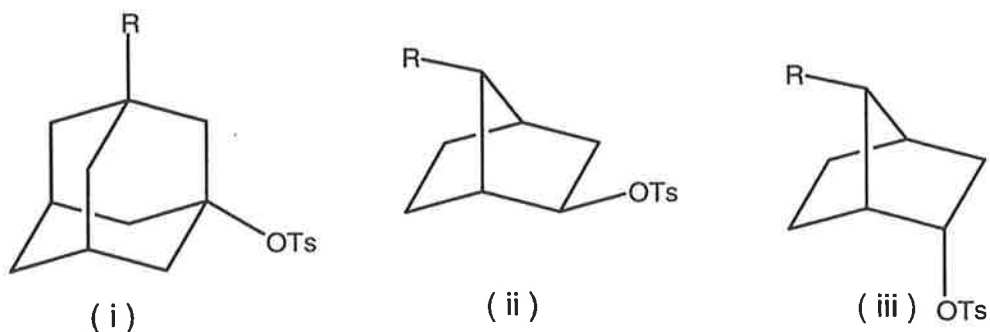


Figure 5.1: (i) 3-substituted 1-adamantyl tosylates.  
(ii) 7-anti-substituted 2-exo norbornyl tosylates.  
(iii) 7-anti-substituted 2-endo norbornyl tosylates.

Through the construction of Hammet plots, based on the solvolysis of the substrates from each series, the authors showed that in each solvent system utilised, a single linear correlation was achieved. This demonstrated that the solvolysis of these systems followed a single mechanism, which was unchanged through changes in the  $\sigma_I$  value of the substituent.

However, through comparison of the slopes of these Hammet relationships, between solvent systems, a difference could be observed (Figure 5.2).

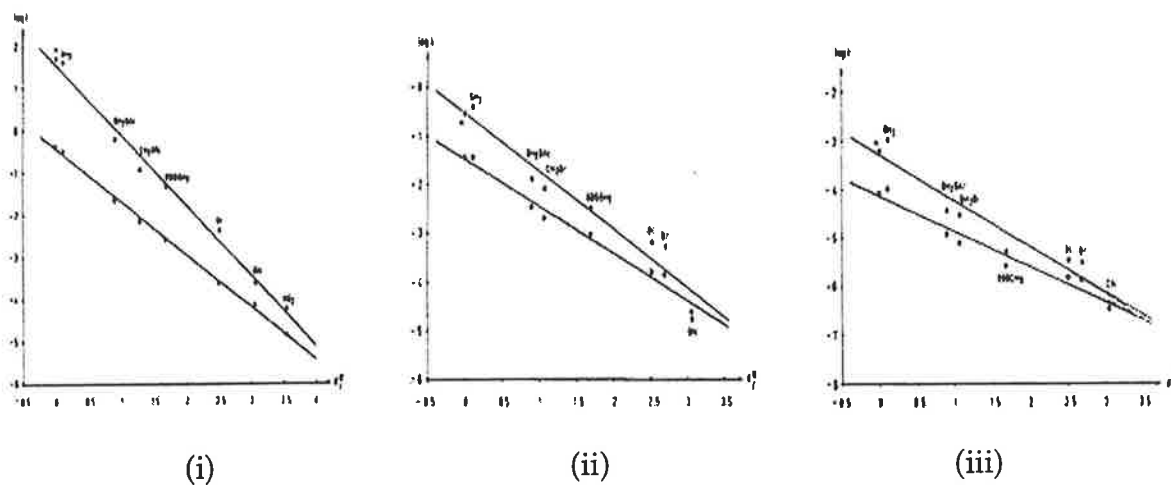


Figure 5.2: Plots of  $\log k$  for (i) 3-substituted 1-adamantyl tosylates v's  $\sigma_I$   
(ii) 7-anti-substituted 2-exo norbornyl tosylates v's  $\sigma_I$   
(iii) 7-anti-substituted 2-endo norbornyl tosylates v's  $\sigma_I$   
in 80E and 97T. Figures from reference.<sup>16</sup>

Through all three series, clear convergence between the Hammett plots generated from the solvolyses in 80% aqueous ethanol (80E) and 97% aqueous 2,2,2-trifluoroethanol (97T) could be seen. While within each solvent system a single mechanism of solvolysis could be observed, through modifying the nucleophilicity and ionising strength of the solvent, a subtle change in the solvolysis could be seen to occur. We postulated that the change observed in the changes in slope of these Hammett plots was due to the same phenomena that caused the changes in "*m*" values noted by Taylor for the bicyclo[1.1.1]pentanes.

In order to test this hypothesis, we anticipated that through analysis of the solvolysis of the substrates we had prepared in a range of solvent systems, reproduction of these converging Hammett plots would be possible. Further, generation of Raber Harris correlations for the substrates would allow us to observe any changes in the "*m*" values through changing the substituent. Through comparing the separation of the converging Hammett plots from differing solvent systems with the changes in "*m*" value for each substrate, we would be able to probe the correlation between the reduction in "*m*" and  $\sigma_I$  as further elucidated within the Introduction.

The BIPCON suite was utilised to carry out all of the kinetic experiments. Through comparison of the collected rate data with known literature values for some of the substrates in some of the solvent systems studied, we were able to validate this method of kinetic data acquisition. Further confirmation of this validity of the BIPCON data was possible through the generation of Raber Harris correlations. The generation of linear correlations for all of the substrates confirmed that the system was operating consistently and that the solvents and substrates were not contaminated.

All kinetic experiments were carried out in triplicate, with the data averaged over the three runs. The solvent systems used for the kinetic experiments were binary solvent systems based on ethanol and 2,2,2-trifluoroethanol in water. The concentration of the substrate required to carry out the solvolytic experiments was approximately 1 mmolL<sup>-1</sup>. In addition, when utilising one of the ethanol based binary solvents, the substrate was buffered with 1.1 molar equivalents of 2,6 lutidine.

## 5.2 Solvolytic study of 1-adamantyl tosylate (10) ( $\sigma_I = 0$ ).

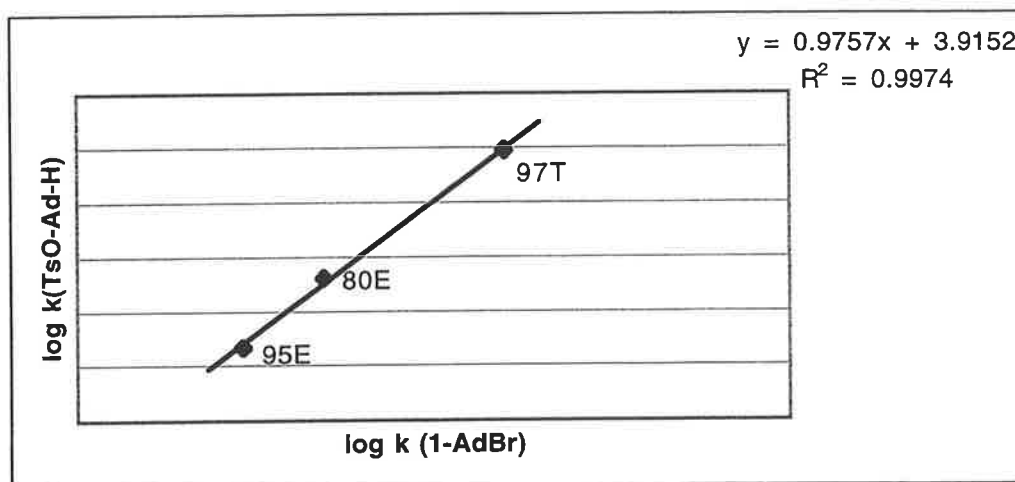
The first substrate analysed with the BIPCON suite was 1-adamantyl tosylate (10). Utilising the prepared 80E and 95E binary solvent systems, the solvolysis of (10) was observed at 25°C.. As the solvolysis of (10) had been previously studied by other groups, we were able to use the accumulated rate data from the BIPCON suite for this substrate as a test of the BIPCON calibration.<sup>14,16</sup>

It is worth noting that the solvolysis of (10) in 80E at 25°C, was carried out with a half life of 168 seconds. It would have been highly difficult if at all possible to follow this solvolysis utilising other kinetic techniques without adjustment of the reaction temperature. Although, unable to follow the solvolysis of (10) in 97T at 25°C, this result allowed us to proceed with the knowledge that with the exception of this one point, that was readily available from the literature, all the kinetic data would be available through analysis at 25°C. This meant that we would be able to carry out the kinetic study without the need to extrapolate our data to allow for temperature changes, which would eliminate one known source of error.

The solvolytic rate data for each of the substrates analysed, in each of the binary solvent systems at 25°C is detailed below (Table 5.1).

Thus, with the inclusion of the kinetic data for the solvolysis of (10) in 97T as described by Grob,<sup>16</sup> we were able to generate a Hammett correlation for the solvolysis of (10) against the known solvolysis of 1-adamantyl bromide (4) (Chart 5.1).<sup>1,12,13</sup>

Chart 5.1: The Raber Harris plot of the solvolysis of 1-adamantyl tosylate (10) versus the solvolytic rate for 1-adamantyl bromide (4).



As can be seen above, upon plotting the kinetic data for 1-adamantyl tosylate (10) against the rate data for 1-adamantyl bromide (4), we obtained a linear correlation, with a slope, or “*m*” of 0.976. This result, close to the anticipated theoretical value of unity, confirmed that the BIPCON system, the solvents and the substrate were all prepared to the required analytical standard.

The slight deviation of the “*m*” value from the theoretical value of unity was anticipated due to the different leaving groups analysed. The literature values used to generate the Raber-Harris plot described the solvolysis of 1-adamantyl bromide (4), which we were comparing to 1-adamantyl tosylate (10). These two leaving groups would be stabilised by the solvent to different extents, and thus there would be minor differences in the rates of these substrates between the bromide and the tosylate.

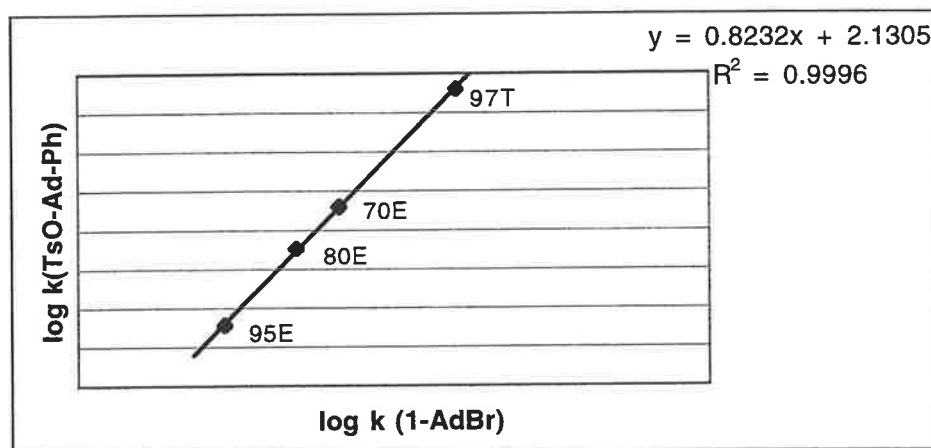
This linear correlation giving an “*m*” value close to unity confirmed that the 1-adamantyl system underwent  $S_N1$  solvolysis, and that while the leaving group would effect the rate of solvolysis, the overall effect on the mechanism was inconsequential.

### 5.3 Solvolytic Study of 3-Phenyl, 1-Adamantyl Tosylate (15) ( $\sigma_I = 0.12$ ).

The next substrate analysed solvolytically with the BIPCON suite 3-phenyl,1-adamantyl tosylate (15). There had not previously been kinetic data published for this substrate and thus, we undertook to observe the solvolysis of this tosylate (15) in 80E, 97T, 95E and 70E.

Once all of the kinetic data had been collected, the results used to generate a Raber Harris plot for this substrate (15) (Chart 5.2).

Chart 5.2: The Raber Harris plot of the kinetic rate data generated through the solvolysis of 3-phenyl-1-adamantyl tosylate (15) versus the solvolytic rate for 1-adamantyl bromide (4).



A linear correlation between the rates of solvolysis of (15) and 1-adamantyl bromide (4) was observed. The "m" value for this substrate was determined to be 0.823. As there had not previously been any data published for the solvolysis of this substrate (15) we were unable to confirm the validity of the data collected. However, the linearity of the plot indicated that the data was consistent across the range of binary solvent systems, and thus indicated that the collected kinetic data was reliable.

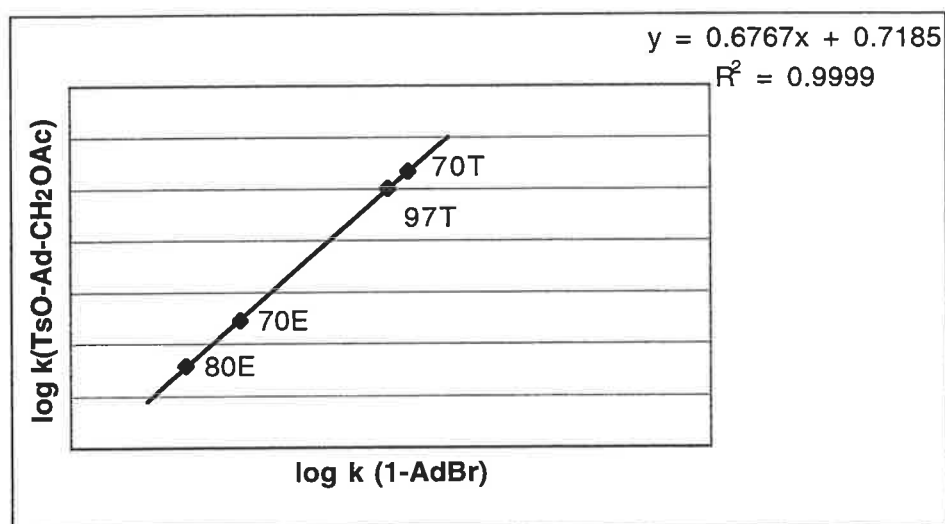
The "m" value determined for this substrate (15) did deviate from the theoretical value of unity, which was consistent with the hypothesis outlined previously.



#### 5.4 Solvolytic Study of (3-[(tosyl)oxy]-1-adamantyl) methyl acetate (22) ( $\sigma_I = 0.15$ ).

The solvolysis of (3-[(tosyl)oxy]-1-adamantyl) methyl acetate (22) was observed in 80E, 97T, 70E and 70T. Again, with the completion of the kinetic experiments, the rate data was used to generate a Raber Harris plot for this substrate (22) (Chart 5.3).

Chart 5.3: The Raber Harris plot of the kinetic rate data generated through the solvolysis of (3-[(tosyl)oxy]-1-adamantyl) methyl acetate (22) versus the solvolytic rate for 1-adamantyl bromide (4).

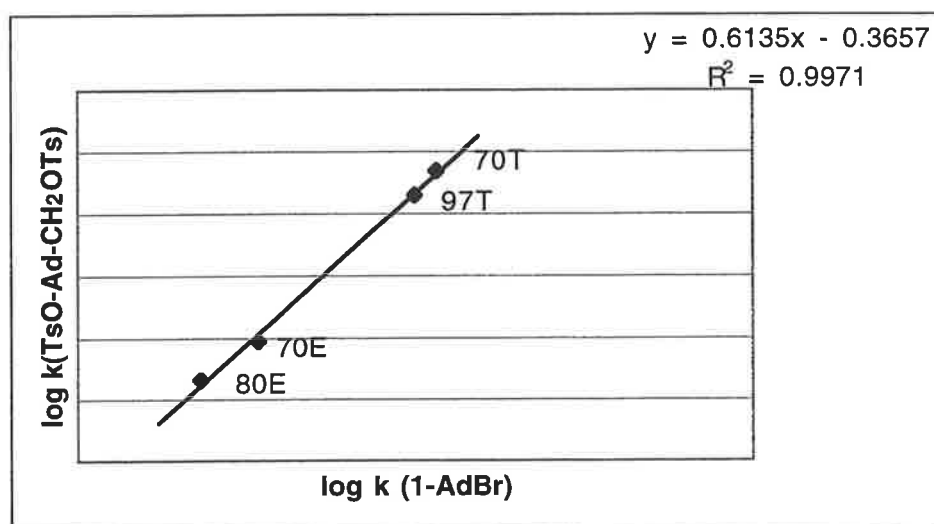


Analysis of this Raber-Harris correlation showed a linear correlation with an "m" value determined to be 0.677. The 80E and 97T data points were able to be confirmed against values from the known literature.<sup>16</sup> This established that the remaining data points were true, given the linearity of the correlation. This linearity indicated that the substrate was undergoing  $S_N1$  solvolysis as anticipated. However, the deviation of the determined "m" value from unity was significantly large to indicate that the mechanism was digressing from a pure  $S_N1$ .

### 5.5 Solvolytic Study of (3-[(tosyl)oxy]-1-adamantyl) methyl tosylate (21) ( $\sigma_I = 0.23$ ).

The solvolysis of (3-[(tosyl)oxy]-1-adamantyl) methyl tosylate (21) was carried out in 80E, 97T, 70E and 70T. The kinetic rate data collected was used to generate a Raber-Harris plot as shown below (Chart 5.4).

Chart 5.4: The Raber Harris plot of the kinetic rate data generated through the solvolysis of (3-[(tosyl)oxy]-1-adamantyl) methyl tosylate (21) versus the solvolytic rate for 1-adamantyl bromide (4).



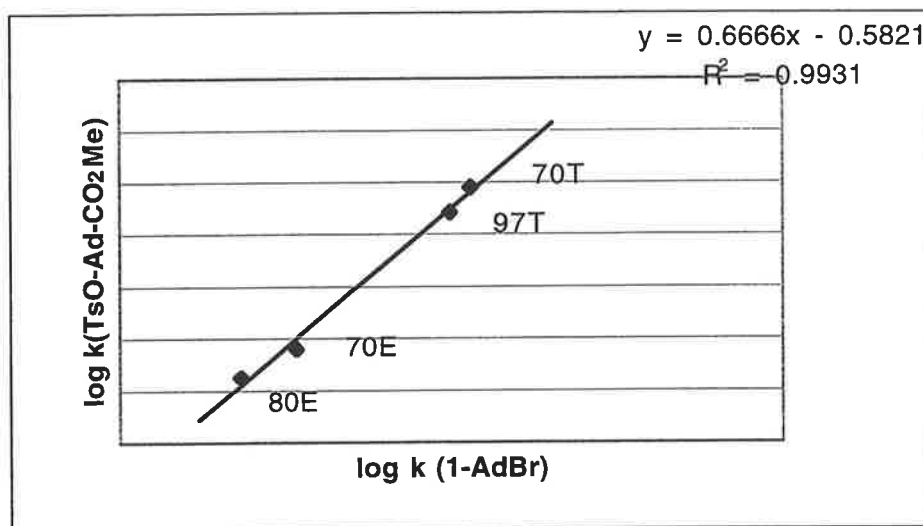
From this linear correlation, an "m" value of 0.614 was determined for this tosylate (21). This again showed a significant deviation from the theoretical value of unity, and was further indicative of the solvolysis moving away from a pure  $S_N1$  mechanism. However, the plot was still linear, which indicated that the nucleophilicity of the solvent was not directly effecting the solvolysis of the substrate (21).

### 5.6 Solvolytic Study of Methyl 3-[(tosyl)oxy]-1-Adamantane Carboxylate (23) ( $\sigma_I = 0.32$ ).

The solvolysis of methyl 3-[(tosyl)oxy]-1-adamantane carboxylate (23) was carried out in 80E, 97T, 70E and 70T. This range of solvents provided a diverse array of solvent conditions and thus gave a wide range of data points. The kinetic rate

data established from these solvolyses was used in the generation of a Raber Harris plot (Chart 5.5).

Chart 5.5: The Raber Harris plot of the kinetic rate data generated through the solvolysis of methyl 3-[(tosyl)oxy]-1-adamantane carboxylate (**23**) versus the solvolytic rate for 1-adamantyl bromide (**4**).



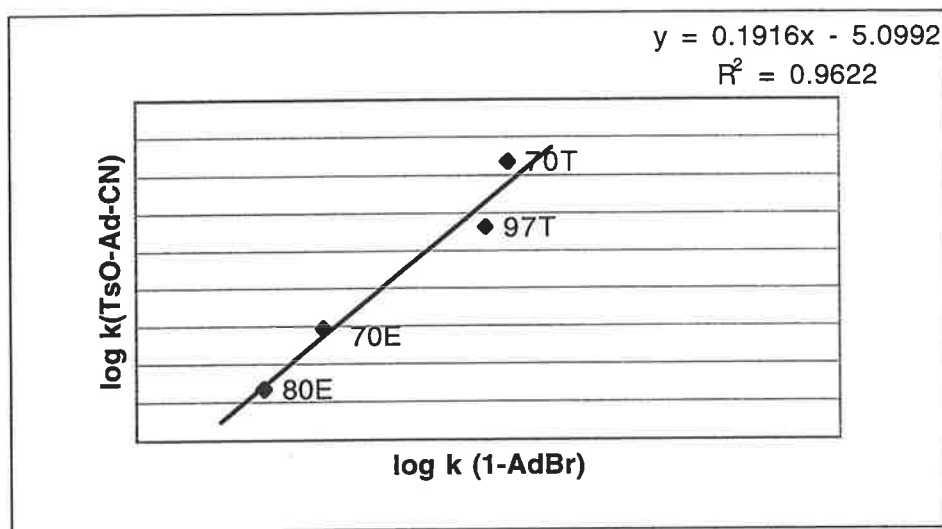
The “*m*” value determined from the Raber Harris plot for this tosylate (**23**) was found to be 0.667. This value, again highly divergent from the theoretical value of unity, was greater than anticipated from the trend developing from the previous experimental data collected, based on a correlation between “*m*” and  $\sigma_I$ .

There was, however, no reason to doubt the validity of the data collected for this substrate (**23**) as the Raber-Harris correlation was again linear, and some of the data collected could be validated against known literature values.<sup>16</sup>

### 5.7 Solvolytic Study of 3-Cyano 1-Adamantyl Tosylate (**11**) ( $\sigma_I = 0.57$ ).

The solvolysis of 3-cyano 1-adamantyl tosylate (**11**) was carried out in 80E, 97T, 70E and 70T. The half lives associated with these solvolytic experiments was significantly greater than any of the previous experiments with some experiments requiring up to a month to complete the required data collection. This time factor, however, proved no obstacle for the BIPCON suite and the collected kinetic data was used in the generation of a Raber Harris plot (Chart 5.6).

Chart 5.6: The Raber Harris plot of the kinetic rate data generated through the solvolysis of 3-cyano 1-adamantyl tosylate (**11**) versus the solvolytic rate for 1-adamantyl bromide (**4**).



From the correlation obtained, an “*m*” value for 3-cyano 1-adamantyl tosylate (**11**) was determined to be 0.192. This value, normally associated with a pure  $S_N2$  mechanism indicated that the rate was now also not reliant on the solvent ionising power. The linearity of the correlation, while not ideal still indicated that this was not an  $S_N2$  mechanism, nor an  $S_N1$ , but falling somewhere in between.

### 5.8 Observation of the Developing Trend in “*m*” Value Decrease.

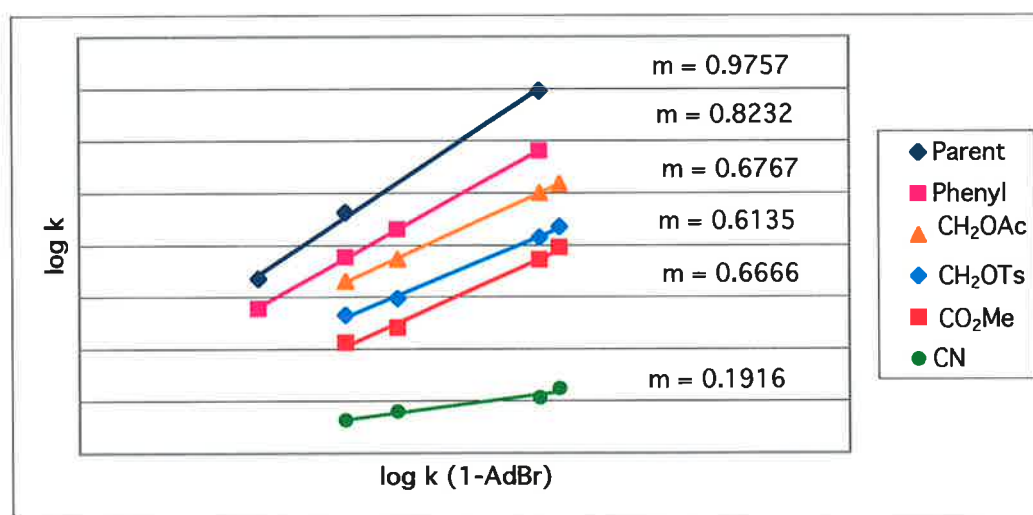
Observation of the kinetic data from all of the solvolytic experiments carried out, shows that the decrease in the “*m*” value generally relates to the electron withdrawing nature of the substituent (Table 5.1).

Table 5.1: The experimental kinetic rate data collected for the tosylates **10**, **11**, **15**, **21**, **22** and **23**. In addition, the generated “*m*” values and the  $\sigma_I$  values for these substrates. The  $\sigma_I$  values were obtained from Progress in Physical Organic Chemistry.<sup>49</sup>

	$\sigma_I$	80E	97T	70T	70E	95E	“ <i>m</i> ” value
H	0	-2.374	-0.041 <sup>16</sup>	-	-	-3.65	0.9757
Ph	0.12	-3.234	-1.196	-	-2.694	-4.219	0.8232
CH <sub>2</sub> OAc	0.15	-3.706	-1.999	-1.831	-3.271	-	0.6767
CH <sub>2</sub> OTs	0.23	-4.342	-2.85	-2.648	-4.027	-	0.6135
CO <sub>2</sub> Me	0.32	-4.875	-3.286	-3.049	-4.596	-	0.6666
CN	0.57	-6.364	-5.937	-5.765	-6.205	-	0.1916
1-Ad-Br <sup>1,12,13</sup>		-6.553	-4.022	-3.767	-5.876	-7.68	

This perceived trend in the decrease in “*m*” value with an increase in the electron withdrawing nature of the substituent can clearly be seen with the presentation of all of the Raber Harris plots for these substrates as a single graph, as shown below (Chart 5.7).

Chart 5.7: The Raber Harris plots of the tosylates **10**, **11**, **15**, **21**, **22** and **23** versus  $k_0$ , 1-adamantyl bromide (**4**).



### 5.9 Hammett Relationship Between the Rate of Solvolysis and the Electron Withdrawing Nature of the Substituent ( $\sigma$ ).

Interpretation of this apparent trend would be inappropriate, unless it could be shown that the observed actions upon each of the tosylates, under solvolytic conditions were conserved across the range of substituents.

In order to show that the observed decrease in the "m" value was not due to isolated fluctuations between the tosylates, Hammett plots of the rates of solvolysis of the substrates against the  $\sigma$ I value of their substituent were generated (Charts 5.8, 5.9, 5.10 and 5.11).

Chart 5.8 Hammett plot of the rate of solvolysis in 80E of tosylates 10, 11, 15, 21, 22 and 23 versus the  $\sigma$ I value of their substituent.

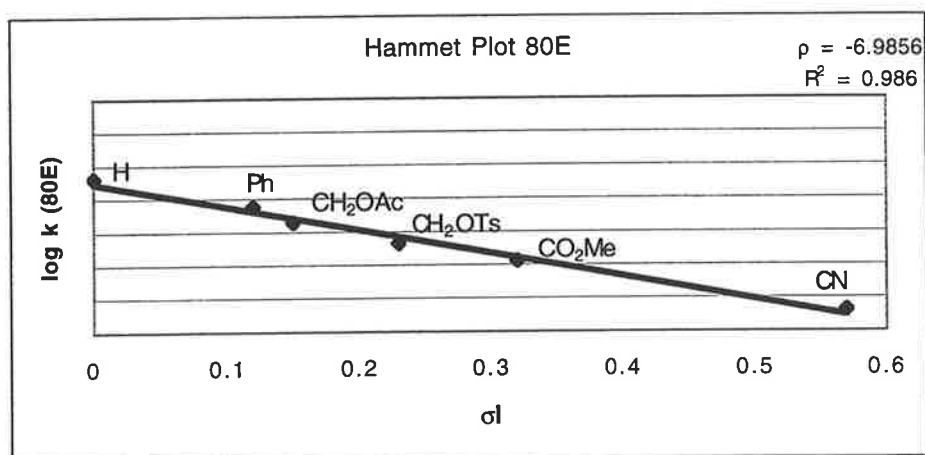


Chart 5.9 Hammett plot of the rate of solvolysis in 97T of tosylates 10, 11, 15, 21, 22 and 23 versus the  $\sigma_I$  value of their substituent.

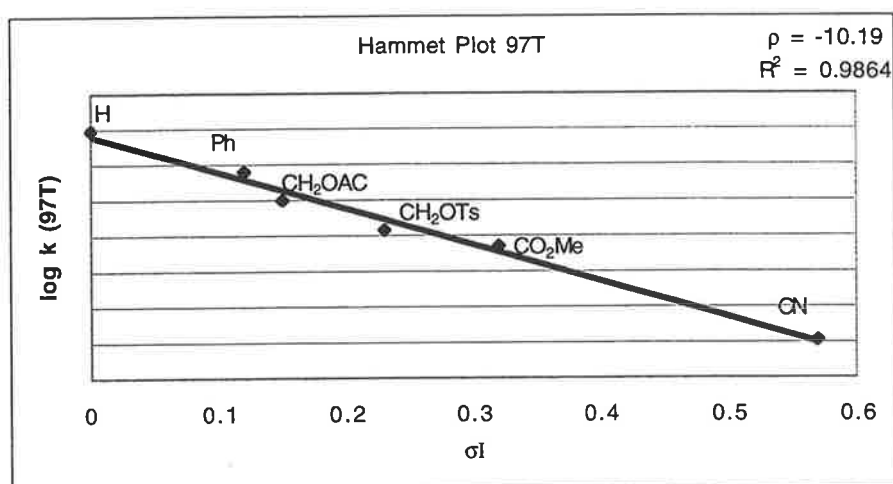


Chart 5.10 Hammett plot of the rate of solvolysis in 70T of tosylates 11, 21, 22 and 23 versus the  $\sigma_I$  value of their substituent.

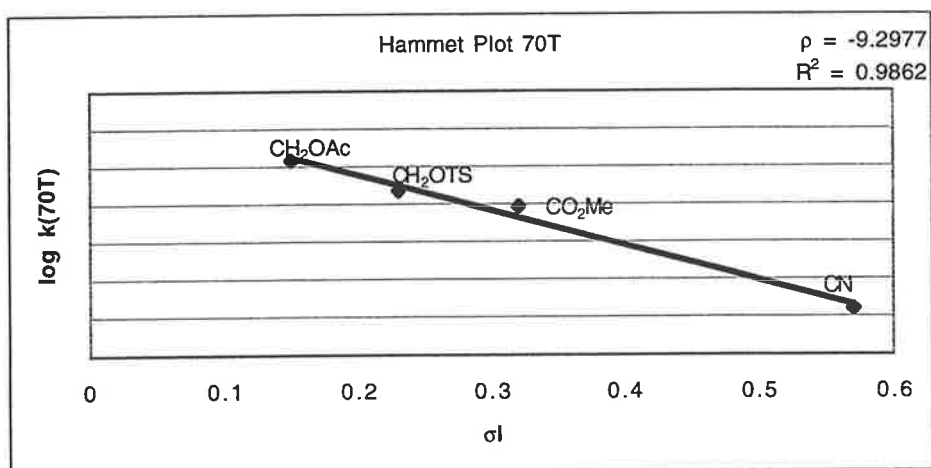
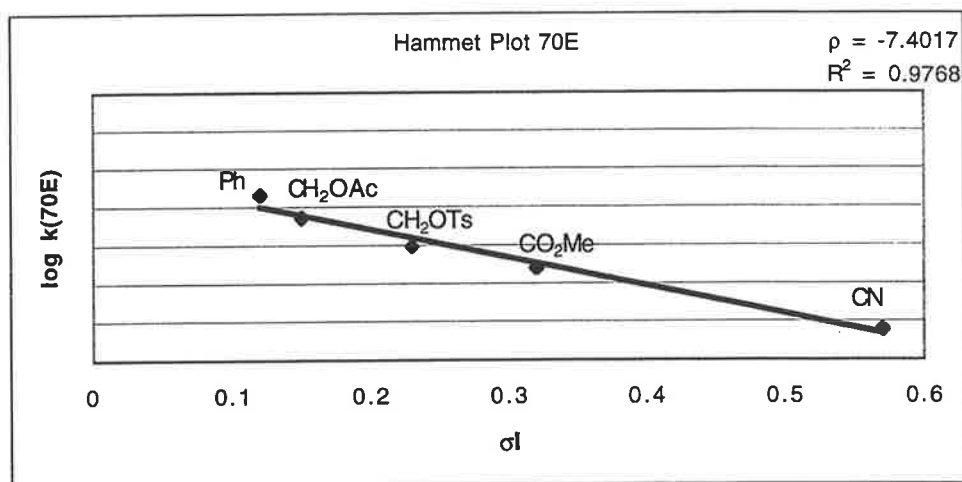


Chart 5.11 Hammett plot of the rate of solvolysis in 70E of tosylates 11, 15, 21, 22 and 23 versus the  $\sigma_I$  value of their substituent.



As can be clearly seen, there is a linear relationship between the rate of solvolysis of the tosylates, against the  $\sigma_I$  values for their substituents in each of the solvent systems. This linearity confirms that there is no change in the mechanism of solvolysis of the tosylates as the 3-substituents on the adamantyl system become more withdrawing.

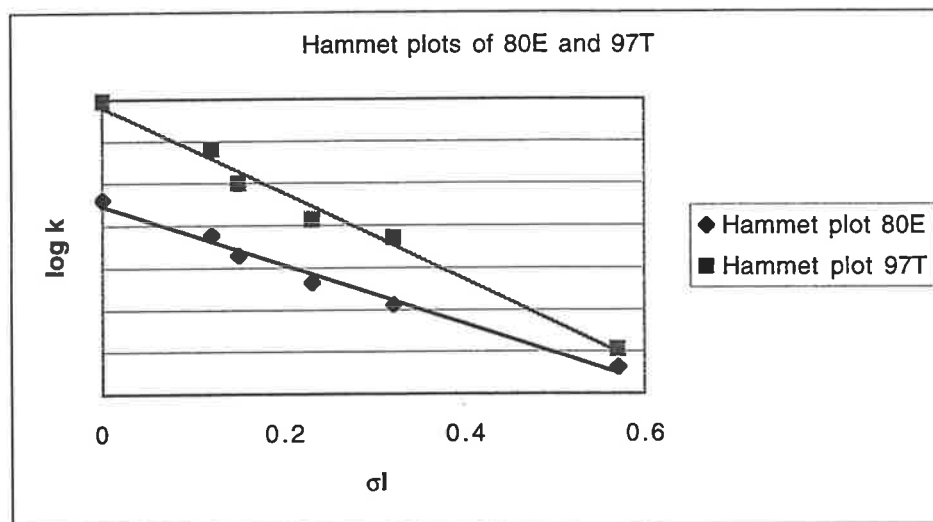
Consequently, the change in "m" value with an increase in the electron withdrawing nature of the substituent could not be dismissed as isolated fluctuations between the tosylates. The observation of the linearity of the Hammett relationships confirmed that while the presence of a remote electron withdrawing group on the adamantyl system would reduce the rate of the solvolysis, this solvolysis proceeded via the same mechanistic pathway.

### 5.10 Investigation of the Convergence Between the Hammett Plots.

In addition, on comparison of the Hammett correlations, it was clear, that while each displayed a linear correlation between the rate of solvolysis of the tosylates and the  $\sigma_I$  value of the substituent, the slope of the plots, referred to as the  $\rho$  value, were significantly different. This indicated that depending on the solvent system used in the solvolysis, the substrates were responding differently. This was the Hammett convergence observed in the kinetic studies carried out by Grob.<sup>16</sup> In order to confirm that this convergence was occurring, the Hammett plots for 80E and 97T were generated simultaneously (Chart 5.12).



Chart 5.12: Hammett plots of the rate of solvolysis in 97T and 80E of tosylates 10, 11, 15, 21, 22 and 23 versus the  $\sigma_I$  value of their substituent.



The convergence of the Hammett plots observed by Grob,<sup>16</sup> was clearly seen to be reproduced from our kinetic data. A comparison of the ratio between the distance between the two Hammett plots, relative to the separation of these plots at the  $\sigma_I$  value for the parent system (10) versus the “*m*” values determined for each of the substituents was carried out (Table 5.2).

Table 5.2: Correlation between the separation of the Hammett plots of the tosylates 10, 11, 15, 21, 22 and 23 in 80E and 97T with the “*m*” values from their individual Raber Harris plots.

R	Plot separation	Ratio	“ <i>m</i> ” value
H	35	1	0.976
Ph	29	0.857	0.823
CH <sub>2</sub> OAc	27	0.771	0.677
CH <sub>2</sub> OTs	22	0.629	0.614
CO <sub>2</sub> Me	20	0.571	0.667
CN	7	0.2	0.192

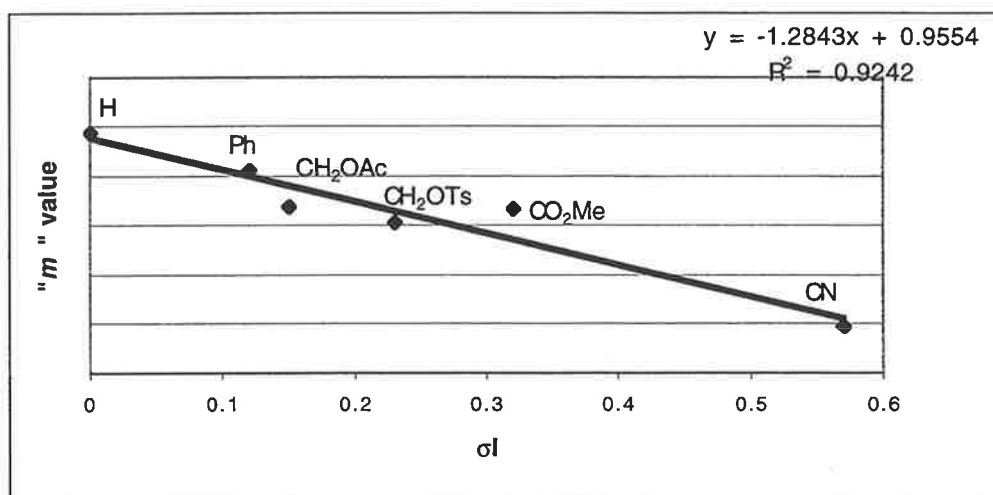
From the ratio of the plot separations, with the assumption that the parent system (10) would have a theoretical “*m*” of one, a close approximation of the decrease in “*m*” value is observed for most substrates. An investigation into presence of a correlation between “*m*” and  $\sigma_I$  was thus undertaken.

### 5.11 Investigation of the Relationship Between “*m*” and $\sigma_I$ .

In order to appreciate the relationship between the “*m*” value and the electron withdrawing nature of the substituent, care was required in ensuring that no other external factors were interfering with the determined rate of solvolysis. As we had carried out all of our kinetic experiments, utilising the BIPCON suite, at a constant temperature of 25°C, and in analytically prepared solvent systems, we were confident that the conditions under which each of the tosylates had been examined was consistent and reliable.

Through the generation of a plot of the “*m*” values of the tosylates 10, 11, 15, 21, 22 and 23 against their respective  $\sigma_I$  values, we could observe a distinct pattern in the response of the substrate to the solvolytic conditions as the substituent became more withdrawing (Chart 5.13).

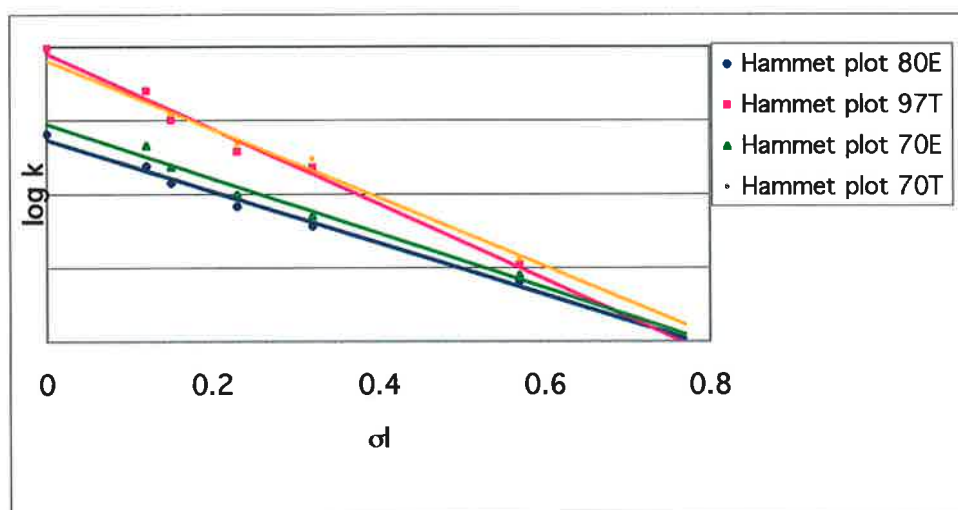
Chart 5.13: The relationship between the determined “*m*” values for the tosylates 3, 6, 21, 23, 18 and 16 and the  $\sigma_I$  values of their substituents.



This trend, however, was not ideal. If we utilised two points that fell on the line of best fit, such as the parent system (10) and the cyano substituted system (11) we could quite accurately predict the rate data for other systems which fell onto this line. However, the use of this correlation to predict data systems, such as the methyl ester substituted system (23) would show considerable deviation from the experimental result. This finding prevented us at this time from describing a general equation for this trend between  $\sigma_I$  and " $m$ ".

Further analysis of the convergence of the Hammett plots generated from the kinetic data, showed a further complication in our attempt to describe the relationship between  $\sigma_I$  and " $m$ ". As anticipated, the Hammett plots from the different solvent systems converged, as seen for 80E and 97T above. However, the convergence was inconsistent. (Chart 5.14).

Chart 5.14: Hammett plots of the rates of solvolysis in 97T, 70T, 70E and 80E of the tosylates 10, 11, 15, 21, 22 and 23 versus the  $\sigma_I$  value of their substituents.



While the convergence of the 80E and 97T Hammett plots could be seen to approximate the decrease in " $m$ " value of the substrates, this was not consistent across a range of solvent systems. The rate of convergence of the Hammett plots was seen to be significantly different between various solvent pairs, and provided multiple points of convergence. Had the correlation between  $\sigma_I$  and " $m$ " been a simple linear association as initially suspected, we would have anticipated a more consistent response between the various solvent pairs.

Consequently, we have been unable at this time to formulate an accurate description of the correlation between  $\sigma_I$  and " $m$ " although, this work does suggest that such a correlation exists. The trend observed from the kinetic analysis of these 3-substituted, 1-adamantyl tosylates indicates that these systems are not undergoing a purely  $S_N1$  solvolysis as described earlier, but undergo this solvolysis with a degree of nucleophilic assistance, the extent of which is dependant on the withdrawing nature of the remote substituent.

The observed solvolytic mechanism appears to be determined by the stability of the intermediate carbocation. In the presence of a poor electron withdrawing substituent, the formation of a stable bridgehead carbocation on the adamantyl system can occur readily. Thus for the low  $\sigma_I$  systems studied, the solvolysis is controlled through the ionising strength of the solvent, and consequently, the observed " $m$ " value is close to the theoretical value of unity. However, as the substituent becomes more withdrawing, the formation of a free carbocation becomes more difficult, as the build up of the positive charge is destabilised by the substituent. Consequently, the effect of the ionising power of the solvent is diminished.

In the presence of a strongly electron withdrawing substituent, formation of a discrete cation will be disfavoured through destabilisation. Trapping will thus occur at the formation of a close ion pair, and not following ionic separation. This process could then be accelerated through the nucleophilicity of the solvent system, which through front side attack of the close ion pair would significantly accelerate the rate of solvolysis. Through this we would no longer be observing a traditional  $S_N1$  mechanism, but a process intermediary to the processes of  $S_N1$  and  $S_N2$  described in text books.

Consequently, although the 1-adamantyl system is able to "model"  $S_N1$  behaviour when unsubstituted, or in the presence of a low  $\sigma_I$  substituent, these results clearly indicate that through the modification of this substituent to a more electron withdrawing group, a subtle change in the mechanism of the solvolysis occurs, resulting in the solvolysis proceeding via a hybrid  $S_N1 / S_N2$  mechanism.

Through further study of this phenomena, a precise description of this trend away from a pure  $S_N1$  mechanism may be possible. This would allow for the

development of an accurate prediction method for kinetic data, from a small subset of solvolytic experiments. This would then possibly lead to the development of an universal equation describing solvolytic behaviour.

Investigation of this phenomena, in other "model  $S_N1$ " systems would provide both an understanding of the general application of this hypothesis, as well as provide more information towards describing the observed trend in the decrease in " $m$ " with an increase in the  $\sigma_I$  of the substituent.

**Synthetic Approach to Further Systems of Kinetic Interest Through the Trapping of the 3-Halobicyclo[1.1.1]pent-1-yl Cation.**

*Abstract:*

The solvolysis of bicyclo[n.1.1]alkanes ( $n = 1 - 3$ ) is known to occur at a rate greater than anticipated from stability of their respective bridgehead cations alone.<sup>50</sup> The intermediate cations for the bicyclo[2.1.1]hexyl and bicyclo[3.1.1]heptyl systems have been previously captured,<sup>20,51</sup> however, there have been few examples of the trapping of the bicyclo[1.1.1]pentyl cation.<sup>52</sup> Through the use of an excess of an external nucleophilic source, we have been able to trap this cation, and synthesise novel, and kinetically interesting substrates, in addition to improving yields of previously synthesised 1,3-disubstituted, bicyclo[1.1.1]pentanes.

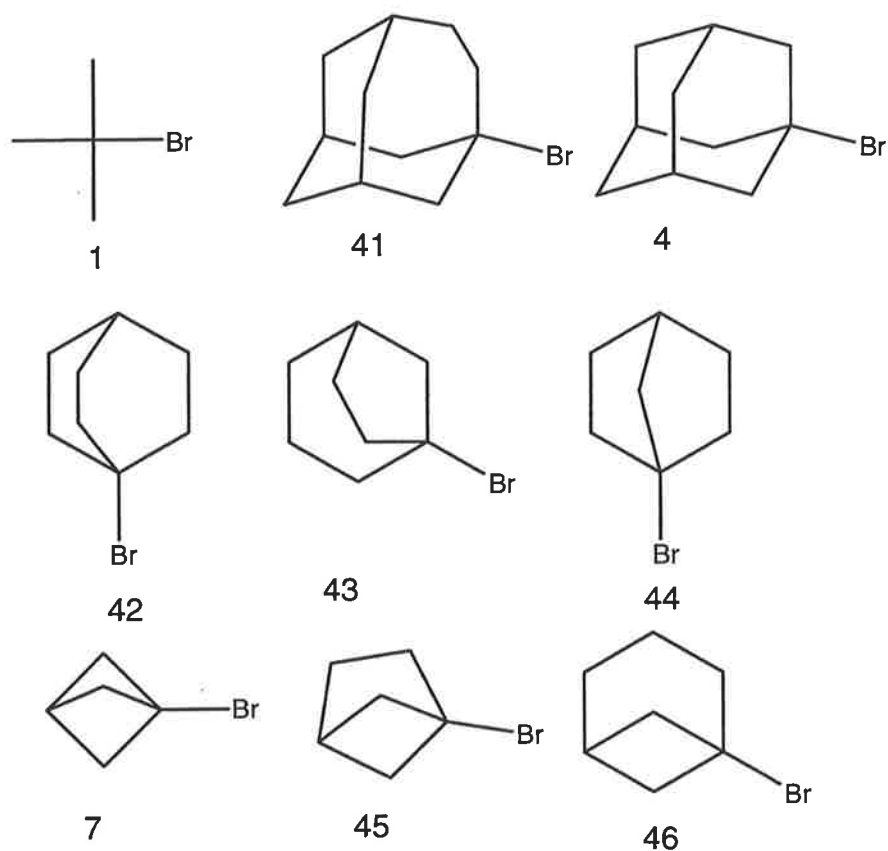
## 6.1 Preparation of Additional Solvolytic Substrates.

With the completion of the kinetic studies on the adamantyl series described in the previous chapter, other substrates of interest were pursued. From the known literature it could be seen that a wide range of polycyclic alkane systems have been utilized to determine rate constants, in order to investigate substitution and solvent effects.<sup>3,21-23,51-54</sup> This provided us with a wide scope in our choice of system to prepare. In making the choice of substrate system, consideration was made not only of the kinetic interest in the target molecules, but also in any synthetic interest that may be approached simultaneously.

The kinetics of one group of substrates was immediately of interest, as they have shown solvolytic activity vastly different to the majority of the polycyclic-alkanes.

In general, the solvolysis of bridgehead substituted polycyclo-alkanes is observed to proceed at reduced rate in comparison to their acyclic analogues.<sup>3,21-23,51-54</sup> As described earlier this has been attributed primarily to the increased difficulty of the system in achieving a planar configuration about the developing positive charge.<sup>22</sup> (Figure 6.1)

The observed trend from the comparison of the polycyclic alkanes (4, 41, 42, 43, 44) is that the greater the angle away from planarity that the carbocation is forced into, the lower the stability of the forming carbocation, and thus the slower the rate of solvolysis, relative to *t*-butyl bromide (1).



Compound	$k_{\text{rel-}t\text{-BuBr}}$	Reference
1	1.0	55
41	0.5	55
4	$10^{-3}$	56
42	$10^{-6}$	57
43	$10^{-6}$	58
44	$10^{-13}$	58
7	$\sim 3$	59
45	$\sim 10^{-6}$	60
46	7 - 10	20

Figure 6.1: Relative rates of solvolysis of some bridgehead substituted halides, relative to *t*-butyl bromide, measured in 80E at 25°C.

This correlation between the rate of solvolysis and the strain energy associated with the angle away from linearity of the forming carbocation was further confirmed by Schleyer and associates<sup>61,62</sup> and more recently by Müller,<sup>18,19,50,63-65</sup>



through comparison of the rate of solvolysis of these substrates (4, 41, 42, 43, 44) with the MM2 calculated strain-energy difference between the parent polycyclic hydrocarbon and the bridgehead carbocation.

From these studies, a linear correlation between the free energy of solvolysis and the strain energy difference was observed and indicates that unimolecular ionisation of these substrates is primarily controlled by the ability of the intermediate carbocation in achieving a planar configuration.

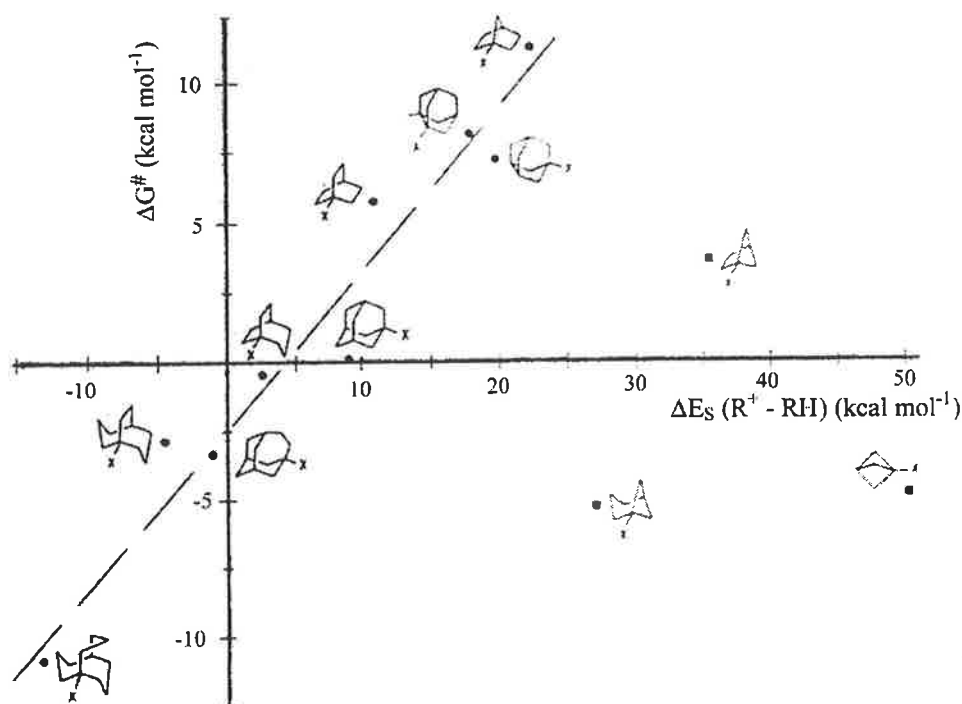


Figure 6.2: "Plots of the free energies of solvolysis ( $\Delta G^\ddagger$ ) versus strain energy differences between cation and parent hydrocarbon ( $\Delta E_s(R^+ - RH)$ ) for the systems of interest."<sup>21</sup>

However, with the solvolysis of the 1-bromobicyclo[n.1.1]alkanes ( $n = 1-3$ ) (7, 45, 46), this linear correlation was no longer seen to apply.<sup>50</sup> Verification of the calculated strain energies at a higher level of calculation (MP2/6-3G\*) by Della and co-workers, confirmed that the bicyclo[n.1.1]bridgehead ( $n = 1-3$ ) (47, 48, 49) cations were indeed aberrant in their solvolytic behaviour.<sup>21</sup>

These bridgehead substituted bicyclic[n.1.1] alkanes had been shown to solvolyse at an enhanced rate with 1-bicyclo[1.1.1]pentyl bromide (7) and 1-

bicyclo[3.1.1]heptyl bromide (**46**) shown to solvolyse even faster than the classical substrate, *t*-butyl chloride (**1**) (Figure 6.1). From interpretation of the positions these molecules took on the plot of free energy of solvolysis and the strain energy difference it was determined that 1-bicyclo[1.1.1]pentyl bromide (**7**) is stabilised by  $\sim 50 \text{ kcal}\cdot\text{mol}^{-1}$ , 1-bicyclo[1.1.1]pentyl bromide (**45**) by  $\sim 25 \text{ kcal}\cdot\text{mol}^{-1}$  and 1-bicyclo[3.1.1]heptyl bromide (**46**) by  $\sim 30 \text{ kcal}\cdot\text{mol}^{-1}$ .<sup>21</sup> It was clear that these substrates had an alternate mode of stabilisation which manifested itself as the enhanced rate of ionisation.

This stabilisation was believed to have been brought about by the close proximity of the bridgehead-bridgehead carbons ( $C^1$  and  $C^3$ ), which in 1-bicyclo[1.1.1]pentyl bromide (**7**) had been measured to be  $1.83 \text{ \AA}$ . It was believed that as this distance approached the typical C-C bond length, that homohyperconjugative interactions between  $C^1$  and  $C^3$  occurred.<sup>22</sup> These through space homohyperconjugative or back lobe orbital interactions would allow for the electron density of the substituent on  $C^3$  to stabilise the forming positive charge at  $C^1$ .<sup>66</sup>

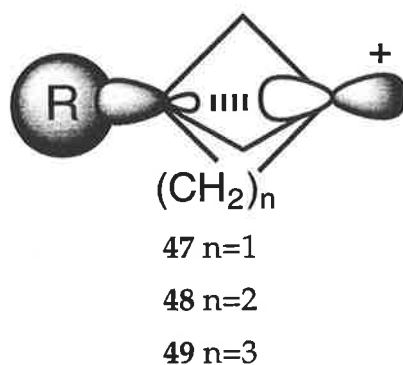


Figure 6.3: The orbital interactions between  $C^1$  and  $C^3$  ( $n=1-3$ ) (**47**:  $n=1$  **48**:  $n=2$  **49**:  $n=3$ )

Through trapping experiments, it has been shown unequivocally that 3-methoxy carbonylbicyclo[2.1.1]hexyl triflate (**50**) and 1-bromo bicyclo[3.1.1]heptane (**46**) solvolyse via the bicyclo[2.1.1]hexyl and bicyclo[3.1.1]heptyl carbocations (**48** and **49**)<sup>20,51</sup> which supports the homohyperconjugative stabilisation theory.

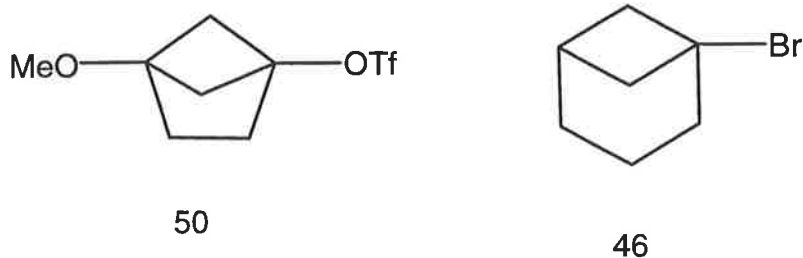


Figure 6.4: 3-Methoxy carbonylbicyclo[2.1.1]hexyl triflate (**50**) and 1-bromobicyclo[3.1.1]heptane (**46**)

However, until recently there was little evidence to support the intermediacy of a discrete carbocation in the solvolysis of the bicyclo[1.1.1] alkanes. It was calculated that the carbocation, if formed would have a half life of so short a period that the carbocation would be expected to ring-open before it had the opportunity to be trapped by a nucleophile.<sup>59,67</sup>

A study of the solvolysis of the 3-R-substituted bicyclo[1.1.1]pentyl bromides (**51**) by Della and co-workers,<sup>22</sup> suggested that the rate determining step (r.d.s.) followed the  $S_N1$  pathway, through the observation of the effect of strong  $\pi$ -donor substituents on the rate of solvolysis. It was predicted that  $\pi$ -donors would provide anchimeric assistance in the ionisation through mesomeric stabilisation of the developing positive charge at C3 in the transition state leading to the ring-opened cation (**52a**) from the concerted ionisation of the substrate (**51**). This associated rate increase was not observed, leading to the conclusion that the  $S_N1$  mechanism through the bridgehead cation (**47**) was the more likely.

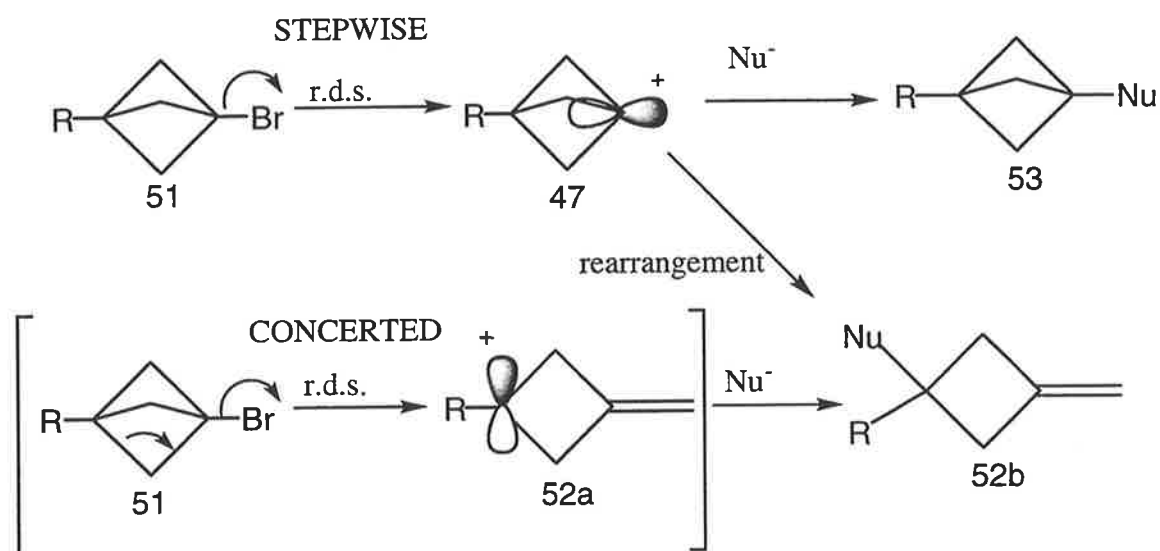


Figure 6.5: The two possible pathways and products available for the solvolysis of the 1,3-disubstituted bicyclo[1.1.1]pentanes.

The best evidence of the formation of the bridgehead cation (47) would be through its direct trapping, with the bicyclo[1.1.1]pentyl skeleton fully retained. Unfortunately, Della and co-workers were unable to successfully isolate any of the non-rearranged product (53) for a large range of substituents (R) and thus were unable to prove unequivocally the intermediacy of the bridgehead cation (47).

Recently however, this was successfully carried out by Wiberg, with the treatment of 1,3-diiodobicyclo[1.1.1]pentane (54) with methanolic KOH to yield 3-methoxybicyclo[1.1.1]pent-1-yl iodide (55) through the trapping of the of the intermediate carbocation (Figure 6.6).<sup>52</sup>

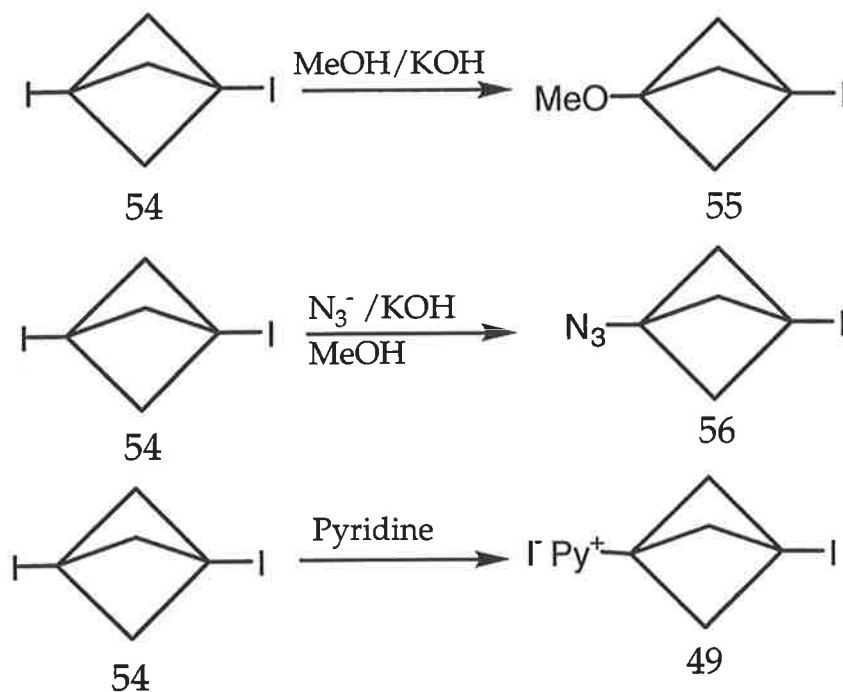


Figure 6.6: Trapping of the intermediate carbocation from the ionisation of 1,3-diiodobicyclo[1.1.1]pentane (54).

In a similar fashion, in the presence of the azide ion, which is "known to intercept most carbocations at every encounter and therefore is probably not very selective"<sup>52</sup> they were able to isolate the 3-iodobicyclo[1.1.1]pent-1-yl azide (56). Adcock and associates also trapped the carbocation of (54) with the weak nucleophile pyridine, yielding the pyridinium salt (57).<sup>53,68</sup>

## 6.2 Choice of Kinetic Model

Consequently, it was seen that an opportunity was present, to prepare solvolytic substrates of both synthetic and kinetic interest. Thus, it was decided to attempt the synthesis of a series of novel 1,3-disubstituted, bicyclo[1.1.1]pentanes. The approach chosen, was to utilise nucleophilic trapping of any intermediate bridgehead cations.

Should this synthesis prove successful, it would be able to provide a range of novel solvolytic substrates, and provide further evidence towards to ionic mechanism of formation of these 1,3-disubstituted, bicyclo[1.1.1]pentanes.

### 6.3 Mechanistic Implications of the Proposed Synthesis.

Prior to the studies by Wiberg and Della,<sup>22,52</sup> it had been assumed that the reaction between [1.1.1]propellane (58) and iodine, which results in a quantitative yield of the 1,3-diiodobicyclo[1.1.1]pentane (54) followed a radical mechanism.<sup>69</sup> The absence of rearranged carbocation products from the reaction was taken as evidence of this radical pathway (Figure 6.7).<sup>69</sup>

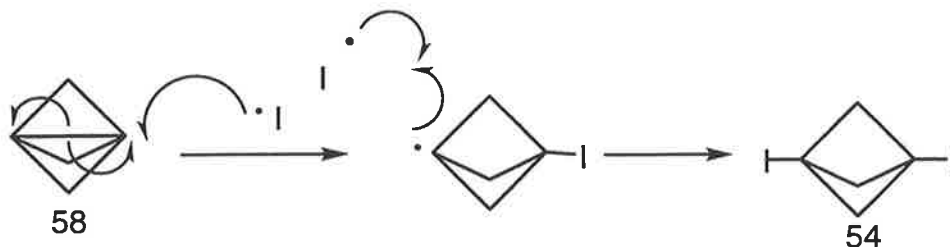


Figure 6.7: Originally proposed radical mechanism<sup>70</sup>

There was, however, conflicting evidence from the addition of bromine and chlorine to the [1.1.1]propellane (58). Direct chlorination of [1.1.1]propellane (58) yielded only 11% of a complex mixture consisting of chloro derivatives, including the products due to rearrangement, that had been absent from the iodine reactions.<sup>71</sup> In the case of direct bromination,<sup>67</sup> a yield of only 36% of 1,3-dibromobicyclo[1.1.1]pentane (59) was obtained after irradiation. Had the reaction followed a radical pathway as assumed, a quantitative yield of the 1,3-dibromobicyclo[1.1.1]pentane (59) would have been anticipated.

These findings resulted in a re-evaluation of much of the early work with these bicyclo[1.1.1]pentanes. In order to account for the presence of rearrangement products, Wiberg, and co-workers forwarded a mechanism that required the facile rearrangement of the radical.<sup>70</sup> This rearrangement is however, known not to occur, and the stability of these bridgehead radicals against rearrangement, has been used in the synthesis of other isolated compounds.<sup>72-74</sup>

The current evidence supports the formation of a discrete carbocation at the bridgehead position as an intermediate. This can then, either be trapped by a nucleophile present in the reaction mixture, or undergo rearrangement as shown below (Figure 6.8). In order to investigate this we attempted to trap cations of type 47 with a range of nucleophilic sources.

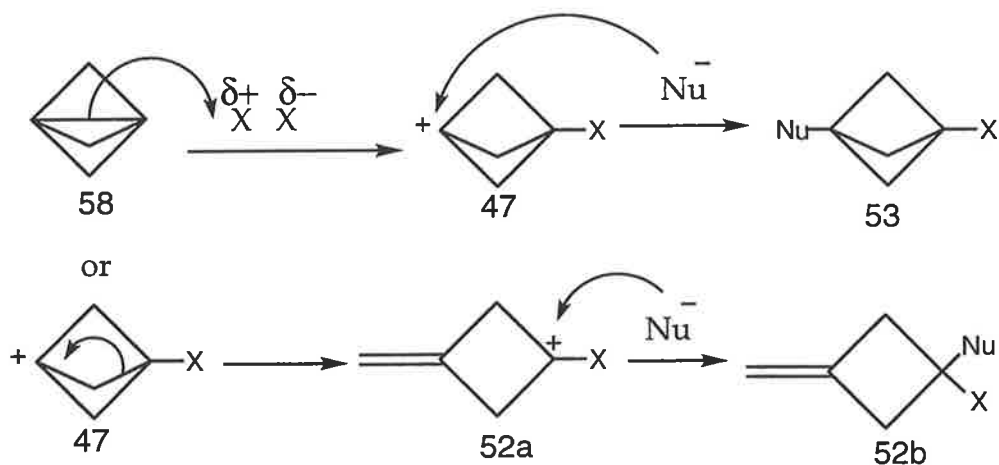


Figure 6.8: Carbocation mechanism, showing formation of (i) trapped bridgehead carbocation with a given nucleophile (53) and (ii) rearranged product (52a/b)

#### 6.4: Synthetic Approach Towards the Desired Di-Substituted, Bicyclo[1.1.1]pentanes.

A solution of [1.1.1]propellane (58) in ether/pentane was prepared from 1,1-dibromo-2,2-bis(chloromethyl)cyclopropane (60) following standard literature procedures.<sup>75</sup>

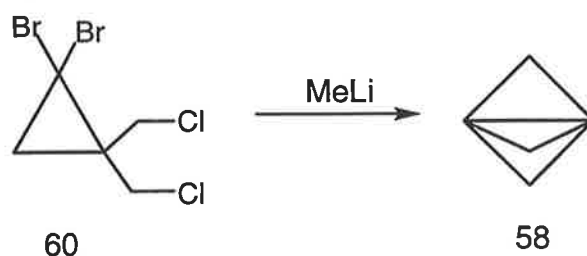


Figure 6.9: Preparation of [1.1.1]propellane (58) from 1,1-dibromo-2,2-bis(chloromethyl)cyclopropane (60).

The customary procedure for determining the extent to which the formation of [1.1.1]propellane (58) had occurred was to react an aliquot of the propellane solution with excess iodine.

### 6.5 Preparation of 1,3-Diodobicyclo[1.1.1]pentane (54).

This reaction between iodine and [1.1.1]propellane (58) is known to yield the 1,3-diodobicyclo[1.1.1]pentane (54) in quantitative yield without the production of any rearrangement products. Consequently, the isolated yield of 1,3-diodobicyclo[1.1.1]pentane (54) can be used to determine the amount of [1.1.1]propellane (58) in the reaction mixture, and consequently allow us to determine the yields from any other reactions utilising this propellane solution.

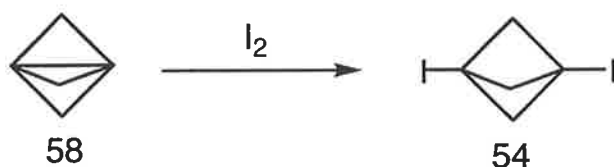


Figure 6.10: Quantitative formation of the 1,3-diodo bicyclo[1.1.1]pentane (54) from the reaction of [1.1.1]propellane (58), with iodine.

The isolated 1,3-diodobicyclo[1.1.1]pentane (54) from this reaction indicated that the reaction aliquot contained 67% of [1.1.1]propellane (58) and this was then used in a series of reactions to attempt to isolate novel di-substituted bicyclo[1.1.1]pentanes and provide further support for the formation of the bridgehead cation.

### 6.6 Synthesis of 1,3-Dibromobicyclo[1.1.1]pentane (59).

As stated earlier, the reaction of bromine with [1.1.1]propellane (58) with irradiation, furnished an optimised yield of only 36% of the desired 1,3-dibromobicyclo[1.1.1]pentane (59). The remaining [1.1.1]propellane (58) was observed to be converted to poly-brominated materials following rearrangement of the ring system. The isolation of these products was consistent with the reaction progressing via a short lived bridgehead carbocation intermediate and not, as previously held, via a radical pathway (Figures 6.7 and 6.8).

We felt that if this short lived bridgehead cation could be trapped immediately after formation, by a nucleophile present in excess in the solution, then the rearrangement could be prevented, leading to a greater isolated yield of the desired 1,3-dibromobicyclo[1.1.1]pentane (59).



Towards this end, a reaction vessel was "spiked" with an excess of lithium bromide. With the addition of bromine and an aliquot of the [1.1.1]propellane (**58**) solution, the resulting reaction yielded 1,3-dibromobicyclo[1.1.1]pentane (**59**) in 66%. This yield however, when calibrated against the concentration of [1.1.1]propellane (**58**) in the reaction mixture, gave the isolated yield of 1,3-dibromo bicyclo[1.1.1]pentane (**59**) as 98% formation from the reaction. The reaction mixture also contained the rearrangement products (**61a/b**), <sup>1</sup>H NMR analysis of the mixture indicated that the formation of these rearrangement products occurred in <5% (Figure 6.11).

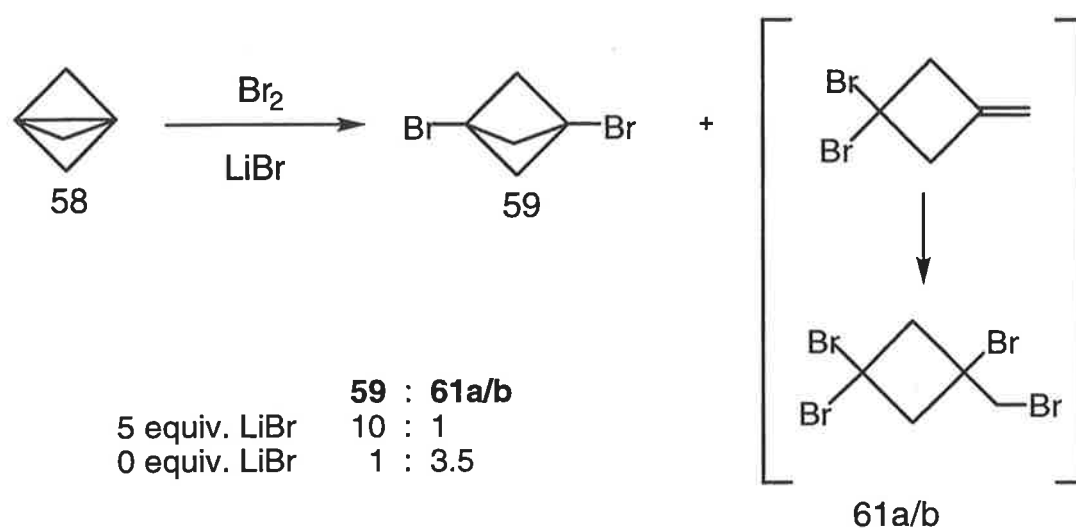


Figure 6.11: Preparation of 1,3-dibromobicyclo[1.1.1]pentane (**59**) through the reaction of [1.1.1]propellane (**58**) with bromine, in the presence of lithium bromide.

This synthesis of 1,3-dibromobicyclo[1.1.1]pentane (**59**) had yielded ~60% more of the desired product than had been available by the previously optimised reaction conditions.<sup>67</sup>

For comparison, a second reaction was carried out between the [1.1.1]propellane (**58**) solution and bromine, this time without the presence of the "spiking" agent. The isolated products were again the desired 1,3-dibromobicyclo[1.1.1]pentane (**59**) and the products of the ionic rearrangement, however, the ratio was now 3.5:1 of the rearrangement products (**61a/b**) to the desired dibromide substrate (**59**), with a calibrated yield of only 35%.

This result provided strong evidence of the presence of a carbocation intermediate in the formation of the dibromo substrate (59). Consequently, the synthesis of other mixed dihalide substrates was attempted.

### 6.7 Synthesis of Mixed Dihalide Bicyclo[1.1.1]pentanes.

Through the addition of various “spiking” agents to the reaction mixture, it was envisioned that we would be able to direct the formation of a series of mixed dihalide substrates. As detailed below (Table 6.1), this synthetic method did in fact allow us to prepare a large range of candidate substrates for potential kinetic analysis.

Table 6.1: Product(s) from the addition of halogens to [1.1.1]propellane (58) in the presence of external nucleophiles. Ratio derived via <sup>1</sup>H NMR analysis of crude mixture, utilising benzene as a internal standard.

Reaction #	Halogen	Additive	Product(s) and (Ratio)	Product Yield (% = rel%)
1	I <sub>2</sub>	-	54	54 (67 = 100)
2	Br <sub>2</sub>	-	59 (1) + 61a/b (3.5)	59 (24 = 35)
3	Br <sub>2</sub>	LiBr	59 (10) + 61a/b (1)	59 (66 = 98)
4	I <sub>2</sub>	LiBr	54 (1) + 62 (10) + 63a/b (1)	62 (49 = 73)
5	I <sub>2</sub>	LiBr *	54 (1) + 62 (2) + 63a/b (6)	-
6	Br <sub>2</sub>	LiCl	59 (1.2)+ 64 (1.5)+ 66 (1) + 65a/b (1)	-
7	Br <sub>2</sub>	LiCl *	59 (16)+ 64 (1)+ 66 (1) + 65a/b (15)	-
8	I <sub>2</sub>	LiCl	54 (3) + 67 (1) + 68a/b (6)	-
9	Br <sub>2</sub>	LiI	54 (15) + 62 (5) + 59 (8) + 69a/b (1)	-
10	I <sub>2</sub>	NaN <sub>3</sub>	54 (5) + 56 (1)	-
11	I-Cl	-	54 (1) + 67 (1) + 70a/b (80)	-
12	I-Cl	LiCl	54 (1) + 67 (1) + 70a/b (4)	-

\* = 15 x excess of external nucleophile.

The formation of the mixed dihalide substrates listed above (Table 6.1) was carried out through the reaction of [1.1.1]propellane (58) and a halogen source (I<sub>2</sub>, Br<sub>2</sub> or I-Cl) in the presence of a nucleophile, present as the respective lithium or sodium salt and are discussed in detail below.

## 6.8 Preparation of 1-Bromo, 3-Iodobicyclo[1.1.1]pentane (62).

The reaction of [1.1.1]propellane (58) with iodine in the presence of excess lithium bromide resulted in the formation of 1-bromo, 3-iodobicyclo[1.1.1]pentane (62) in 49% isolated yield. This yield represents a formation of 73% of the 1-bromo, 3-iodo substrate (62) based on the concentration of [1.1.1]propellane (58) in the reaction mixture.

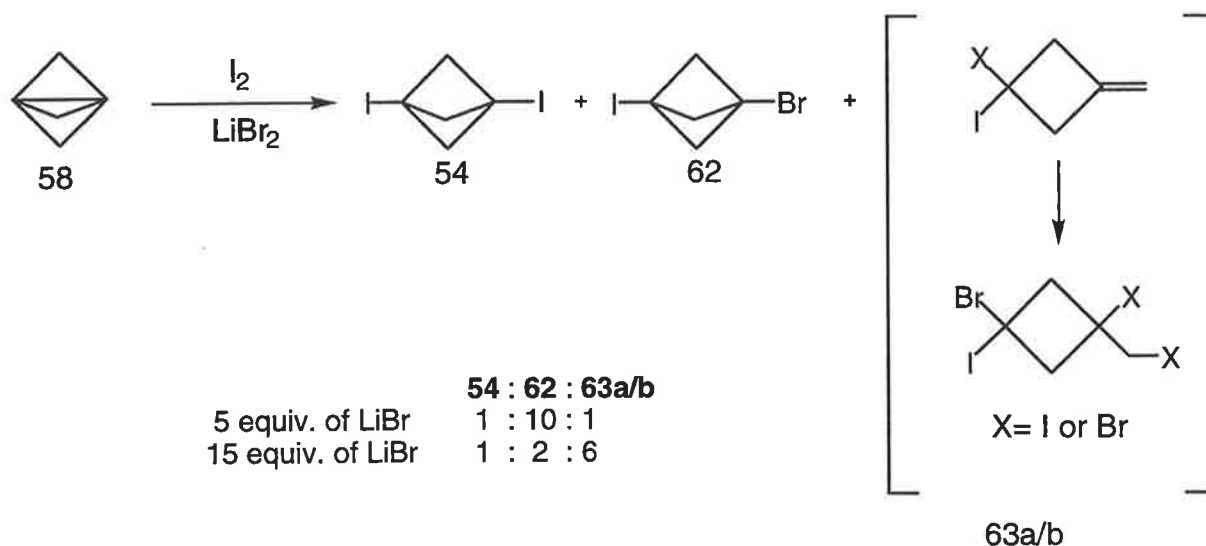


Figure 6.12: Synthesis of 1-bromo, 3-iodobicyclo[1.1.1]pentane (62).

While the isolated products also contained a small quantity of the 1,3-diiodo substrate (54) and the rearrangement products (63a/b), the reaction represented a significant increase in the isolated yield of 1-bromo, 3-iodobicyclo[1.1.1]pentane (62) over previous syntheses, which had relied on halide exchange, or the formation of a bridgehead radical through Barton decarboxylation, which would be trapped with a halide donating solvent. In the latter case, while the formation of the radical was successful, elimination to give [1.1.1]propellane (58) resulted in the loss of the majority of the product.

In addition, the isolated product from either traditional approach contained significant quantities of rearranged by-products. The difficulty with which the purification of the desired 1-bromo, 3-iodobicyclo[1.1.1]pentane (62) required resulted in the inability of this system to be utilised for kinetic studies with any degree of reliability.<sup>22,52,76</sup> This new synthetic approach consequently provided a significant improvement over the previous approach to this mixed dihalide.

Via this new synthetic route, it was possible to generate yields of up to five grams of the desired 1-bromo, 3-iodobicyclo[1.1.1]pentane (62) in a purified state. It was, however, necessary to take extra care in the handling and preparation of these substrates due to the high volatility of bicyclo[1.1.1]pentanes. It was found that small scale synthetic preparations were generally unsuccessful, as a significant portion of the desired product would be lost through the removal of the solvent system that the reaction was carried out in, and also through purification by recrystallisation or sublimation.

Of synthetic importance, was the finding that the external nucleophile must not be present in greater than ten molar equivalents. Through a repeat reaction between [1.1.1]propellane (58) and iodine in the presence of fifteen equivalents of lithium bromide, the isolated yield of the desired mixed dihalide was significantly reduced, while the amount of rearrangement products increased eight fold (Figure 6.12).

It was theorised that this significant difference in the isolated products could be attributed to the change in polarity and dielectric constant of the solvent due to the higher salt concentration. These factors assist in the ionisation of the rapidly formed dihalides (54 and 62), which then may undergo ionic rearrangement, to afford the ring opened cations which are subsequently trapped by nucleophiles present in the reaction mixture.

#### **6.9 Formation of 1-Bromo, 3-Chlorobicyclo[1.1.1]pentane (64).**

The reaction between [1.1.1]propellane (58) and bromine was carried out in the presence of lithium chloride. Crude analysis of the reaction mixture indicated that the expected 1-bromo, 3-chlorobicyclo[1.1.1]pentane (64) had been formed, in similar quantities to the formation of the 1,3-dibromo substrate (59). Additionally, the presence of the rearrangement products (65a/b) was again observed, along with the hydrolysis product, 3-bromobicyclo[1.1.1]pentan-1-ol (66) (Figure 6.13).

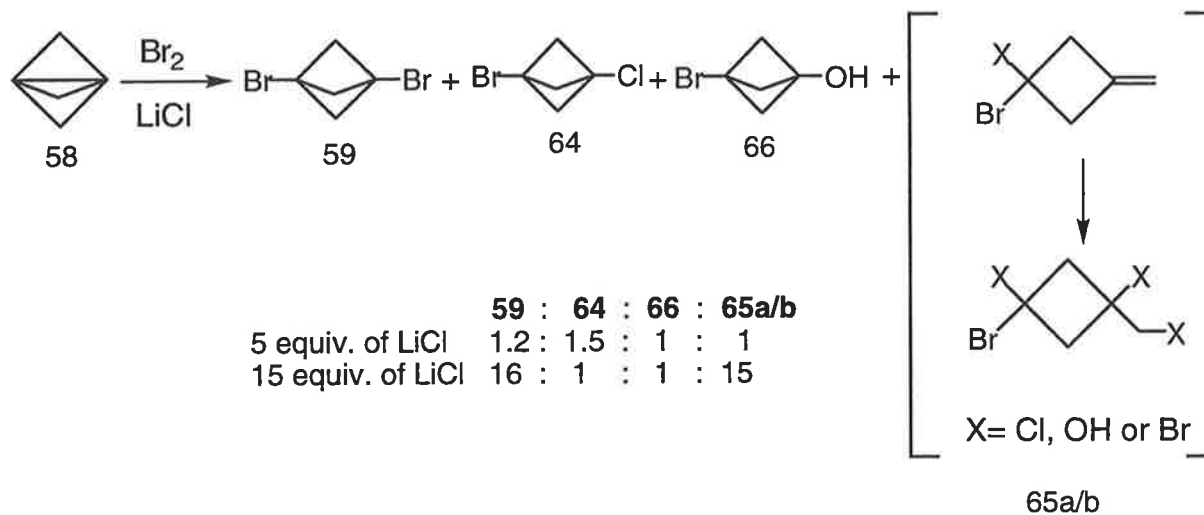


Figure 6.13: Formation of 1-bromo, 3-chlorobicyclo[1.1.1]pentane (64).

Unfortunately, due to the high volatility of the constituents of this complex product mixture it was difficult to isolate any of the dihalide species in significant quantities or purity. This reaction did, however, provide yet further evidence of the discrete carbocation intermediate and a pathway to the synthesis of novel mixed dihalides should appropriate measures be taken in the purification.

In order to see if the observed increase in formation of the products of ionic rearrangement (65a/b) with a large amount of the nucleophilic spiking agent present, this reaction was repeated in the presence of 15 equivalents of lithium chloride. As expected, the reaction mixture again showed a lower formation of the desired mixed dihalide (64) and a corresponding increase in the formation of the rearrangement products (65a/b) (Figure 6.12). This result was significant in both showing that the consequence of a high concentration of nucleophilic salts in the formation of the ionic rearrangement products (65a/b) was not isolated in its effect, but also in the relative stabilities of the di-substituted bicyclo[1.1.1]pentanes.

If the hypothesis that the high concentration of nucleophiles present in the reaction mixture promotes the decomposition of di-substituted bicyclo[1.1.1]pentanes to give the ionic rearrangement products, then the increased concentration of 1,3-dibromobicyclo[1.1.1]pentane (59) in relation to 1-bromo, 3-chlorobicyclo[1.1.1]pentane (64) would indicate that under these conditions the bromo substituted substrate had an increased stability, relative to that of the chloro substituted substrate.

### 6.10 Synthetic Approach to 1-Chloro, 3-Iodobicyclo[1.1.1]pentane (67).

We were able to prepare 1-chloro, 3-iodobicyclo[1.1.1]pentane (67) <sup>76,77</sup> through the reaction of [1.1.1]propellane (58) with iodine in the presence of excess lithium chloride (Figure 6.14).

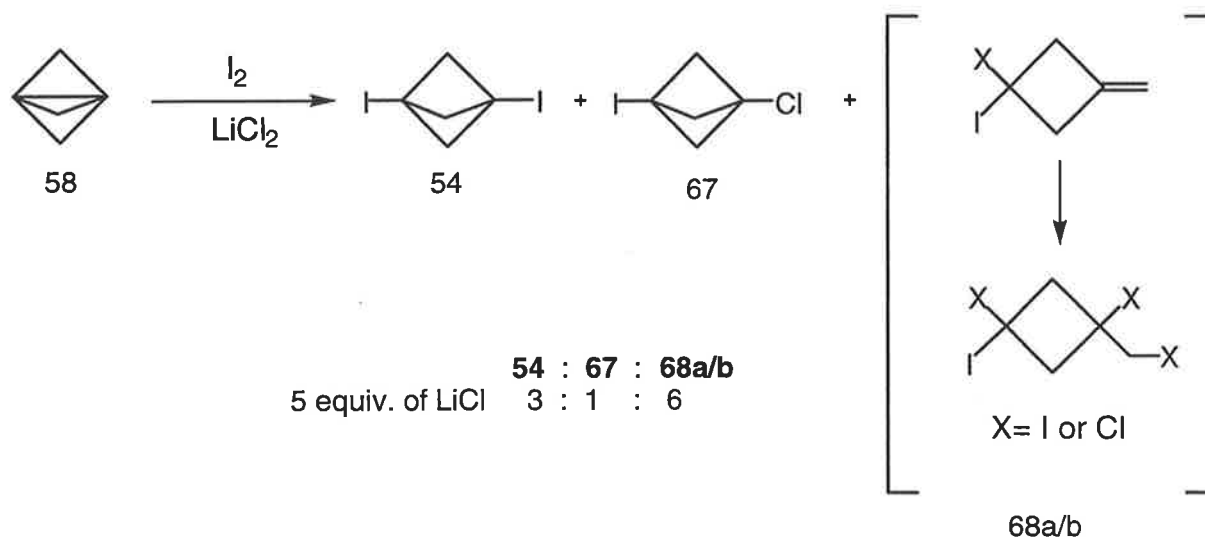


Figure 6.14: Preparation of 1-chloro, 3-iodobicyclo[1.1.1]pentane (67).

In addition to the desired dihalide (67) the reaction also yielded a mixture of 1,3-diiodobicyclo[1.1.1]pentane (54), and the products of the ionic rearrangement of the intermediary cation (68a/b) in a ratio of 1 : 3 : 6 of the desired 1-chloro, 3-iodo substrate (67) : 1,3-diiodo substrate (54) : rearrangement products (68a/b). Unfortunately, once again, the high volatility of the product mixture prevented the isolation of the desired substrate, and consequently accurate yield calculations could not be prepared.

### 6.11 Alternate Synthetic Approach to the Formation of 1-Bromo, 3-Iodobicyclo[1.1.1]pentane (62).

We attempted to form 1-bromo, 3-iodobicyclo[1.1.1]pentane (62) from the reaction of [1.1.1]propellane (58) with bromine in the presence of lithium iodide (Figure 6.15).

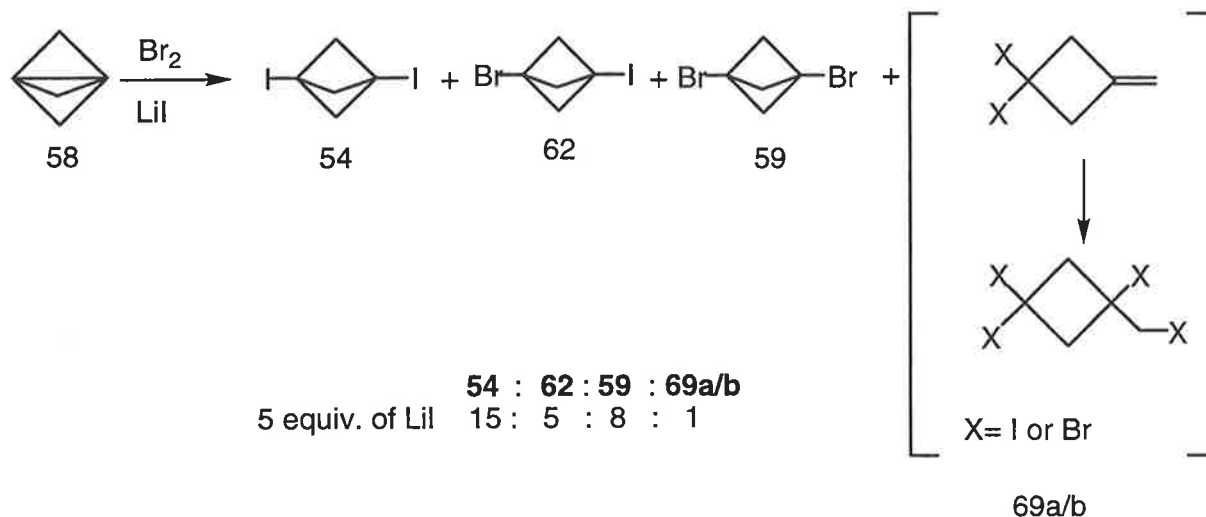


Figure 6.15: The attempted synthesis of 1-bromo, 3-iodobicyclo[1.1.1]pentane (62), through the reaction of [1.1.1]propellane (58) and bromine, in the presence of lithium iodide.

The observed product mixture, however, was found to consist significantly of the 1,3-diiodo (54) and 1,3-dibromo (59) substrates, at the exclusion of the formation of the desired mixed dihalide (62). This result was not surprising, as in the dissolution of lithium iodide, it is known that a portion of free iodine is observed to be released. This iodine would consequently react preferentially with the [1.1.1]propellane (58) in solution, and bias the formation of 1,3-diiodobicyclo[1.1.1]pentane (54).

### 6.12 Formation of 1-Azido, 3-Iodobicyclo[1.1.1]pentane (56)

As mentioned previously, the azide ion acts as a non-selective nucleophile and has been seen to be very successful in trapping the intermediate carbocation from a reaction of [1.1.1]propellane (58) with iodine.<sup>52</sup> Preparation of the 1-azido, 3-iodo substrate (56) was carried out, utilising sodium azide as the nucleophilic spiking agent (Figure 6.16).

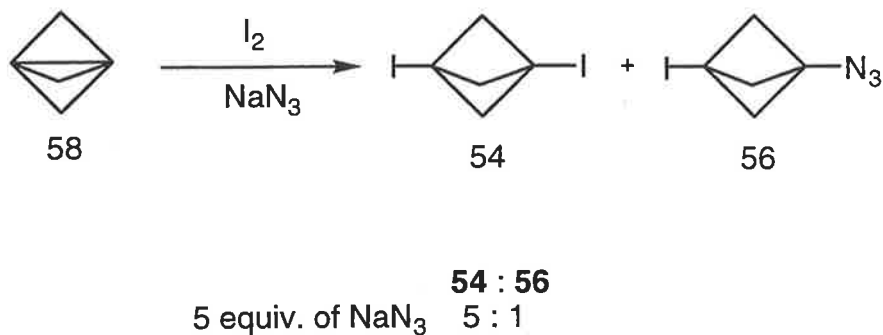


Figure 6.16: Formation of 1-azido, 3-iodobicyclo[1.1.1]pentane (56).

Product analysis indicated that there was no discernible rearrangement of the carbocation, giving only the diiodo derivative (54) and the known 1-azido, 3-iodobicyclo[1.1.1]pentane (56)<sup>52</sup> in a 5 : 1 ratio.

### 6.13 Attempted Syntheses Utilising Iodine Monochloride as the Halogen

#### Source.

The final reactions trailed were using iodine monochloride. The addition of neat iodine monochloride to [1.1.1]propellane (58) resulted in essentially complete rearrangement of the propellane system to the rearrangement products (70a/b) (Figure 6.17).

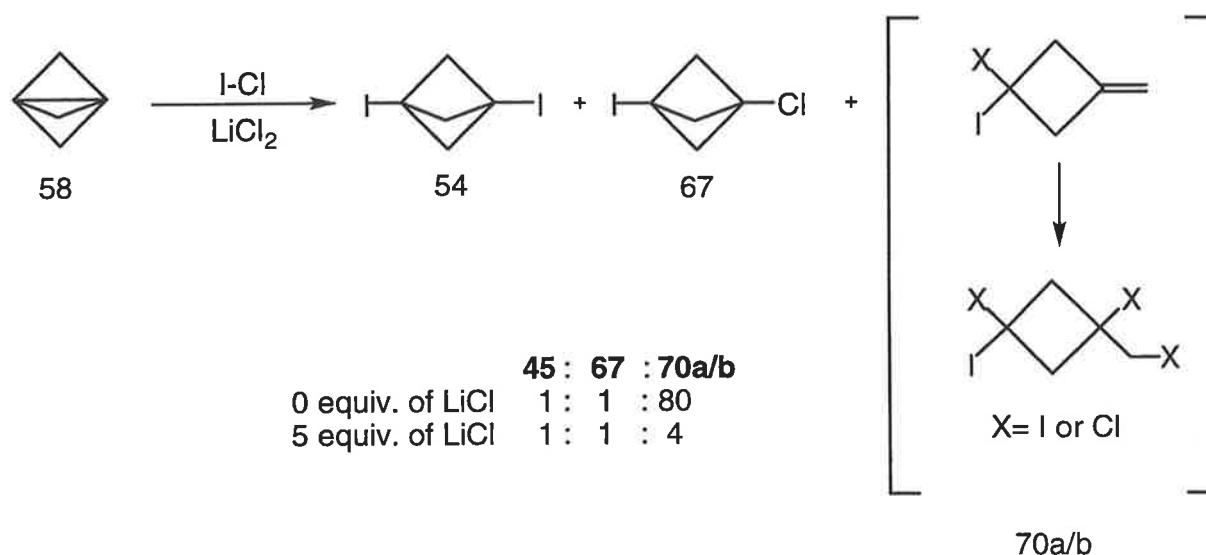


Figure 6.17: The reaction between [1.1.1]propellane (58) and iodine monochloride.



In the presence of five equivalents of lithium chloride, there was a relative increase in the yield of the desired 1-chloro, 3-iodobicyclo[1.1.1]pentane (67), however, due to the complexity of the product mixture isolation of a pure sample was impossible.

#### 6.14 Hypothesis for the observed stability of the bridgehead cations.

The results from these syntheses indicate that the formation of the intermediate bridgehead carbocation in the bicyclo[1.1.1]pentane systems is indeed possible and is stabilised to a far greater extent than could be predicted from analysis of the aforementioned plot, based on the relative strain energies associated with the carbocationic centre.<sup>3</sup>

This degree of stabilisation and ultimate product formation, appears to be dependant upon which halogen is utilized to attack the [1.1.1]propellane (58), leading to the formation of the bridgehead bicyclo[1.1.1]pentane cation. It could be theorized that in the case of iodo substitution, the stabilisation of the developing charge through homohyperconjugation is significantly high, thus disfavoring the ionic rearrangement and allowing the formation of the diiodo substrate (54) in quantitative yield.

In a similar fashion, the introduction of a bromo substituent, provides similar stabilisation of the developing charge. The "attack" by the bromine, and the homohyperconjugative stabilisation it creates, is however, weaker than that observed for the iodo system, and consequently a competing radical approach is able to operate simultaneously as observed by Della.<sup>67</sup>

In addition, the bromine seems less able to prevent the rearrangement mechanism through stabilisation of the bridgehead cation and thus some rearrangement products are observed to form. This was particularly noted when the nucleophiles present were less nucleophilic in nature, providing a greater period of time for the rearrangement to occur.

The introduction of a chloro substituent does not appear to be able to prevent the rearrangement mechanism, and the respective cation clearly undergoes facile rearrangement.

This apparent pattern of behaviour has tentatively been attributed to the outer shell electron density of the halogen substituent. Because of the relatively larger electron shell of the iodo system, the homohyperconjugative stabilisation of the bridgehead cation is significantly high. The bromo system also displays this stabilisation, yet to a lesser extent. This has been attributed to the smaller, more dense outer shell of electrons in the bromo system, which is less able to stabilise the forming bridgehead cation through homohyperconjugation.

This apparent trend could also account for the lack of bridgehead stabilisation observed for the chloro system, which again has a smaller outer shell of electrons, which would conceivably prevent the stabilisation of the bridgehead cation.

### **6.15 Future directions.**

Although these syntheses had provided a range of both novel and known di-substituted bicyclo[1.1.1]pentanes, due to the difficulty in preparation, isolation and purification of many of the substrates, this system could not be utilized for kinetic studies within this research project.

The work did, however, provide a significant portion of evidence towards the existence of an intermediary cation in the formation of these di-substituted bicyclo[1.1.1]pentanes, as well as providing synthetic approaches to several novel substrates.

## Chapter 7

### Experimental

## General:

Unless otherwise indicated, all melting points were carried out in sealed tubes, utilising a Gallenkamp melting point apparatus and are uncorrected. All NMR ( $^1\text{H}$  and  $^{13}\text{C}$ ) were carried out utilising a Varian Gemini 300 MHz spectrometer. All NMR shifts ( $\delta$ ) in parts per million (ppm) are reported in deuteriochloroform ( $\text{CDCl}_3$ ) and measured relative to an internal standard of trimethylsilane (TMS) at the reference of 0 ppm, unless otherwise specified. The abbreviations used are : s (singlet), d (doublet), t (triplet), q (quartet), m (multiplet),  $J$  (coupling constant).

Purification of bulk solvents and commercially available precursor compounds was carried out following literature procedures.<sup>78</sup> Purification of synthesised products was carried out through standard techniques as described. Flash chromatography was carried out on Merck #9385 silica gel 230-400 mesh. TLC was carried out using Merck TLC plates of silica gel 60  $\text{F}_{254}$ .

The solvent systems utilised for kinetic analysis were prepared following standard techniques as described in the main body of the text, following purification from literature procedures.<sup>24,78</sup>

The water used to make the aqueous solutions was sourced from a Millipore Continental Water system, utilising reverse osmosis feed water passed through two mixed bed ion exchange columns, a carbon filter, and Organo-X filter and finally a  $0.22\mu\text{m}$  filter. The typical reading from the system was found to be  $>10\text{ M}\Omega$ . This was then degassed through vigorous boiling for ten minutes and allowed to cool utilising a drying tube containing "Carbasorb"<sup>®</sup> to prevent the absorption of carbon dioxide.

Ethanol was purified through reflux over freshly prepared magnesium ethoxide, followed by fractional distillation under dry nitrogen.<sup>78</sup> The ethanol system solvents were then prepared as volume for volume solutions utilising the known densities from the literature.<sup>32</sup>

2,2,2-Trifluoroethanol was purified by reflux over a mixture of anhydrous calcium sulfate and potassium carbonate for two hours, followed by fractional distillation under dry nitrogen.<sup>24</sup> The 2,2,2-trifluoroethanol system solvents were prepared as weight for weight solutions.

### 3,3-Dimethyl-2-butyl brosylate (Pinacolyl brosylate) (12)<sup>27</sup>

To brosyl chloride (14) (5 g, 19.56 mmol, 1.05 equiv.) in anhydrous pyridine (10 ml) was added pinacolyl alcohol (13) (2.11 g, 2.6 ml, 20.66 mmol) and allowed to stir at room temperature for six days. Pentane (100 ml) was then added. The solution was washed with sulfuric acid (0.1M). The aqueous layer was back extracted with pentane (2 x 7 5ml) and the combined organic layers washed with sodium bicarbonate solution and water. The organic phase was dried over sodium sulfate, and the pentane removed by evaporation. The resulting white precipitate was recrystallised from pentane, and kept in the mother liquor at -4°C. (80-90%). m.p. 53-54°C (lit. m.p. 52.5-53.2°C)<sup>27</sup>. <sup>1</sup>H NMR (CDCl<sub>3</sub>, 300 MHz) δ 0.85 (s, 9H), 1.23 (d, 3H, J = 6.0 Hz), 4.44 (q, 1H, J = 6.0 Hz), 7.56 (d, 2H, J = 9.6 Hz), 7.78 (d, 2H, J = 9.6 Hz)<sup>27</sup>.

### 1-Adamantyl bromide (4)<sup>43</sup>

A three neck round bottom flask fitted with a dropping funnel, thermometer and condenser was charged with adamantane (19) (10 g, 83.21 mmol). Bromine (29.25g, 9.43 ml, 183.07 mmol, 2.2 equiv.) was added dropwise over thirty minutes. The mixture was then heated under reflux (95°C) for six hours with the evolving hydrogen bromide gas trapped in an aqueous potassium hydroxide bath. The mixture was allowed to cool to room temperature as it stirred overnight, then dichloromethane (150 ml) was added and the solution poured carefully onto iced chilled saturated sodium metabisulfite solution to destroy the excess bromine. The organic phase was separated, and the aqueous phase extracted with dichloromethane (3 x 150 ml). The combined organic phases were dried over magnesium sulfate, the solvent removed and the title product purified by sublimation (105°C @0.02 mm Hg) yielding 13.5 g (85%). m.p. (sealed tube) 117°C (lit. m.p.. 118°C)<sup>43</sup>. <sup>1</sup>H NMR (CDCl<sub>3</sub>, 300 MHz) δ 1.73 (s, 6H), 2.11 (s, 3H), 2.37 (s, 6H); <sup>13</sup>C (CDCl<sub>3</sub>, 300 MHz) δ 32.59 35.54, 49.34, 66.62.

### 1-Adamantyl tosylate (10)<sup>42</sup>

Silver tosylate (1.995 g, 9.675 mmol 1.5 equiv.) was desiccated under high vacuum for one hour. Then under a dry nitrogen atmosphere, acetonitrile (10 ml) and 1-adamantyl bromide (4) (1 g, 4.65 mmol) were added. The reaction mixture was

stirred at room temperature for 2 hours. The silver bromide precipitate was removed by filtration, and the acetonitrile removed under reduced pressure. Under a dry nitrogen blanket, the residue was taken up in diethyl ether (5 ml) and filtered to remove any remaining silver salts. The diethyl ether was then removed by evaporation, giving the title compound as a white crystalline solid (1.3 g, 93%). m.p. (sealed tube) 69-71°C (there are two lit. m.p. reordered, due to crystal packing, 72.5-74.5°C and 80.5-81.5°C)<sup>79</sup>. <sup>1</sup>H NMR (CDCl<sub>3</sub>, 300 MHz) δ 1.62 (s, 6H), 2.17 (s, 9H), 2.43 (s, 3H), 7.22-7.27 (m, 2H), 7.73-7.78 (m, 2H); <sup>13</sup>C NMR (CDCl<sub>3</sub>, 300 MHz) δ 20.95, 22.45, 38.11, 40.85, 54.98, 127.82, 130.73, 131.99, 143.68.

### 1-Phenyl adamantane (26)<sup>43</sup>

1-Adamantyl bromide (4) (10 g, 46 mmol) was dissolved in benzene (80 ml). This solution was added slowly to a stirring solution of ferric chloride (2 g, 1.23 mmol 0.3 equiv.) in benzene (50 ml). When combined, the mixture was heated to reflux (100°C) for 3 hours and then allowed to stir overnight. The solution was poured onto an aqueous mixture of hydrochloric acid in ice (100 ml). The phases were separated and the aqueous phase back extracted with benzene. The combined organic layers were washed with water and dried over magnesium sulfate. The solvent was removed at reduced pressure, yielding 15.5 grams (75%) of the title compound which was purified by sublimation (60°C @ 0.04 mmHg). m.p. (sealed tube) 86-87°C (lit. m.p. 87-89°C)<sup>43</sup>. <sup>1</sup>H NMR (CDCl<sub>3</sub>, 300 MHz) δ 1.77 (s, 6H), 1.92 (s, 6H), 2.09 (s, 3H), 7.30-7.36 (m, 5H); <sup>13</sup>C NMR (CDCl<sub>3</sub>, 300 MHz) 28.99, 36.19, 36.84, 43.19, 124.82, 125.48, 128.08, 151.32.

### 1-Phenyl adamantan-1-ol (28)<sup>44</sup>

Chromium trioxide (7.5 g, 75 mmol) was dissolved in acetic acid (65 ml) and acetic anhydride (65 ml) and cooled to 0°C. 1-Phenyl adamantane (26) (4.6 g, 21.6 mmol) was added and the solution stirred and allowed to warm to room temperature over night, under a dry nitrogen atmosphere. The mixture was poured onto water (500 ml) and extracted with benzene. The organic phase was washed with brine, the solvent removed at reduced pressure, and the pH neutralised with the addition of 1N aqueous sodium hydroxide solution. Methanol (100 ml) and sodium hydroxide solution (2N, 100ml) were added and the mixture stirred at room temperature for 20 hours. The solution was acidified with 2N sulfuric acid and extracted with diethyl ether. The organic phases were washed with saturated

sodium bicarbonate solution and dried over magnesium sulfate. The solvent was removed at reduced pressure yielding off white crystals of the title compound (4.7 g, 59%), which were purified by sublimation (120°C @ 0.05 mmHg). m.p. (sealed tube) 108-110°C (lit. m.p.. 107-114°C)<sup>44</sup>. <sup>1</sup>H NMR (CDCl<sub>3</sub>, 300 MHz) δ 1.72 (s, 2H), 1.77 (s, 2H), 1.81 (s, 4H) 1.88 (s, 2H), 1.96 (s, 4H), 2.34 (s, 1H), 7.30-7.36 (m, 5H); <sup>13</sup>C NMR (CDCl<sub>3</sub>, 300 MHz) 23.82, 25.42, 38.39, 43.87, 44.71, 50.19, 60.66, 125.67, 126.75, 128.20, 144.88.

### **3-Phenyl, 1-adamantyl bromide (29)<sup>44</sup>**

3-Phenyl adamantan-1-ol (28) (4 g, 17.5 mmol) was dissolved in 30% hydrogen bromide in acetic acid (75 ml) and heated to 70°C for 30 minutes. Water was added to the reaction mixture, which was then extracted with diethyl ether. The organic phase was washed with brine and saturated sodium bicarbonate solution and dried over sodium sulfate. The solvent was removed at reduced pressure and the residue purified by column chromatography on silica gel (hexane, R<sub>f</sub> = 0.3) providing the title compound (3.8 g, 75%). m.p. (sealed tube) 99-101°C (lit. m.p.. 100-101°C)<sup>44</sup>. <sup>1</sup>H NMR (CDCl<sub>3</sub>, 300 MHz) δ 1.98 (s, 4H), 2.41-2.46 (m, 8H), 2.57 (s, 2H), 7.36-7.41 (m, 5H); <sup>13</sup>C NMR (CDCl<sub>3</sub>, 300 MHz) δ 26.21, 28.77, 31.98, 37.43, 42.89, 45.66, 51.18, 125.74, 126.69, 128.18, 144.83.

### **3-Phenyl, 1-adamantyl tosylate (15)**

Silver tosylate (1.437 g, 5.15 mmol, 1.5 equiv.) was desiccated under high vacuum for one hour. Then under a dry nitrogen atmosphere, acetonitrile (35 ml) and 3-phenyl, 1-adamantyl bromide (29) (1 g, 3.434 mmol) were added. The reaction mixture was heated to 60°C for two hours. The silver bromide precipitate was removed by filtration, and the acetonitrile removed under reduced pressure. The residue was taken up in diethyl ether (5 ml) and filtered to remove any remaining silver salts. The diethyl ether was then removed by evaporation, giving the title compound as a yellow oil (0.75 g, 57%). <sup>1</sup>H NMR (CDCl<sub>3</sub>, 300 MHz) δ 1.64 (s, 4H), 1.83 (s, 4H), 2.22 (s, 2H), 2.32 (s, 2H), 2.38 (s, 2H), 2.46 (s, 3H), 7.21-7.26 (m, 5H), 7.29-7.32 (m 2H), 7.79-7.84 (m, 2H).

### 3-Bromo-1-adamantane carboxylic acid (31) (Method A) <sup>46</sup>

Bromine (70 ml, 210 g, 1.32 mol, 12 equiv.) was added to aluminium bromide (20.54 g, 77 mmol, 0.7 equiv.) with stirring at 0°C. 1-Adamantane carboxylic acid (24) (20 g, 0.11 mol) was added and the mixture warmed to room temperature and stirred for nine days. When the evolution of hydrogen bromide gas was observed to have ceased, the solution was poured slowly onto ice chilled saturated sodium metabisulfite solution. Solid sodium metabisulfite was added to the mixture until the remainder of the bromine had been destroyed. The solution was extracted with dichloromethane, and the solvent removed by evaporation to give the desired product (20.1g, 70%). Purification by sublimation (120°C @ 5 mmHg) was only partially successful, and the resulting product was found to contain trace impurities, consequently <sup>13</sup>C NMR analysis was not carried out. m.p. (sealed tube) 141-142°C (lit. m.p.. 146.5°C)<sup>46</sup>. <sup>1</sup>H NMR (CDCl<sub>3</sub>, 300 MHz) δ 1.92 (s, 4H), 2.23 (s, 2H), 2.31 (s, 4H), 2.49 (s, 2H).

### Methyl 3-bromo-1-adamantane carboxylate (32)<sup>42,80</sup>

In clear glass jointed quick-fit<sup>®</sup> glassware, potassium hydroxide (14 g, 24.9 mmol) was dissolved in ethanol (25 ml) and water (20 ml) and heated to 65°C. DIAZALD<sup>®</sup> (11.14 g, 51.99 mmol) in diethyl ether (100 ml) was added dropwise. Upon reaction, diazomethane was formed *in situ* and distilled into the reaction vessel containing a stirring solution of 3-bromo-1-adamantane carboxylic acid (32) (4 g, 15.38 mmol) in diethyl ether (220 ml). All evolved gasses were bubbled through a trap containing acetic acid (10ml) in diethyl ether (250 ml) to ensure complete trapping of any excess diazomethane. Upon completion of diazomethane formation the reaction was allowed to stir at room temperature for two days. The reaction mixture was dried over magnesium sulfate and the solvent removed under reduced pressure. The residue was dissolved in minimal dichloromethane and filtered. The dichloromethane was removed and the product was dissolved in minimal hexane and filtered. Removal of the hexane under reduced pressure, it yielded 3.7 grams (97%) of an off yellow low melting point solid. m.p. 34-35°C (lit. m.p. 35-36°C)<sup>42</sup>. <sup>1</sup>H NMR (CDCl<sub>3</sub>, 300 MHz) δ 1.58 (s, 2H), 1.88 (s, 4H), 2.20 (s, 2H), 2.31 (s, 4H), 2.48 (s, 2H), 3.68 (s, 3H); <sup>13</sup>C NMR (CDCl<sub>3</sub>, 300 MHz) δ 26.01, 31.19, 31.89, 35.89, 37.13, 44.09, 45.32, 51.02, 175.32.

### 3-Hydroxy, 1-adamantane carboxylic acid (33)<sup>47</sup>



1-adamantane carboxylic acid (**24**) (10 g, 55.48 mmol) was added to a warm (40°C) solution of potassium permanganate (10 g, 63.28 mmol, 1.1 equiv.) in 2% potassium hydroxide solution (125 ml). The solution was then heated to reflux until a colour change to deep brown was observed (approximately one hour). When the reaction mixture had cooled to room temperature, it was acidified with concentrated hydrochloric acid, and the solid sodium bisulfite was added until all of the manganese dioxide was destroyed. The white precipitate was washed with water and cold diethyl ether and recrystallised from acetone : water (9 : 1) to give the title compound which was further purified by sublimation (130°C @ 0.04 mmHg) (8.2 g, 75%). m.p. (sealed tube) 202-203°C (lit. m.p. 202-203°C)<sup>47</sup>. <sup>1</sup>H NMR (CDCl<sub>3</sub>, 300 MHz) δ 1.61 (s, 2H), 1.71 (s, 6H), 1.91 (s, 4H), 2.02 (s, 2H); <sup>13</sup>C NMR (CDCl<sub>3</sub>, 300 MHz) δ 23.57, 31.31, 36.62, 38.10, 42.97, 44.45, 60.41, 180.30.

### **3-Bromo, 1-adamantane carboxylic acid (31) (Method B)**

3-Hydroxy, 1-adamantane carboxylic acid (**33**) (4 g, 20.4 mmol) was dissolved in 30% hydrogen bromide in acetic acid (60 ml) and heated to reflux for two hours. The mixture was extracted with diethyl ether (2 x 100 ml), and the organic phases washed with water and sodium bicarbonate solution. Acidification of the bicarbonate solution caused the desired product to precipitate. This was dissolved in diethyl ether and dried over sodium sulfate. The solvent was removed under reduced pressure to give the title product. All sublimable material was first collected through rapid sublimation (130°C @ 0.005 mmHg) then further slow sublimation (70°C @ 0.005 mmHg) afforded the pure title compound (3.8 g, 72%). m.p. (sealed tube) 145-147°C (lit. m.p. 146.5°C)<sup>46</sup>. <sup>1</sup>H NMR (CDCl<sub>3</sub>, 300 MHz) δ 1.92 (s, 4H), 2.23 (s, 2H), 2.31 (s, 4H), 2.49 (s, 2H); <sup>13</sup>C NMR (CDCl<sub>3</sub>, 300 MHz) δ 26.07, 31.84, 33.72, 35.66, 37.08, 43.83, 45.35, 180.31.

### **Methyl-3[(tosyl) oxy]-1-adamantane carboxylate (23)<sup>42</sup>**

Silver tosylate (2.3 g, 6.30 mmol, 1.2 equiv.) was desiccated under high vacuum for one hour. Then under a dry nitrogen atmosphere, acetonitrile (25 ml) and methyl-3-bromo-1-adamantane carboxylate (**32**) (2 g, 7.32 mmol) were added. The reaction mixture was warmed to 45°C for six hours. The silver bromide precipitate was removed by filtration, and the acetonitrile removed under reduced

pressure. Under a dry nitrogen blanket, the residue was taken up in diethyl ether (25 ml) and filtered to remove any remaining silver salts. The diethyl ether was then removed by evaporation, furnishing the title compound as a white crystalline solid (23 g, 86%). The sample was then purified through recrystallisation from hexane. m.p. (sealed tube) 73-75°C (lit. m.p. 74.5-76°C)<sup>42</sup>. <sup>1</sup>H NMR (CDCl<sub>3</sub>, 300 MHz) δ 1.59 (s, 2H), 1.80 (s, 4H), 2.13 (m, 2H), 2.17 (s, 2H), 2.30 (s, 4H), 2.44 (s, 3H), 3.66 (s, 3H), 7.28-7.33 (m, 2H), 7.76-7.81 (m, 2H); <sup>13</sup>C NMR (CDCl<sub>3</sub>, 300 MHz) δ 20.96, 23.63, 28.81, 36.93, 38.12, 39.60, 40.82, 51.06, 52.39, 127.85, 130.74, 131.98, 143.61, 173.57.

### **3-Cyano, 1-adamantyl bromide (34)<sup>48</sup>**

3-Bromo,1-adamantane carboxylic acid (31) (1 g, 3.86 mmol) was dissolved in anhydrous dichloromethane (20 ml). Chlorosulfonyl isocyanate (0.655 g 0.4 ml, 4.63 mmol, 1.2 equiv.) in anhydrous dichloromethane (20 ml) was added drop wise, and the mixture heated to reflux for three hours. The reaction mixture was allowed to cool to room temperature, and triethylamine (0.43 g, 0.6 ml, 4.25 mmol, 1.1 equiv.) was added. The mixture was then heated under reflux for a further five hours. The mixture was washed with aqueous 2N sodium bicarbonate solution, 0.5N hydrochloric acid solution and water, and dried over potassium carbonate. The solvent was removed and the residue sublimed (room temperature @ 0.001 mmHg, as the title compound was noted to decompose with heating, above 60°C).<sup>48</sup> The title compound afforded from this purification was 0.53 grams (58%). m.p. (sealed tube) 117-119°C (decomposition) (lit. m.p. 118-121°C decomposition)<sup>48</sup>. <sup>1</sup>H NMR (CDCl<sub>3</sub>, 300 MHz) δ 1.73 (s, 2H), 2.01 (s, 4H), 2.12 (s, 2H), 2.30 (s, 4H), 2.58 (s, 2H); <sup>13</sup>C NMR (CDCl<sub>3</sub>, 300 MHz) δ 30.27, 30.87, 33.82, 38.27, 47.32, 49.97, 59.34, 122.70.

### **3-Cyano, 1-adamantyl tosylate (11)<sup>42</sup>**

To a freshly desiccated sample of silver tosylate (0.49 g, 1.77 mmol, 1.7 equiv.) were added 3-cyano-1-adamantyl bromide (34) (0.25 g, 1.04 mol) and acetonitrile (15 ml). The mixture was stirred under a dry nitrogen atmosphere at 60°C for seven days. Upon completion of the reaction, the silver bromide precipitate was removed by filtration, and the acetonitrile removed under reduced pressure. Under a dry nitrogen blanket, the residue was taken up in dichloromethane (20 ml) and filtered to remove any remaining silver salts. The dichloromethane was

then removed by evaporation, and the residue purified by column chromatography (100% dichloromethane,  $R_f = 0.35$ ). This yielded 0.12 grams of the title compound (35%). m.p. (sealed tube) 106-108°C (lit. m.p.. 106-107.5°C)<sup>42</sup>. <sup>1</sup>H NMR (CDCl<sub>3</sub>, 300 MHz)  $\delta$  1.63 (s, 2H), 2.11 (s, 2H), 2.27 (s, 4H), 2.39 (s, 4H), 2.45 (s, 2H), 2.58 (s, 3H), 7.27-7.33 (m, 2H), 7.72-7.77 (m, 2H); <sup>13</sup>C NMR (CDCl<sub>3</sub>, 300 MHz)  $\delta$  20.96, 28.51, 31.31, 37.99, 45.01, 47.80, 50.05, 52.11, 122.73, 127.88, 130.68, 131.90, 143.69.

### **(3-Bromo, 1-adamantyl) methyl alcohol (38)<sup>44</sup>**

To a stirring mixture of lithium aluminium hydride (0.2 g, 1.4 equiv.) in diethyl ether (10 ml), methyl 3-bromo-1-adamantane carboxylate (32) (1 g, 3.66 mmol) was added and the mixture heated under reflux for two hours. The solution was allowed to cool to room temperature, and saturated sodium sulfate solution (0.5 ml) was added. The precipitate was removed by gravity filtration. The diethyl ether was removed by evaporation, and the residue taken up in minimal diethyl ether and recrystallised from hexane, yielding 0.55 grams of the purified title compound (62%). m.p. (sealed tube) 86-87°C (lit. m.p.. 86-87°C)<sup>44</sup>. <sup>1</sup>H NMR (CDCl<sub>3</sub>, 300 MHz)  $\delta$  1.43 (s, 4H), 1.70 (s, 2H), 2.15 (s, 4H), 2.29 (s, 2H), 2.31 (s, 2H), 3.27 (s, 2H); <sup>13</sup>C NMR (CDCl<sub>3</sub>, 300 MHz)  $\delta$  23.18, 26.62, 32.45, 36.85, 37.41, 45.00, 45.69, 74.73.

### **(3-Bromo, 1-adamantyl)methyl acetate (39)<sup>42</sup>**

(3-Bromo, 1-adamantyl) methyl alcohol (38) (0.2 g, 0.816 mmol) was dissolved in triethylamine (5 ml). Dimethyl aminopyridine (DMAP, 0.05g, 0.408 mmol, 0.5 equiv.) was added and the mixture stirred at room temperature under a dry nitrogen atmosphere. Acetic anhydride (0.166 g, 0.15 ml, 1.63 mmol, 2 equiv.) was added and the mixture allowed to stir for sixteen hours. Diethylether (20 ml) was added, and the organic phase washed with sulfuric acid (0.5M), sodium bicarbonate solution and brine, and dried over potassium carbonate. The diethyl ether was removed by evaporation, leaving a yellow oil, found to be the desired title compound in a pure state (0.18g, 78%). <sup>1</sup>H NMR (CDCl<sub>3</sub>, 300 MHz)  $\delta$  1.56 (s, 4H), 1.71 (s, 2H), 2.08 (s, 3H), 2.17 (s, 4H), 2.30 (s, 2H), 2.37 (s, 2H), 3.72 (s, 2H); <sup>13</sup>C NMR (CDCl<sub>3</sub>, 300 MHz)  $\delta$  17.31, 19.85, 26.38, 32.16, 37.07, 37.49, 45.21, 45.66, 98.13, 171.02.

### **(3-[(Tosyl)oxy]-1-adamantyl)methyl acetate (22)<sup>42</sup>**

To a freshly desiccated sample of silver tosylate (0.262 g, 0.94 mmol, 1.5 equiv.) was added anhydrous acetonitrile (10 ml) and (3-Bromo-1-adamantyl)methyl acetate (39) (0.18 g, 0.627 mmol). The mixture was warmed to 50°C, with stirring under a dry nitrogen atmosphere for three hours. The silver bromide formed in the reaction was removed by filtration, and the acetonitrile removed under reduced pressure. The residue was taken up in dry dichloromethane (15 ml) and filtered to remove any silver salts present. With the removal of the dichloromethane, the products were purified by rapid sublimation (120°C @ 0.005 mmHg) yielding the desired title compound (0.18 g, 79%). m.p. 72-74°C (lit. m.p.. 72.5-74°C)<sup>42</sup>. <sup>1</sup>H NMR (CDCl<sub>3</sub>, 300 MHz) δ 1.42 (s, 2H), 1.49 (s, 4H), 2.06 (s, 3H), 2.11 (s, 2H), 2.19 (s, 4H), 2.30 (s, 2H), 2.46 (s, 3H), 3.60 (s, 2H), 7.34-7.39 (m, 2H), 7.75-7.80 (m, 2H).

### **(3-Bromo-1-adamantyl) methyl tosylate (40)**

(3-Bromo-1-adamantyl) methyl alcohol (38) (0.5 g, 2.04 mmol), dimethyl aminopyridine (DMAP, 0.06 g, 0.51 mmol, 0.25 equiv.) and triethylamine (0.413 g, 0.57 ml, 4.08 mmol, 2 equiv.) were dissolved in anhydrous dichloromethane (15ml) and stirred under a dry nitrogen atmosphere. *p*-Toluene sulfonyl chloride (0.47 g, 2.45 mmol, 1.2 equiv.) in anhydrous dichloromethane (10 ml) was added and the reaction mixture heated under reflux for two days. Having allowed the mixture to return to room temperature, it was washed with cold solutions of sulfuric acid (1M), water and saturated sodium bicarbonate, and dried over magnesium sulfate. The solvent was removed, and the residue purified by rapid sublimation (120°C @ 0.005 mmHg). This provided 0.25 grams of the title compound (30%). m.p. (sealed tube) 108-109°C (lit. m.p.. 108.5-110)<sup>42</sup>. <sup>1</sup>H NMR (CDCl<sub>3</sub>, 300 MHz) δ 1.26 (s, 2H), 1.43 (s, 2H), 1.72 (s, 4H), 2.02 (s, 2H), 2.21 (s, 4H), 2.35 (s, 3H), 3.45 (s, 2H), 7.38-7.43 (m, 2H), 7.79-7.84 (m, 2H); <sup>13</sup>C NMR (CDCl<sub>3</sub>, 300 MHz) δ 19.56, 20.98, 26.60, 32.48, 36.81, 37.42, 45.07, 45.69, 73.15, 127.83, 130.72, 131.94, 143.61.

### **(3-[(tosyl)oxy]-1-adamantyl)methyl tosylate (21)<sup>42</sup>**

(3-Bromo-1-adamantyl)methyl tosylate (40) (0.25 g, 0.626 mmol) was dissolved in anhydrous acetonitrile (15 ml) and stirred under a dry nitrogen atmosphere. A

freshly desiccated sample of silver tosylate (0.27 g, 0.965 mmol, 1.5 equiv.) was added and the reaction mixture warmed to 40°C for eighteen hours. The resulting silver bromide precipitate was removed by filtration under a dry nitrogen blanket, and the solvent removed from the reaction mixture under reduced pressure. The residue was taken up in dichloromethane (15 ml) and filtered to remove any remaining silver salts. With the removal of the dichloromethane, the desired title compound was furnished. Purification was carried out through recrystallisation from diethyl ether, yielding 0.14 grams (47%). m.p. 93-95°C (lit. m.p.. 93-94.5°C)<sup>42</sup>. <sup>1</sup>H NMR (CDCl<sub>3</sub>, 300 MHz) δ 1.26 (s, 2H), 1.42 (s, 2H), 1.71 (s, 4H), 1.89 (s, 2H), 2.11 (s, 4H), 2.37 (s, 6H), 3.55 (s, 2H), 7.19-7.25 (m, 4H), 7.71-7.78 (m, 4H).

### [1.1.1]Propellane (58)<sup>75</sup>

To a stirring solution of 1,1-dibromo-2,2-bis(chloromethyl)cyclopropane (60) (50 g, 0.168 mol) in diethylether (300 ml) at -30°C, was added methyl lithium (1.4 M solution in diethylether, 7.7 g, 0.353 mmol, 252 ml, 2.1 equiv.) dropwise. The mixture was allowed to warm to room temperature with stirring over an hour. When the formation of a white precipitate was seen to be complete, the solvents and volatile products were distilled under reduced pressure (14 mmHg) and collected into a Schlenk flask and kept at -78°C. This solution was found to contain 67% of the desired [1.1.1]propellane (58), and used for the formation of all of the described 1,3-disubstituted bicyclo[1.1.1]pentanes.

### General procedures associated with the formation of 1,3-disubstituted bicyclo[1.1.1]pentanes.

The formation of the described 1,3-disubstituted bicyclo[1.1.1]pentanes followed similar conditions for all reactions. All salts used were dried by applying gentle heat under vacuum overnight. Both bromide and iodine monochloride were added neat in a slow dropwise manner, while iodine was added as a pentane solution, until the typical halogen colour persisted. All salts were dissolved in THF (tetrahydrofuran) except for sodium azide which was dissolved in DMF (dimethylformamide). All reactions were carried out at -5°C under an inert atmosphere.

To describe the synthesis of these 1,3-disubstituted bicyclo[1.1.1]pentanes, the example of the novel synthesis of 1,3-dibromo bicyclo[1.1.1]pentane (**59**) and 1-bromo, 3-iodobicyclo[1.1.1]pentane (**62**) will be given. The percentage yields quoted are calibrated against the known concentration of the [1.1.1]propellane (**58**) solution.

### **1,3-Dibromo bicyclo[1.1.1]pentane (**59**)<sup>54</sup>**

To a mixture of lithium bromide (26g, 0.3 mol) dissolved in anhydrous THF (100ml) at  $-5^{\circ}\text{C}$  was added an aliquot of the prepared [1.1.1]propellane (**58**) in diethylether solution described above (65 ml). Bromine was then added in a slow dropwise manner until the colour persisted. After one hour, the solution was washed with a saturated sodium metabisulfite solution (2 x 50 ml) and dried over magnesium sulfate. The solution was then carefully concentrated under reduced pressure, and the residue recrystallised from methanol to afford the desired title compound (**59**) (4.5 g, 98%) m.p.  $121-122^{\circ}\text{C}$  (lit. m.p.  $119.5-120.5^{\circ}\text{C}$ ).<sup>81</sup>  $^1\text{H}$  NMR ( $\text{CDCl}_3$ , 300 MHz)  $\delta$  2.57 (s, 6H);  $^{13}\text{C}$  NMR ( $\text{CDCl}_3$ , 300 MHz)  $\delta$  30.52, 64.67.

### **1-Bromo, 3-iodobicyclo[1.1.1]pentane (**62**)<sup>54</sup>**

To a mixture of lithium bromide (23.4 g, 0.27 mol) dissolved in anhydrous THF (100 ml) at  $-5^{\circ}\text{C}$  was added an aliquot of the prepared [1.1.1]propellane (**58**) in diethylether solution described above (60 ml). Iodine dissolved in pentane, was then added in a slow dropwise manner until the colour persisted. After one hour, the solution was washed with a saturated sodium metabisulfite solution (2 x 50 ml) and dried over magnesium sulfate. The solution was then carefully concentrated under reduced pressure, and the residue sublimed ( $100^{\circ}\text{C}$  @ 80 mmHg) to remove any 1,3-diiodo bicyclo[1.1.1]pentane (**54**) present. The sublimation was then continued, to afford the desired title compound (**62**) (3.62 g, 73%) as a volatile colourless solid. m.p.  $140-141^{\circ}\text{C}$  (lit. m.p.  $141-142^{\circ}\text{C}$ )<sup>52</sup>  $^1\text{H}$  NMR ( $\text{CDCl}_3$ , 300 MHz)  $\delta$  2.62 (s, 6H);  $^{13}\text{C}$  NMR ( $\text{CDCl}_3$ , 300 MHz)  $\delta$  32.49, 66.43.

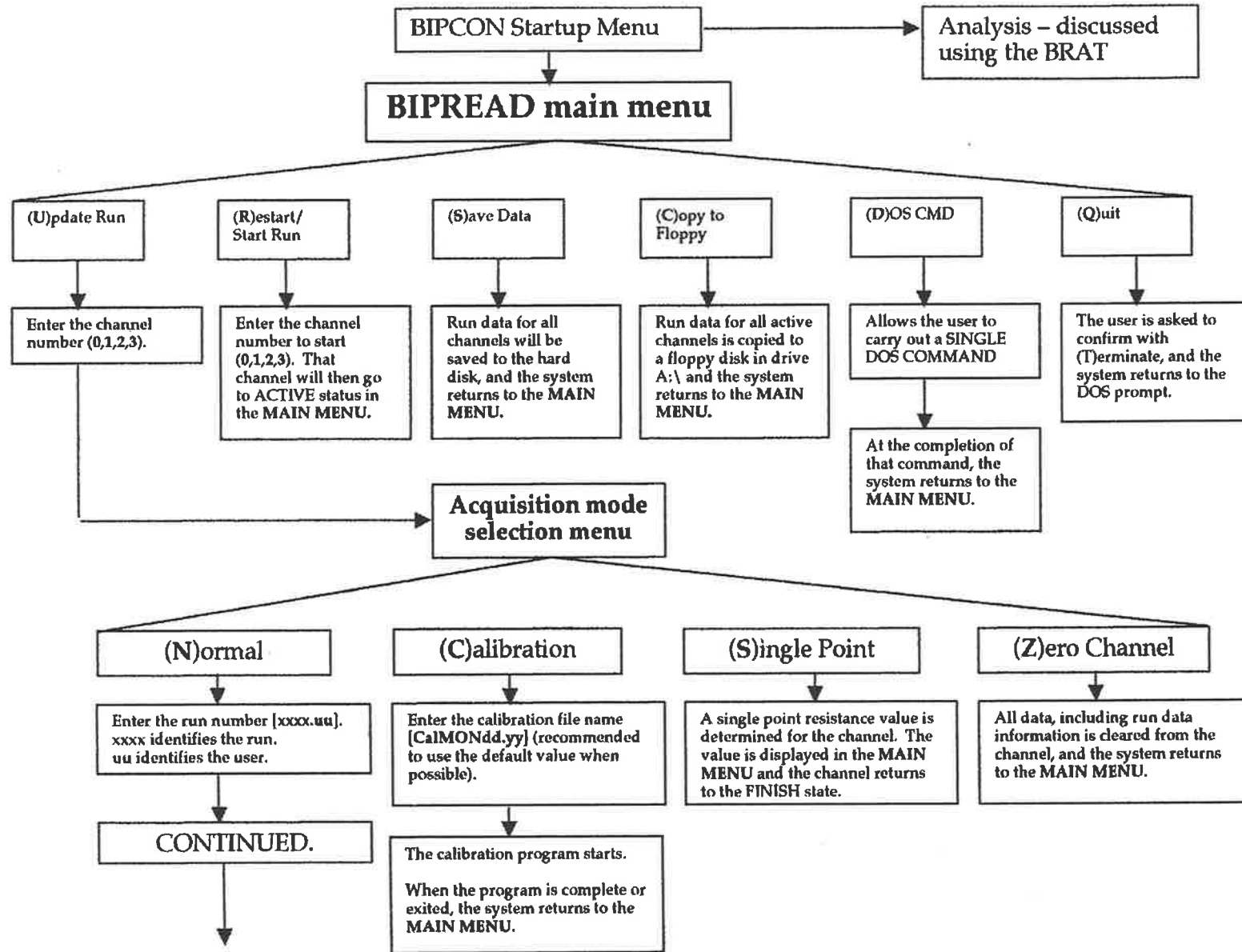
## Appendices

### DOS Glossary:

This Glossary provides a very brief list of the vital MS-DOS commands required to operate the BIPCON suite. This is not intended to be an exhaustive compendium of MS-DOS commands, nor will it cover all of the commands that a user may wish to use in the operation of the BIPCON suite. For more information on the use of Ms-DOS and the commands there in, please refer to reference material specific to the MS-DOS operating system or the MS-DOS online help, accessible through typing HELP at the DOS prompt.

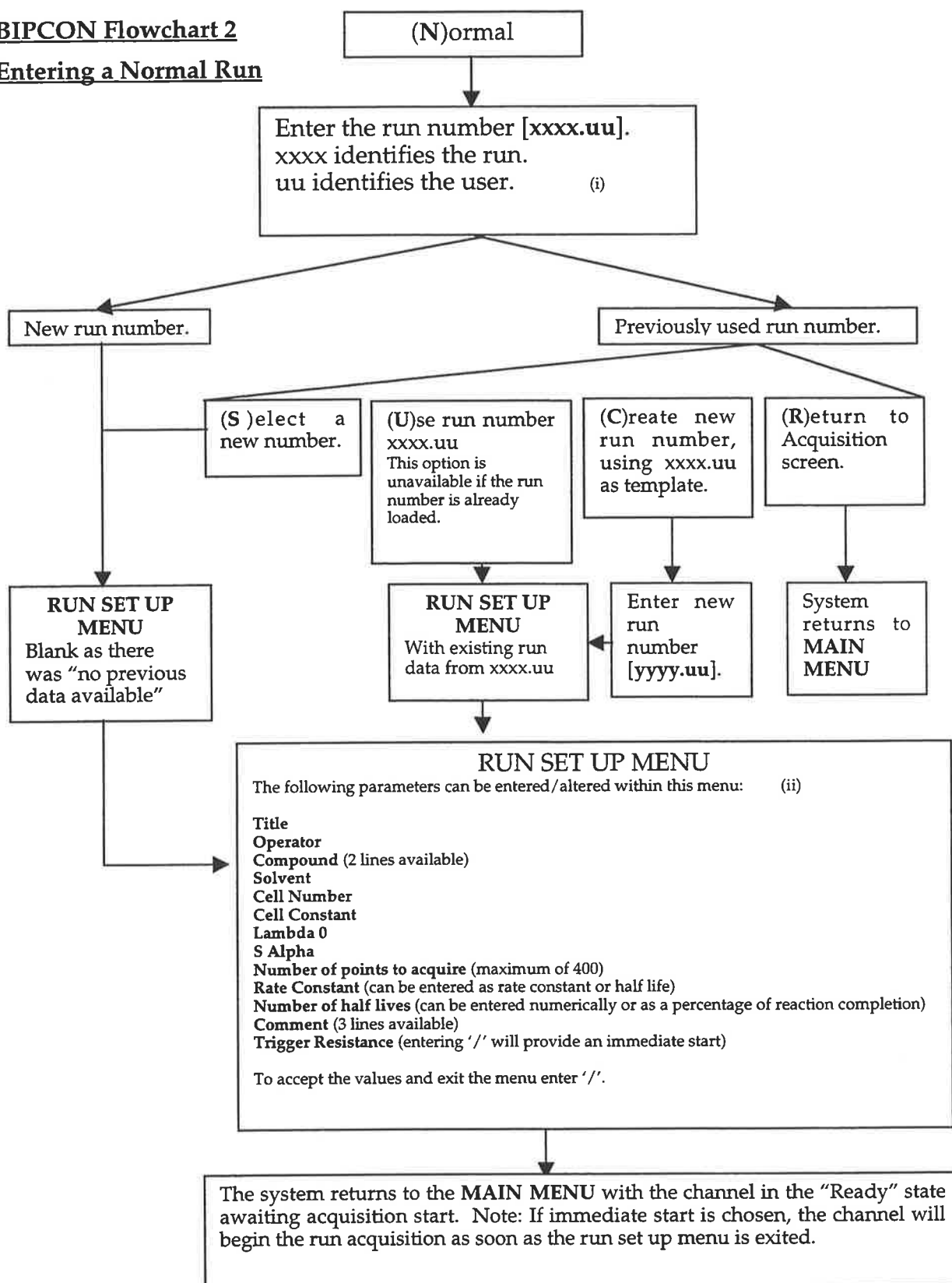
A:	move to DRIVE "A" (The BIPCON has A:\ (floppy disk) and C:\ (Hard Disk) drives)
DIR	directory list (can specify directory)
CD	change directory
..	signifies moving up in the directory tree
DEL (filename)	delete (filename)
MKDIR (directoryname)*	make directory (directoryname) in current directory
RENAME (filename) (newfilename)*	change the name of a file
MOVE (filename) (directory)	move the file to a new location
COPY (filename) (directory)	make a copy of a file in another directory
EDIT (filename)	open a file in the EDIT program (basic text editing)
BIPREAD	start the BIPCON acquisition program
BIPREAD	
TRANSHDR	start the translation program
TRANSHDR	
KINPROG	start the kinetic calculation program
KINPROG	

\* It is important to remember that the MS-DOS operating system uses an 8.3 naming system. Consequently a document or directory name can have a maximum of 8 characters in its name, followed by the 3 digit code for that item. It is not possible to exceed this naming limit.



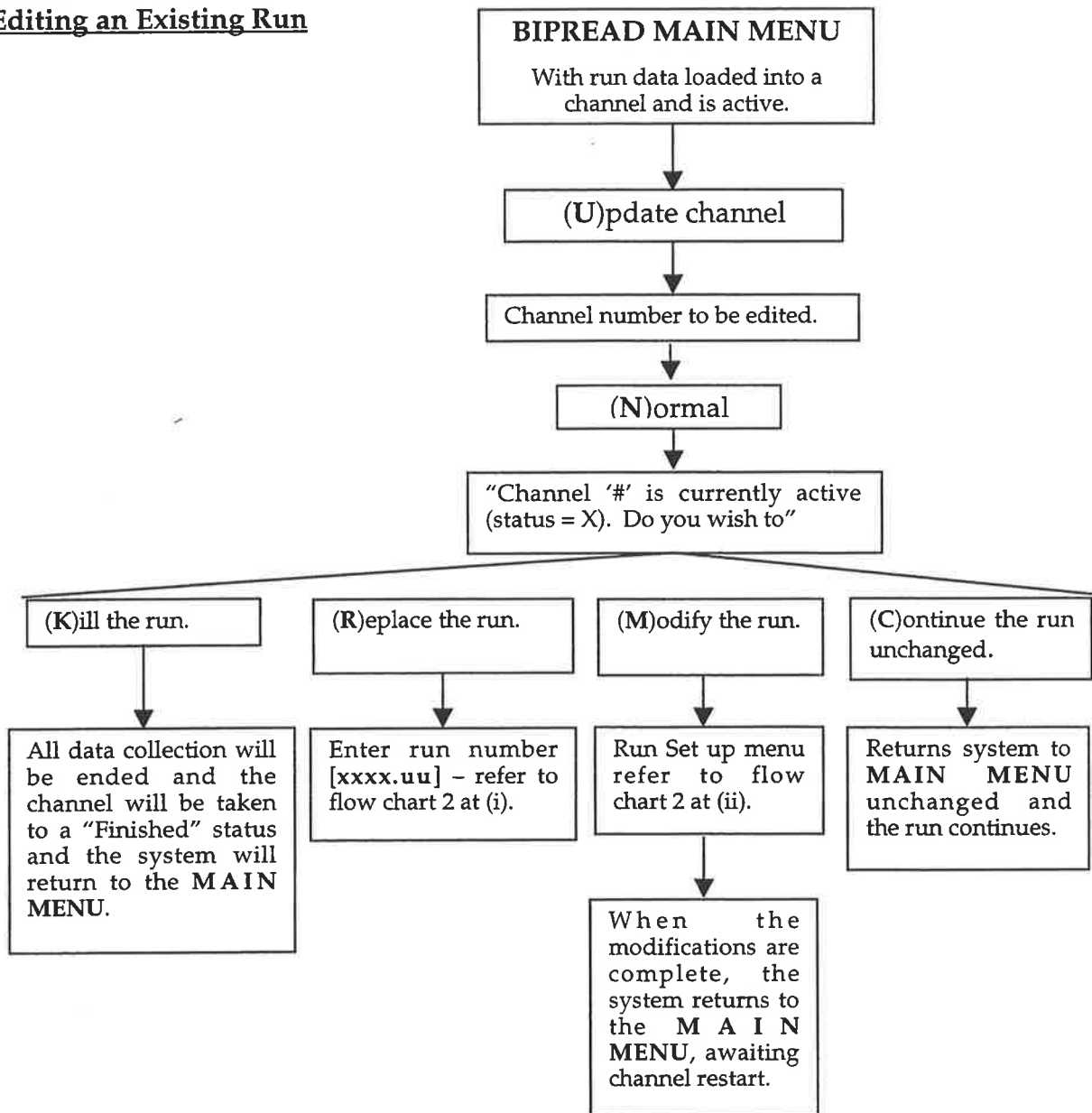


**BIPCON Flowchart 2**  
**Entering a Normal Run**



### BIPCON Flowchart 3

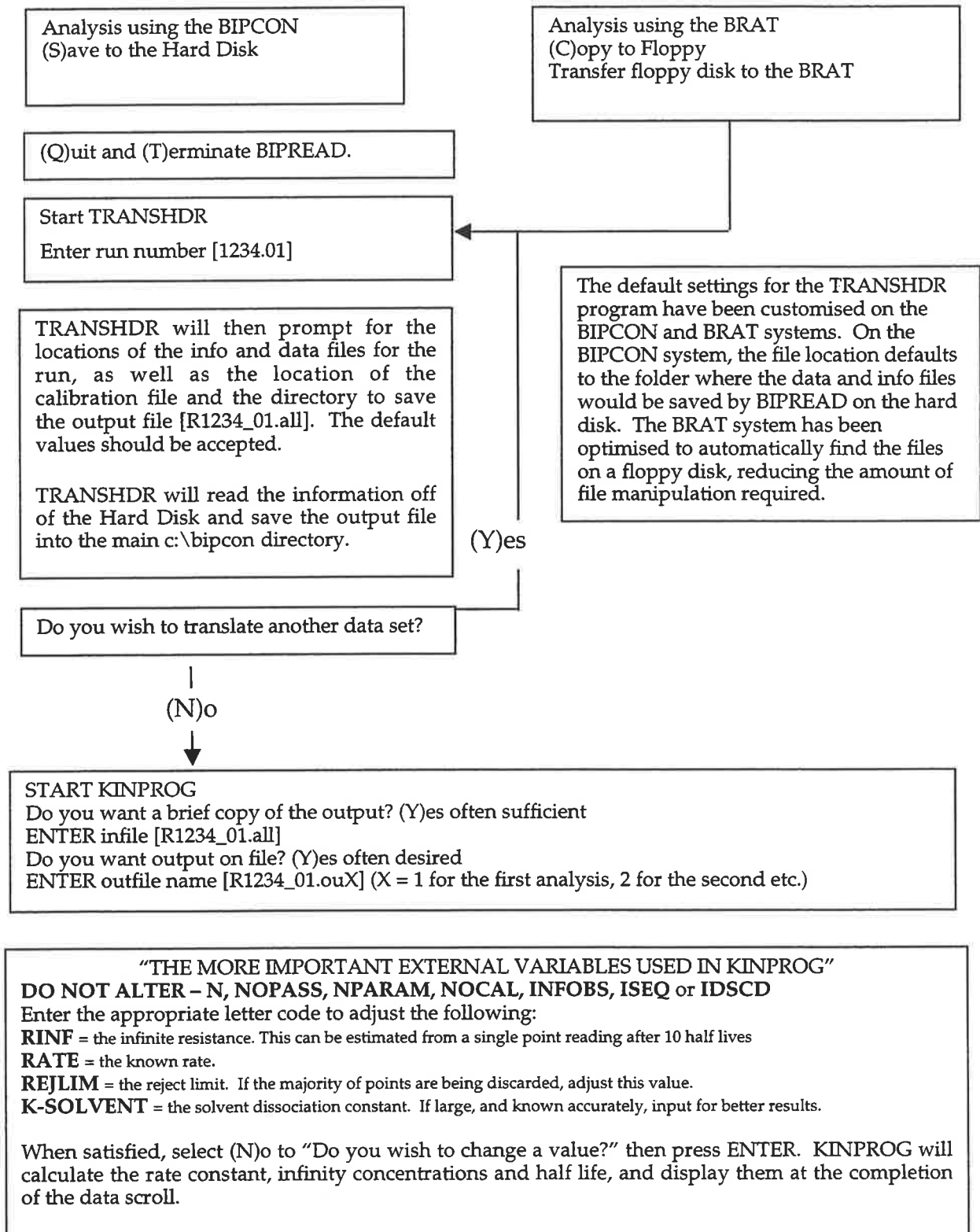
#### Editing an Existing Run



#### Channel Status Numbers

-4	=	Paused
-3	=	Ready to start (run parameters defined, awaiting user activation)
-2	=	Calibration Hold (awaiting user input to read calibration point)
-1	=	Finish
0	=	Inactive/Passive
1	=	Run acquisition
2	=	Awaiting Resistance Trigger to start run
3	=	Calibration acquisition (acquire 1 point)
4	=	Single point acquisition (acquire 1 point)

## BIPCON Analysis Flowchart



### **About this thesis:**

This thesis has been written utilising Australian-English spelling and grammar. The text was entered using Microsoft Word 98/2001, the technical diagrams created using AppleWorks 5.1, the photographic images were manipulated using Adobe Photoshop 5.0, the charts were generated using Microsoft Excel 2001 and the chemical diagrams created using ChemDraw. The thesis was created on a Apple Macintosh PowerPC 6500, and typeset in Palatino 12 point.

## References

- (1) Raber, D. L.; Neal, W. C. J.; Djukes, M. D.; Harris, J. M.; Mount, D. L. *J. Am. Chem. Soc.* **1978**, *100*, 8137-8146.
- (2) Carroll, F. A. *Perspectives on Structure and Mechanism in Organic Chemistry*; Brooks/Cole Publishing Company: Pacific Grove, CA, USA, 1998.
- (3) Della, E. W.; Elsey, G. M. *Aust. J. Chem.* **1995**, *48*, 967-985.
- (4) Elsey, G. M. Ph.D., Flinders University of South Australia, 1992.
- (5) Schadt, F. L.; Bentley, T. W.; Schleyer, P. v. R. *J. Am. Chem. Soc.* **1976**, *98*, 7667-7674.
- (6) Shiner, V. J., Jr.; Dowd, W.; Fisher, R. D.; Hartshorn, S. R.; Kessick, M. A.; Milakofsky, L.; Rapp, M. W. *J. Am. Chem. Soc.* **1969**, *91*, 4838-4843.
- (7) Grunwald, E.; Winstein, S. J. *J. Am. Chem. Soc.* **1948**, *70*, 846.
- (8) Winstein, A. H.; Grunwald, E.; Jones, H. W. *J. Am. Chem. Soc.* **1951**, *73*, 2700.
- (9) Winstein, S.; Fainberg, A. H.; Grunwald, E. *J. Am. Chem. Soc.* **1957**, *79*, 4146.
- (10) Raber, D. J.; Harris, J. M.; Hall, R. E.; Schleyer, P. v. R. *J. Am. Chem. Soc.* **1971**, *93*, 4821-4828.
- (11) Raber, D. J.; Harris, J. M.; Schleyer, P. v. R. *J. Am. Chem. Soc.* **1971**, *93*, 4829-4834.
- (12) Raber, D. J.; Bingham, R. C.; Harris, J. M.; Fry, J. L.; Schleyer, P. v. R. *J. Am. Chem. Soc.* **1970**, *92*, 5977-5981.
- (13) Bentley, T. W.; Carter, G. E. *J. Am. Chem. Soc.* **1982**, *104*, 5741-5747.
- (14) Grob, A. G.; Schaub, B. *Helvetica Chim Acta* **1982**, *65*, 1720-1727.
- (15) Grob, C. A. *Acc. Chem. Res.* **1983**, *16*, 426.
- (16) Biemann, R.; Christen, M.; Flury, P.; Grob, A. G. *Helvetica Chim. Acta* **1983**, *66*, 2154-2164.
- (17) Müller, P.; Mareda, J. *Helvetica Chim Acta* **1987**, *70*, 1017.
- (18) Müller, P.; Blanc, J.; Mareda, J. *Helv. Chim. Acta* **1986**, *69*, 635.
- (19) Müller, P.; Mareda, J. *Tetrahedron. Lett.* **1984**, 1703.

- (20) Della, E. W.; Gill, P. M. W.; Schiesser, C. H. *J. Org. Chem.* **1987**, *53*, 4354-4357.
- (21) Della, E. W.; Gill, P. M. W.; Schiesser, C. H. *J. Org. Chem.* **1988**, *53*, 4354-4357.
- (22) Della, E. W.; Grob, C. A.; Taylor, D. K. *Journal of the American Chemical Society* **1994**, *116*, 6159-6166.
- (23) Della, E. W.; Janowski, W. K. *J. Org. Chem.* **1995**, *60*, 7756-7759.
- (24) Ferber, P. H.; Gream, G. E.; Wagner, R. D. *Aust. J. Chem.* **1980**, *33*, 1569-1588.
- (25) Abboud, J. M.; Herreros, M.; Notario, R.; Lomas, J. S.; Mareda, J.; Müller, P.; Rossier, J. *J. Org. Chem.* **1999**, *64*, 6401-6410.
- (26) Creary, X.; Wang, Y. *J. Org. Chem.* **1992**, *57*, 4761-4765.
- (27) Tilley, L. Ph.D., University of Indiana, 1996.
- (28) Murr, B. L. Ph.D., University of Indiana, 1961.
- (29) Jones, G.; Josephs, R. *J. Am. Chem. Soc.* **1928**, *50*, 1049-1092.
- (30) Johnson, D. E.; Enke, C. G. *Anal. Chem.* **1970**, *42*, 329-335.
- (31) Following consultation with the Shiner group, r. t. u. o. t. B. i.
- (32) *C.R.C. Handbook of Chemistry and Physics*; 6th ed.; Chemical Rubber Publishing Company:, 1980.
- (33) Shiner, V. J. J.; Verbanz, C. J. *J. Am. Chem. Soc.* **1957**, *79*, 373-375.
- (34) Shiner, V. J. J.; Murr, B. L. *J. Am. Chem. Soc.* **1962**, *84*, 4672-4677.
- (35) Fuoss, R. M.; Accascina, F. *Electronic Conductance*; Interscience: New York, 1959.
- (36) Onsager, L. *Physik Z.* **1927**, *28*, 277.
- (37) Coope, J. L. Ph.D., University of Indiana, 1990.
- (38) Rapp, M. W. Ph.D., University of Indiana, 1968.
- (39) Stoelting, D. T. Ph.D., University of Indiana, 1990.
- (40) Wilgis, F. P. Ph.D., University of Indiana, 1989.
- (41) March, J. *Advanced Organic Chemistry - 4th Edition*; 4 ed.; Wiley-Interscience: New York, 1993; Vol. 4th Edition.
- (42) Biemann, R.; Grob, A. G.; Schaub, B. *Helvetica Chim Acta* **1982**, *65*, 1728-1733.
- (43) Stetter, H.; Schwarz, M.; Hirschhorn, A. *Chem. Ber.* **1959**, *92*, 1629-1635.

- (44) Ficsher, W.; Grob, C. A.; Katayama, H. *Helvetica Chimica Acta* **1976**, *59*, 1953-1962.
- (45) Baughman, G. L. *Journal of Organic Chemistry* **1964**, *29*, 238-240.
- (46) Stetter, H.; Mayer, J. *Chem Ber* **1962**, *95*, 667-672.
- (47) Anderson, G. L.; Burks, W. A.; Harruna, I. I. *Synthetic Communications* **1988**, *18*, 1967-1974.
- (48) Fischer, W.; Grob, C. A. *Helvetica Chim Acta* **1978**, *61*, 1588-1608.
- (49) Progress in Physical Organic Chemistry; Taft, R. W., Ed. 1981; Vol. 13, p 143-150.
- (50) Müller, P.; Milin, D. *Helv. Chim. Acta* **1991**, *74*, 1808.
- (51) Della, E. W.; Janowski, W. K. *J. Chem. Soc., Chem. Commun.* **1994**, 1763-1764.
- (52) Wiberg, K. B.; McMurdie, N. J. *Am. Chem. Soc.* **1994**, *116*, 11990-11998.
- (53) Adcock, J. L.; Gakh, A. A. *J. Organic Chemistry* **1992**, *57*, 6206-6210.
- (54) Milne, I. R.; Taylor, D. K. *J. Org. Chem* **1997**, *64*, 2618-2625.
- (55) Fainberg, A. H.; Winstein, S. *J. Am. Chem. Soc.* **1957**, *79*, 1602.
- (56) Schlyer, P. v. R.; Nicholas, R. D. *J. Am. Chem. Soc.* **1961**, *83*, 2700.
- (57) Brenneisen, P.; Grob, C. A.; Jackson, R. A.; Ohta, M. *Helv. Chim. Acta.* **1965**, *48*, 146.
- (58) Fort, R. C. J.; Schleyer, P. v. R. *Adv. Alicyclic. Chem.* **1966**, *1*, 283.
- (59) Wiberg, K. B.; Williams, V. Z. *J. Am. Chem. Soc.* **1967**, *89*, 3373.
- (60) Wiberg, K. B.; Lowry, B. R. *J. Am. Chem. Soc.* **1963**, *85*, 3188.
- (61) Bingham, R. C.; Schlyer, P. v. R. *J. Am. Chem. Soc.* **1971**, *93*, 3189.
- (62) Parker, W.; Tranter, R. L.; Watt, C. I. F.; Chang, L. W. K.; Schlyer, P. v. R. *J. Am. Chem. Soc* **1974**, *96*, 7121.
- (63) Müller, P.; Blanc, J.; Marada, J. *Chimia* **1984**, *38*, 389.
- (64) Müller, P.; Mareda, J. *Helv. Chim. Acta* **1987**, *70*, 1017.
- (65) Müller, P.; Marada, J. *J. Comput. Chem.* **1989**, *10*, 863.
- (66) Adcock, W. A.; Krstic, A. R. *Tetrahedron Letters* **1992**, *33*, 7397-7398.

- (67) Della, E. W.; Taylor, D. K. *J. Org. Chem.* **1994**, *59*, 2986-2996.
- (68) Adcock, J. L.; Gakh, A. A. *Tetrahedron Lett.* **1992**, *33*, 4878.
- (69) Wiberg, K. B.; Waddell, S. T.; Laidid, K. *Tetrahedron Letters* **1986**, *27*, 1553-1556.
- (70) Wiberg, K. B.; Waddell, S. T. *Tetrahedron Letters* **1987**, *20*, 151-154.
- (71) Robinson, R. E.; Michl, J. *J. Org. Chem.* **1989**, *54*, 2051-2053.
- (72) Della, E. W.; Pigou, P. E.; Schiesser, C. H.; Taylor, D. K. *J. Org. Chem.* **1991**, *56*, 4659-4664.
- (73) McGarry, P. F.; Johnston, L. J.; Scaiano, J. C. *J. Am. Chem. Soc.* **1989**, *111*, 3750-3751.
- (74) McGarry, P. F.; Johnson, L. J.; Scaniano, J. C. *J. Org. Chem.* **1989**, *54*, 6133-6135.
- (75) Belzner, J.; Bunz, U.; Semmler, K.; Szeimies, G.; Opitz, K.; Schluter, A. D. *Chem. Ber.* **1989**, *122*, 397-398.
- (76) Adcock, W.; Binmore, G. T.; Krstic, A. R.; Walton, J. C.; Wilkie, J. *J. Am. Chem. Soc.* **1995**, *117*, 2758-2766.
- (77) Adcock, W.; Krisic, A. R. *Magn. Reson. Chem.* **1997**, *35*, 663.
- (78) Perrin, D. D.; Armarego, W. L. F.; Perrin, D. R. *Purification of Laboratory Chemicals*; 2nd ed.; Pergamon Press: Oxford, 1980.
- (79) Kevill, D. N.; Kolwyck, K. C.; Weitzel, F. L. *J. Am. Chem. Soc.* **1970**, *92*, 7300-7306.
- (80) Black, T. H. *Aldrichimica Acta* **1983**, *16*, 3-9.
- (81) Gleiter, R.; Pfeifer, K. H.; Szeimies, G.; Bunz, U. *Angew. Chem., Int. Ed. Engl.* **1990**, *29*, 413.



## Addendum.

Throughout this thesis, the term “Hammett” has been misspelt, and should be read as “Hammett.” In addition the following terms were misspelt through typographical error. The term “adamantyl” should replace “adamantly,” the term “halide” replace “hailde,” the term “trial” replace “trail,” the term “requisite” replace “requisit,” the term “sulfonate” replace “solfonate,” the term “unequivocally” replace “unequivically,” the term “quantitative” replace “quantatative,” and the term “deutero” replace “durtero.” Where used, the symbol for electron withdrawing nature shown as “ $\sigma$ ” should appear as “ $\sigma_1$ ”.

For clarity, where discussed, the withdrawing nature of a substituent refers to the electron withdrawing nature. Further discussion of the  $\rho$  value describes the polar susceptibility value.

On pages 144, 145, 146, 148, 149, 150, 156, 158, 159, 160 and 163, the chemical name “phenyl adamantane” should appear as one word, as “phenyladamantane.” Further, where mentioned 1-phenyladamantan-3-ol should appear as 3-phenyladamantan-1-ol.

Where named, dihalide bicyclo[1.1.1]pentanes should be named in a the manner of, for example, 1-bromo-3-iodobicyclo[1.1.1]pentane, and not as shown in the text separated with a comma. The naming of substituted adamantanes should appear in a similar fashion without spacing, such as 3-methyl-1-adamantyl tosylate.

Where mentioned 1-bromo-adamantane-3-carboxylic acid should appear as 3-bromo-adamantane-1-carboxylic acid.

Pinacolyl should refer to 3,3-dimethyl-2-butyl and not 2,2-dimethyl-2-butyl as shown in the text.

On page 136 “3-methoxy carbonylbicyclo[2.1.1]hexyl triflate” should be read as “3-methoxycarbonylbicyclo[2.1.1]hex-1-yl triflate”

On page 32, Section 1.4, reference to Figure 1.9 should read 1.8.

On page 135, compound **45** is misnamed, and should be read as 1-bicyclo[1.1.1]hexyl bromide.

On page 135, compound **46** is misnamed, and should be read as 1-bicyclo[1.1.1]heptyl bromide.

For clarity, on page 151, the sentence beginning “This has been attributed...” should read “We have attributed this...”

All references to *Journal of the American Chemical Society*, should read *J. Am. Chem. Soc.*

All references to *Helvetica Chim Acta*, should read *Helv. Chem. Acta*.

All references to University of Indiana should be suffixed with "Bloomington."

All references to *Journal of Organic Chemistry*, should read *J. Org. Chem.*

All references to *Tetrahedron Letters* should read *Tetrahedron Lett.*

References 20 and 21 should be read as the same reference. The correct reference is Della, E. W.; Gill, P. M.; Schiesser, C. H. *J. Org. Chem.* **1988**, *53*, 4354.

Reference 31 should read "Following consultation with the Shiner group, regarding the use of their BIPCON instrument.

Reference 49 is incorrect and should read Charton, M. *Prog. Phys. Org. Chem.* **1981**, *13*, 143-150.

Reference 54 is incorrect and should read Milne, I. R., Taylor, D. K. *J. Org. Chem.* **1988**, *63*, 3769.

The following recent references were kindly highlighted by an examiner and are of interest to this project:

*J. Am. Chem. Soc.* **2000**, *122*, 7351

*J. Org. Chem.* **2001**, *66*, 2034

*J. Am. Chem. Soc.* **2001**, *123*, 10, 877

*Org. Lett.* **2001**, *3*, 2225

An examiner suggested that for clarity, further definition of an  $S_N1$  process, as described on page 20 be given. For an  $S_N1$  reaction the important rate determining step may be either ionisation to give the intimate ion-pair (the most common situation) or the separation of the initially formed intimate ion-pair into a solvent separated ion-pair. A well known example of the latter is the solvolysis of 2-adamantyl tosylate which is the standard compound for defining the solvent parameter  $Y(OTs)$ .

It was highlighted by an examiner that alternative syntheses for 1,3-dibromoadamantane are present in the known literature (*Helv. Chim. Acta.* **1976**, *57*, 1953) which may have allowed us to prepare other substrates of interest.

An alternative theory that may explain the observed decrease in " $m$ " values was proposed by an examiner. The varying " $m$ " values could be rationalised within the framework of the existing mechanistic model for  $S_N1$  solvolyses. The important point is that a very low " $m$ " value for a reaction that is unambiguously an  $S_N1$  process indicates that the transition state has a moderate degree of polarity. A low result should not be taken as a reliable indicator that a reaction is not  $S_N1$ . Obviously, the position of the transition state along the reaction coordinate is shifted by varying the electron withdrawing power of the substituent. Thus, the degree of polarity of the transition state is changed in a regular fashion. Decreasing the polarity lessens the demand for solvation and hence causes a lower response to  $Y_{OTs}$ . It is important to consider that the mechanism of  $S_N1$  solvolysis of the standard compound (2-adamantyl tosylate) involved rate-determining separation of the intimate ion-pair, hence, charge development is maximised in the transition state and the

09PH  
M6593  
c.2

system is very sensitive to solvation factors. By definition any substrate solvolysing by a similar scenario should yield an “*m*” value of unity. With respect to the notion that there is “frontside” bimolecular substitution it is worthwhile noting that even in the case of the tert-butyl cation it has been shown that the carbocation is not diffusionally equilibrated but reacts at the ion-pair stage within the pool of solvent molecules that are present when the bond to the leaving group is broken (*J. Am. Chem. Soc.* **1996**, *118*, 11434). It is reasonable to assume that a similar situation may occur for the 1-adamantyl cation.

The generous gift of 1,1-dibromo-2,2-bis(chloromethyl)cyclopropane utilised in the formation of [1.1.1]propellane from Dr. W. Adcock (Flinders University of South Australia) is kindly acknowledged.